# Effective Fiber Bandwidth Utilization in TDM WDM Optical Networks

**Yoong Cheah Huei**

**National University of Singapore**

**2007**

# Effective Fiber Bandwidth Utilization in TDM WDM Optical Networks

**Yoong Cheah Huei**

**(B.Sc. and M.Sc., Iowa State University, USA)**

**A THESIS SUBMITTED**

**FOR THE DEGREE OF DOCTOR OF PHILOSOPHY**

**DEPARTMENT OF COMPUTER SCIENCE**

**NATIONAL UNIVERSITY OF SINGPORE**

**2007**

# Acknowledgements

First and foremost, I wish to express my sincere and deepest gratitude to my supervisor, Dr. Pung Hung Keng. His guidance, kindness, and support have made this work possible. Dr. Mohan Gurusamy, Dr. Roger Zimmermann, Dr. Lillykutty Jacob, and Dr. A. L. Ananda have served as my reviewers at different stages of this thesis. I would like to express my sincere appreciation for their time in reviewing this thesis, and their valuable comments and suggestions.

I am grateful to the School of Computing, National University of Singapore (NUS) for giving me the opportunity to pursue this doctorate of philosophy. The services and facilities provided by NUS are fantastic. This helps me to carry out the research smoothly. I am also grateful to the management of the School of Infocomm Technology, Ngee Ann Polytechnic, Singapore for their continuous support.

I wish to thank Dr. Nikolai Krivulin for sharing his expertise and many discussions.

I would like to thank all my colleagues and friends at the Network Systems and Services Laboratory, especially Gu Tao, Long Fei, and Chua Hui Lin for laboratory support.

I want to sincerely thank my colleagues, Miss Yang Sook Chiat and Miss Irene Tan who have spent a lot of time to proofread this thesis.

Finally, I would like to thank my family members, especially my wife, Ng Hong Kian and my three children for their strength, love, support, and patience during the course of my doctoral studies.

# TABLE OF CONTENTS

# List of Tables

# List of Figures

# Abbreviation List

| | |
|---|---|
| FDL | Fiber Delay Lines |
| GMPLS | Generalized Multiprotocol Label Switching |
| IP | Internet Protocol |
| LCR | Least-Cost Routing |
| LCR-FTL | Least-Cost Routing with At Least A Free Time-Slot in a Fiber Link |
| MHFR | Minimum Hop Fixed Routing |
| MTWR | Mini-Slot Time-Slot Wavelength Router |
| OCS | Optical Circuit Switching |
| OEO | Optical-Electrical-Optical |
| OMSI | Optical Mini-Slot Interchanger |
| OMSS | Optical Mini-Slots Switches |
| OTDS | Optical Time-Division Switch |
| OTSI | Optical Time-Slot Interchanger |
| OTSS | Optical Time-Slot Switches |
| RWA | Routing and Wavelength Assignment |
| SSWC | Slot-by-Slot fast Wavelength Converter |
| STSWR | Shared Time-Slot Wavelength Router |
| TEB-SC | Total Established Bandwidth for Successful Connections |
| TSI | Time-Slot Interchanger |
| WC | Wavelength Converter |
| WCB | Wavelength Converter Bank |
| WDM | Wavelength Division Multiplexing |

# Summary

There has been a wide deployment of Wavelength Division Multiplexing (WDM) transmission technology in the core networking arena. WDM is a very favorable technique to exploit the high bandwidth in the optical fiber. A wavelength typically operates in hundreds of Mbps or even Gbps needs to be better utilized if the connection request is less than 100 Mbps bandwidth. Otherwise, there is a tremendous wastage of bandwidth in a fiber for data transmission.

Though the fiber bandwidth has been improving due to the advancement of fiber-optics technologies and the increases of number of wavelengths in a fiber, there has not much research being carried out in the area of optical traffic grooming at the time-slot wavelength level. In this thesis, we propose two methods of traffic grooming to effectively and efficiently utilizing the fiber bandwidth.

The first method deals with sharing of time-slots in a wavelength. The second method involves further division of each time-slot in a wavelength into mini-slots. For each method, a corresponding optical data transport network architecture enabling the respective traffic grooming has also been proposed; they are namely the shared time-slot time division multiplexing (TDM) wavelength optical WDM network and the mini-slot TDM wavelength optical network. The shared time-slot TDM wavelength optical WDM network is effective for heavy volume of data traffic going to the same destination router from the same source router. In this thesis, the effectiveness of the router architecture and behavior of shared time-slot TDM wavelength optical WDM network are studied intensively. The simulated results indicate this type of network has the lowest blocking probability when compared with the typical wavelength optical network without

Wavelength Converter (WC) and the TDM wavelength optical network. Our simulation study also shows that the blocking probability of the network under different routing algorithms like fixed routing, least cost routing, and least cost routing with at least an available time-slot at each fiber link is almost the same. The mini-slot TDM wavelength optical network has a lower blocking probability than the typical wavelength optical network. The total established bandwidth for successful connections (TEB-SC) and blocking probability of this network varies with the number of mini-slot requested by each connection. The NSFNET topology, *3x5* mesh torus topology, and 40-node irregular topology were studied in the simulation. In general, our simulation results show that the shared time-slot network has a lower blocking probability than the mini-slot network. The two proposed optical networks are technically feasible to implement based on the results of our analysis and the availability of the network components. Generally, the cost of implementing a shared time-slot TDM wavelength optical WDM node is much lower than a mini-slot TDM wavelength optical node. At present, the high development cost of an optical time-slot interchange (OTSI) is the major hindering factor for the shared time-slot TDM wavelength optical WDM network to be economically viable. The optical technologies are still immature for the mini-slot TDM wavelength optical network to be commercially implemented.

In addition to simulation, we have also proposed an analytical model for TDM wavelength optical networks with OTSIs and without WC using the partition based approach with two objectives: (1) to validate the simulation results of this network, and (2) to calculate the average network blocking probabilities of this network. To make the analysis tractable, we propose a schema that can work for any number of partition patterns, regardless of the numbers of links, wavelengths in each link, and time-slots in each wavelength. The results obtained from the analysis agreed closely with that of the simulation results.

# Publications

[1] Cheah Huei Yoong and Hung Keng Pung, “A Framework for Shared Time-Slot TDM Wavelength Optical WDM Networks,” Journal of Optical Networking, Special Issue – Convergence, vol. 5, no. 7, pp. 554-567, July 2006. Printed by the Optical Society of America (OSA).

[2] Cheah Huei Yoong and Hung Keng Pung, “Mini-slot TDM WDM Networks,” Journal of Photonics Network Communications, vol. 5, no. 2, pp. 91-100, Apr. 2008. DOI: 10.1007/s11107-007-0090-1. Printed by Springer (Netherlands).

[3] Cheah Huei Yoong, Hung Keng Pung, and Nikolai Krivulin, “Calculating the Approximate Blocking Probabilities in TDM Wavelength Optical Network with OTSIs and without WC,” Journal of High Speed Networks (Accepted – 20 pages). Printed by IOS.

[4] Cheah Huei Yong and Hung Keng Pung, “A Mini-slot Router Architecture for TDM Optical WDM Networks,” in 20th IEEE Advanced Information Networking and Applications Conference (AINA), Vienna, Austria, 18th-20th Apr. 2006, vol. 1, pp. 605-610.

[5] Cheah Huei Yoong and Hung Keng Pung, “A Shared Time-Slot Router Architecture for TDM Wavelength Optical WDM Networks,” in 13th IEEE International Conference on Networks (ICON), Kuala Lumpur, Malaysia, 16th-18th Nov. 2005, vol. 2.

[6] Cheah Huei Yoong and Hung Keng Pung, “Optical Architecture For Traffic Ungrooming and Grooming at Intermediate Destinations,” in 4th Australia Network and Telecommunications Applications Conference (ANTAC), Sydney, Australia, 8th-10th Dec. 2004, pp. 194-198.

[7] Cheah Huei Yoong, Hung Keng Pung, and Nikolai Krivulin, “Average Network Blocking Probabilities for TDM WDM Optical Networks with OTSIs and without WC,” in 15th IEEE / ACM International Symposium on Modeling, Analysis, and Simulation of Computer and Telecommunication Systems (MASCOTS), Istanbul, Turkey, 24th-26th Oct. 2007 (Accepted – 9 pages).

# CHAPTER 1

# Introduction

Telecommunications networks have evolved in the last century with technological advances and social changes. In the beginning, telephone networks require intervention of friendly local operators to make a successful voice connection. Today, voice connections in these networks are automated and gigabits of data per second can be transmitted. Transmission of data at such high speeds can be equivalent to thousands of encyclopedias per second. Throughout this history, digital networks have evolved from asynchronous networks to synchronous networks to optical networks.

The first digital networks were asynchronous where each network node had an internal clock to time its transmitted signal. Signals arriving and transmitting had large time variations because timing of each clock was not always synchronized. This resulted in transmission bit errors. The need for optical standards led to the formation of Synchronous Optical Network (SONET). SONET defines standardized line rates, coding schemes, bit-rate hierarchies, operations and maintenance functionality, required network elements, network architectures, and functionality for vendors to follow. This definition allowed network providers to use different vendor optical equipment with least problem of interoperability. As higher bit rates are used, physical limitation in laser sources on each signal becomes a constraint. In addition, connection to the networks through access rings has increased the requirements of different network services such as speed rates. In the light of these issues, optical networks with WDM are preferred choice to provide full end-to-end connectivity that is able to meet customer service demands and transmit at high capacity bandwidth. The standard of WDM optical networks defines the network elements and architectures; the components of the optical network are defined according to how the wavelengths are transmitted, groomed, or implemented in the network. In addition to the WDM services and SONET layers, an optical layer is required. This layer defines the requirements for non-SONET optical signals that can bypass the SONET layer and is transparent to the SONET layer in providing restoration, performance monitoring, and provision of individual wavelengths instead of electrical SONET signals.

Despite the limitations of optical networks, some important factors that are currently driving the interest and advancement of the optical network are:

(i) Continual increase of fiber bandwidth and the number of wavelengths in each fiber;

(ii) Economical restoration in the optical layer can perform faster switching protection than the electrical SONET layer;

(iii) Reduction in equipment cost by only having electrical nodes for those wavelengths that add or drop traffic at a site;

(iv) Selling wavelengths, rather than fibers by service providers to customers;

(v) Discovery and development of new enabling optical technologies like erbium-doped fiber amplifiers, dense wavelength division multiplexing, fiber bragg gratings, and semi-conductor optical amplifiers.

For further advancement of the optical technology, there are some important outstanding issues that need to be addressed, especially in the areas of traffic grooming, convergence of IP intelligence with optical networks, economic viability of optical buffer, and the invention of a specialized purpose optical processor. As there is constant increase in fiber bandwidth and not much research being carried out in grooming data traffic optically at time-slot wavelength level (see Sections 1.2.2.1 and 1.2.2.2 for more details), the objectives of this thesis are to (i) investigate the different ways of effectively and efficiently utilizing fiber bandwidth at time-slot wavelength level and mini-slot time-slot wavelength level, and (ii) carry out a performance analysis at the time-slot wavelength level.

The next two sections of this chapter present the survey that was conducted in deriving the research objectives of this thesis. Section 1.1 gives an overview of the WDM technology; Section 1.2 examines the state of research in traffic grooming.

## 1.1 Wavelength Switching and GMPLS

WDM is a method of sending many light-paths of different wavelengths down the core of an optical fiber. A typical high level WDM network is shown in Figure 1.1.

WDM is a very favorable technique to exploit the high bandwidth in the optical fiber [1]. WDM networks satisfy the growing demand for protocol transparency [2] and

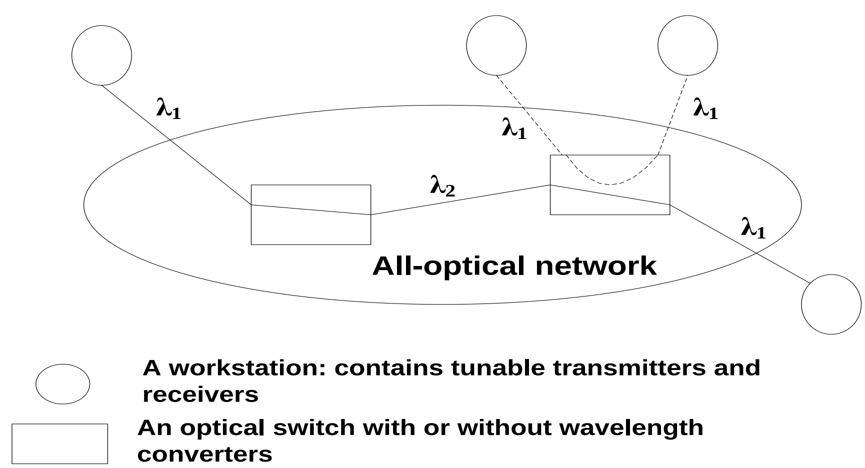


Figure 1.1: Typical WDM

have simple operations and management [3]. The MONET project using the multi-location test-bed in New Jersey has demonstrated the feasibility of deploying wide scale WDM optical networks [4]. Then there are commercial optical networking vendors like Alcatel-Lucent [5], CISCO [6], Calient Networks [7], ADVA [8], Tejas Networks [9], and others who have developed WDM network technologies. All these developments and commitments by vendors show that the WDM technology has a huge future in high speed broadband networking.

With the rapid advancement and evolution of optical technologies, it is possible to move towards an all-optical data transfer wavelength network that can take full advantage of the available fiber bandwidth. Such a network would consist of a number of optical multiplexers, optical de-multiplexers, optical switches or optical cross-connects, optical selective splitters, optical selective combiners, and high speed input/output packet synchronizers arranged in some arbitrary topologies like a mesh network with the same degree of connectivity at each node [10].

In order to establish a light-path [11], we must deal with both routing and wavelength assignment. This is known as a routing and wavelength assignment (RWA) problem. The performance of the RWA algorithm is generally measured in terms of call blocking probability. Currently, extensive research [12-19] has been carried out in RWA problem. The three main routing methods are fixed routing, adaptive routing, and alternate routing. Fixed routing is an example of static routing. In fixed routing, the route is computed and stored for later use. Hence, it has low latency in establishing the light-path. A connection request is blocked if no wavelength is available along the designated route at the time of the connection request. In alternate routing, each source destination pair is assigned a set of routes. The set is searched in a fixed [14] or arranged order [17] to find an available route for a new connection. In adaptive routing, the route is computed using an adaptive algorithm depending on the current state of the network. The algorithm is executed at the time a light-path set-up request arrives and the network nodes are required to exchange information regarding their network states. Light-path set-up time may be longer than that of fixed routing but generally adaptive algorithms improve network performance, such as having lower blocking probability. Once the routing method is decided, the next step is to determine the wavelength selection method [18]. Several common approaches have been proposed. For example, the First-fit method is to pack all the in-use wavelengths to be selected first so that wavelengths towards the end have a higher probability of being available over long continuous routes. This method saves network communication and computational time as it does not need to know the usage wavelength in real time. First-fit method is the easiest and least expensive to implement compared to adaptive methods. In an adaptive method, the wavelengths are selected based on usage – least or most used. Data is transmitted optically after the route is established and the wavelength is assigned.

Generally, three switching techniques [20] can be used to transport data optically in the WDM networks: optical packet switching (OPS), optical burst switching (OBS), and optical circuit switching (OCS). Extensive research has been conducted in the area of OPS [21-26]. The major advantage of OPS is its flexibility and efficient bandwidth usage [27]. The main disadvantage of OPS is the relatively immature techniques and technologies for optical processing of packet header [25,28-29] and optical buffering; the OPS fabric technologies today are still not able to delivery cost-effective commercial high-performance optical packet switches. In OBS, data is switched all-optically at the burst level, and only a few control channels go through O-E-O conversion. Different OBS architecture and protocols are studied in [30] and [31-34] respectively; OBS takes advantage of both the huge capacities in fiber for switching and transmission, and the sophisticated processing capability in electronics. Several issues need to be addressed before OBS can be deployed such as the offset time between the control packet and data burst, how to resolve resource conflicts without optical buffering, and optical burst switch architecture. Currently, there are still no commercial OBS networks. Lastly, OCS is a mature technology which is currently employed in the commercial WDM networks. It works in the same way as electronic circuit switching except that data is transferred optically. However, OCS requires longer set-up time [29].

Generalized Multi-protocol Label Switching (GMPLS) is becoming an integral part of optical networking and supports WDM technology [35-36]. GMPLS provides control and management for the WDM technology. It incorporates (i) Open-Shortest Path First (OSPF) [37] or Intermediate System-Intermediate System [38] protocols to exchange resource availability information for path computation, (ii) Resource Reservation Protocol (RSVP) [39-40] or Label Distribution Protocol [41] for path establishment process, (iii) Link Management Protocol to manage links in the control plane [42], and (iv) Multiprotocol Label Switching (MPLS) to forward data based on a label. MPLS control plane has been extended to recognize packets, time slot, and lambdas [43-45] in GMPLS. GMPLS control plane is used for session establishment once the route is calculated, and data plane is used to forward data once the route is connected. The separation of the control channel and the data channel in GMPLS optical switching provides two main advantages over the sharing of channels by the routing and signaling protocol in electronic switching. The two advantages are to reduce technical complexities and failure risks. The current RSVP used in GMPLS unfortunately does not deal with further reservation of time-slots within a wavelength and mini-slots within a time-slot. It only handles the reservation of wavelengths which typically represents multiple gigabits per second. Hence, there is a concern of efficiency of bandwidth utilization here. However, since OCS is used in commercial WDM network and circuit switching protocol is well established, no further development of protocol is necessary in our research for path establishment.

As the number of wavelengths per fiber increases, and each wavelength operates at the rate of 10Gbps or higher, it is important to better utilize this huge bandwidth per wavelength in a WDM network which has many lambda of wavelength. Assuming that each connection request is only one wavelength ($\lambda$ or $W$), the maximum number of connections for each fiber is $w$ if there are $\lambda_1\lambda_2...\lambda_w$ in a fiber. If a connection request is in the range of Mbps, an entire wavelength which typically represents a multiple gigabits per second will be allocated. This causes a tremendous wastage of bandwidth in a fiber for data transmission. Thus, there is a great need for traffic grooming.

## 1.2 Traffic Grooming

Traffic grooming is defined as a procedure of efficiently multiplexing/de-multiplexing and switching low-speed traffic streams onto/from high-capacity lightpaths [46]. In a situation of efficient traffic grooming, the fiber bandwidth utilization is improved. Thus, bandwidth wastage in a fiber is reduced. This leads to more successful connections and lower blocking probability. The three main types of traffic grooming methods are traffic grooming in OCS, OBS, and OPS. Since traffic grooming in OCS is the focus of our research, we shall discuss two main types of OCS traffic grooming methods which are waveband switching and time-slot wavelength switching in more details in the next two subsections. Readers can find out details of OBS and OPS traffic grooming from [47-48] and [49].

### 1.2.1 Waveband Switching

Waveband switching is to group several wavelengths together as a band and switch the band using one or more ports [50]. [51-52] present a two-layer optical cross-connect (OXC) architecture with a two-stage multiplexing and de-multiplexing scheme. The size of the OXC can be reduced using waveband switching [53]. Waveband switching also provides traffic grooming [50] at the coarse granularity and introduces two overhead layers when compared with the wavelength switching. The two overhead layers are waveband cross-connect layer and fiber cross-connect layer. Figure 1.2 illustrates these two additional layers in a hierarchical OXC switch. Furthermore, waveband switching introduces additional complexities in routing. The two common routing models for waveband switching are integrated routing and separate routing [54]. The hop-by-hop routing scheme or centralized routing scheme can be used in the two routing models. The integrated-routing model computes routes for both wavelength and waveband routes, whereas the separate routing model computes the wavelength and waveband routes separately. Electrical TDM switching can be integrated into the all-optical waveband architecture to provide Optical-Electrical-Optical (O-E-O) TDM switching [55]. This adds complexity to the already complex architecture, and the processing of electrical TDM switching is slow.

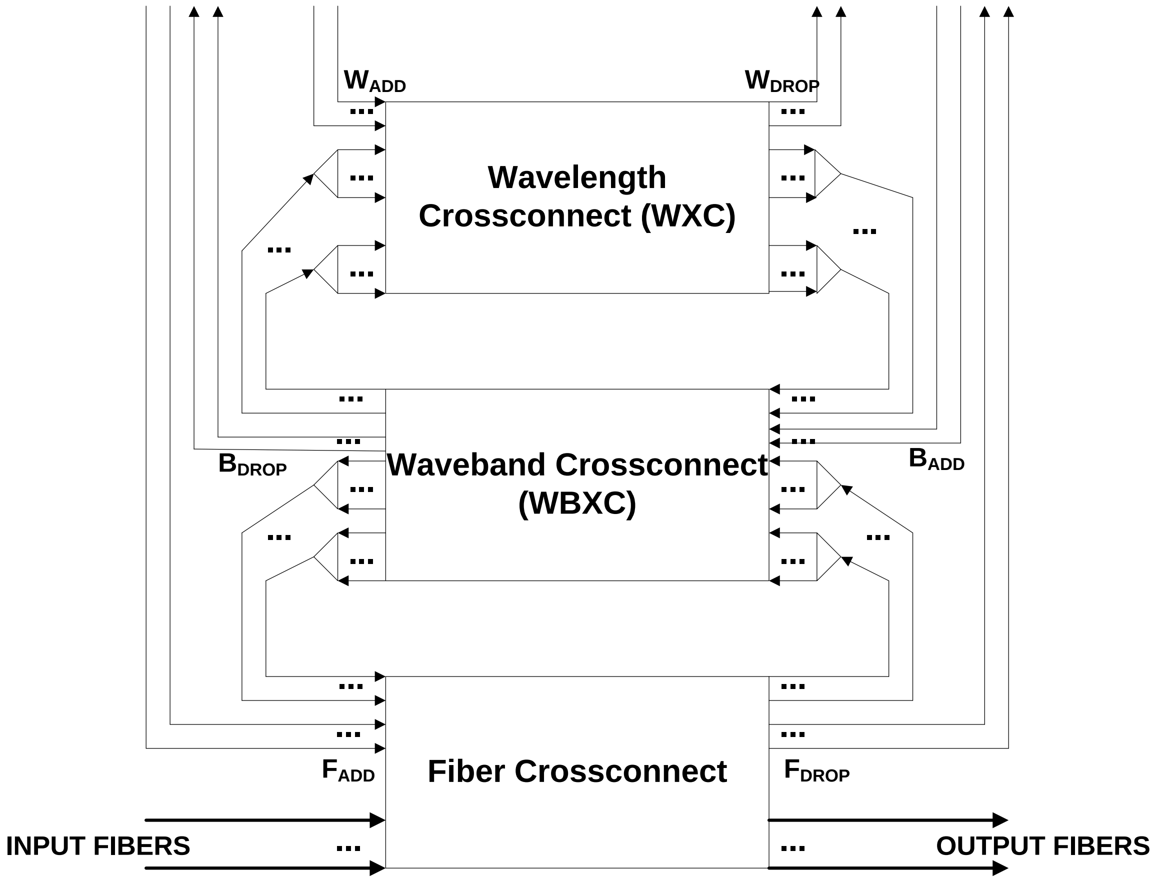


Figure 1.2: Overview hierarchical OXC architecture

### 1.2.2 Time-Slot Wavelength Switching

Time-slot wavelength switching is to aggregate lower rate traffic at the time-slot level into a wavelength in order to improve bandwidth utilization. This technique provides traffic grooming at finer granularity. This technique does not have the two overhead layers in waveband switching and the complexity of waveband routing. Hence, the complexity of the switch architecture is reduced.

In the earlier traffic-grooming research, most of the work focused on network design and optimization for SONET/WDM ring networks [56-63]. By employing wavelength add-drop multiplexers (W-ADMs), efficient wavelength assignment, and time-slot assignment algorithms have been designed for SONET/WDM ring network such that all traffic requests can be accommodated and at the same time, thus minimizing the network cost. Network cost is mostly dominated by SONET components like

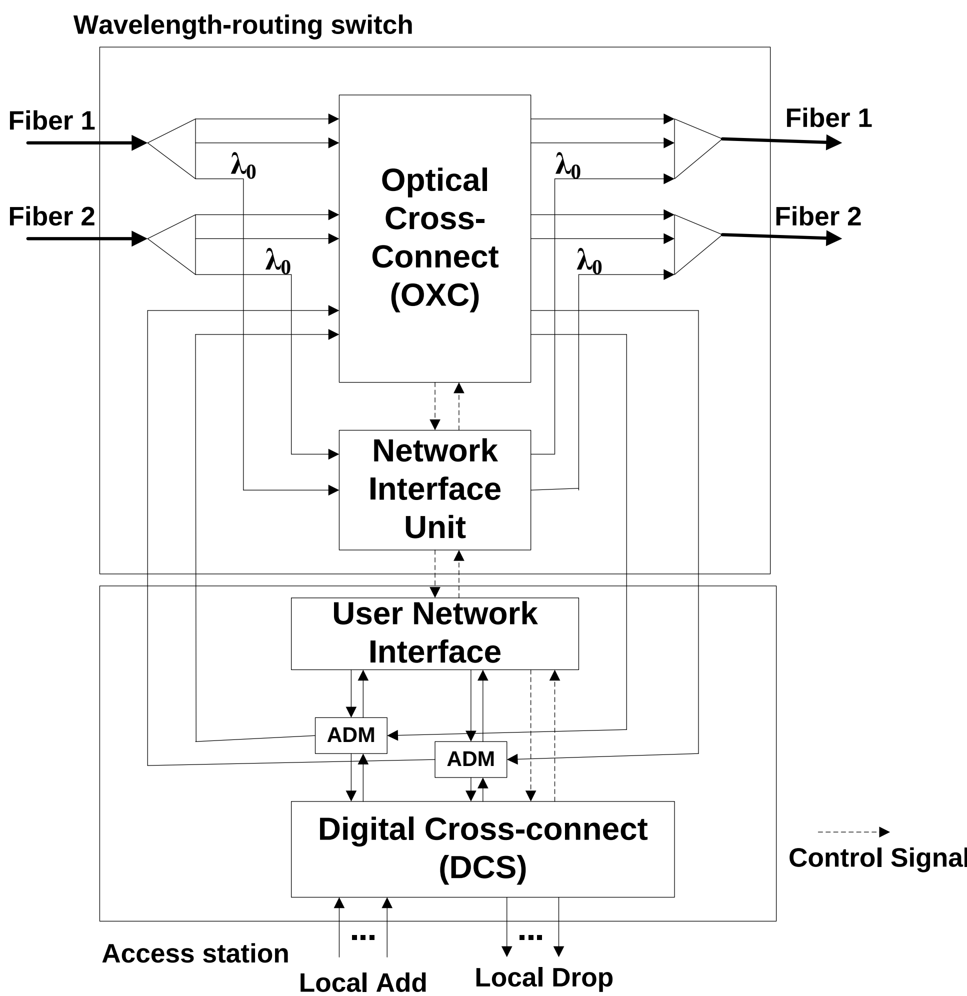


Figure 1.3: Node architecture of SONET in WDM

electrical SONET add-drop multiplexers (SONET-ADMs) and digital cross-connect (DCS). Figure 1.3 presents the architecture of a node using SONET in WDM. The disadvantage of using this approach is the high cost of SONET-ADMs and DCSs.

In recent years, optical transport networks have evolved from interconnected SONET/WDM ring networks to mesh-based optical WDM networks. The use of W-ADMs can be used for through traffic without terminating them in SONET equipment. This reduces the number of SONET ADMs needed in the network and thus helps to reduce the overall network cost significantly. Moreover, the WDM mesh network provides more bandwidth, easy expansion in core networks, and alternate paths to destination nodes. Since there is continual increase of fiber bandwidth, increasing the number of wavelengths in each fiber and ineffective bandwidth utilization in each wavelength, research efforts [64-73] are being conducted on different aspects of traffic-grooming problem in optical WDM mesh networks. In this thesis, we investigate traffic grooming at the time-slot wavelength level, its architectural requirements and study the performance of our proposed methods using both simulation and analytical techniques.

#### 1.2.2.1 TDM WDM Network Aspect

[74-75] propose many different types of grooming architectures. The multi-hop partial grooming OXC architecture provides all-optical or electronic wavelength switch and an electronic grooming fabric that can switch low-speed traffic streams. A multi-hop full-grooming OXC architecture is built for switching with electronic optical conversion technology. Data in a time-slot can be electrically switched from one time-slot of a

wavelength to another time-slot of a different wavelength at every intermediate node which it traverses.

[76] studies the problem of scheduling multi-rate connections in TDM wavelength-routing networks supporting multi-rate circuit-switched sessions. [77] studies the problem of routing, wavelength, and time-slot-assignment in wavelength routed TDM/WDM optical networks with the goal of maximizing throughput in the network. [78] studies the switch reconfiguration capability in TDM wavelength routing networks. [79] maximizes the performance of optical TDM networks with a small number of optical buffers. [80] proposes an optical architecture that is able to transmit data optically at the time-slot wavelength level without using OTSI and WC. [81] proposes the time-domain wavelength interleaved network (TWIN) which requires complex scheduling algorithm to deal with substantial delays arising from propagation of signals across the network, and burst traffic collision at the core node [82].

[74-75] proposed the use of electronic TSI to interchange time-slots. [76-82] assigned one or more time-slots for each connection request, and each time-slot is not shared. Our scheme, however, allows a time-slot to be shared by one or more successful connections of different speed in a TDM wavelength optical network with OTSIs and we studied the behavior of this type of network because no such work is published in the literature. An OTSI works the same way as the well known electronic TSI [83] except that data is switched optically. The data is optically transferred, and all the connections going to the same destination share the same time-slot from the source router to the destination router. In order to eliminate the problem of complex scheduling algorithm and burst traffic collision, the OCS is used. Each node in this network which employs least-

cost routing method is assumed to use the OSPF of GMPLS to exchange information for path computation.

We also proposed the mini-slot TDM wavelength optical network, where each time-slot is further divided into mini-slots so that we can compare the performance of this network with the shared time-slot TDM wavelength optical WDM network. The behavior of this network is also studied through extensive simulations.

In addition, we considered the viability of the proposed shared time-slot TDM wavelength optical WDM network and mini-slot TDM wavelength optical network from the availability of optical components prospective. A survey on related optical components is carried out and the total cost of implementation is estimated. The following briefly describe our findings:

- Optical switches can be constructed using Microelectromechanical Systems [84] technology, thermo-optical technology [85], opto-mechanical switches technology, liquid crystals technology, thermo-optic switches technology, and other known technologies. Currently, wavelength optical switches are widely available in the optical networking industry. In addition, wavelength multiplexers and de-multiplexers, fiber optical cables, optical selective splitters, and optical selective combiners are also commercially available. Optical add-drop multiplexers for optical TDM [86] and de-multiplexing of optical TDM stream have been shown to be feasible [87]. Upgradeable TDM wavelength optical switches are commercially available [5]. The use of fiber delay lines (FDLs) in an OTSI has been proposed in [88-89]. Design and simulation study on OTSIs producing encouraging results can be found in [90]. An OTSI has been demonstrated to be feasible in [91]. All these development can help to make OTSI commercially available in the near future. Optical input/output packet synchronizers were demonstrated in the KEOPS project [92] and experimented in [93]. These developments of optical components enhance the view that our proposed network, shared time-slot TDM wavelength optical WDM network is possible to be implemented in the near future.

- The main optical components of mini-slot TDM wavelength optical network are optical switches, wavelength multiplexers, wavelength de-multiplexers, fiber optical cables, faster optical splitters and optical combiners, TDM multiplexers and de-multiplexers, optical mini-slot interchangers (OMSIs), and faster optical input/output packet synchronizers. An OMSI works in the same way as the well known electronic TSI [83] except that data is switched optically in a mini-slot. The current state of optical components from optical switches to TDM multiplexers and de-multiplexers is explained in the previous paragraph. In chapter 3, we show that OMSIs and optical input/output synchronizers for mini-slot streams are feasible. Chapter 3 also explains in more detail the working operations of our mini-slot TDM wavelength optical network with the current state of optical technologies.

We present in the following the proposed cost model that is used to calculate the implementation cost. Our WDM network set-up cost model consists of link provisioning cost ($C_{lp}$), mux-demux cost ($C_{mux\text{-}demux}$), trans-recv cost ($C_{trans\text{-}recv}$), and cross-connect cost ($C_{cc}$). The set-up costs of our proposed networks are respectively calculated from an extended WDM network set-up cost model from [94]. The operational cost is the cost of operating the network and is not considered in our model. The maintenance cost is the cost of maintaining the network. Normally, the maintenance cost is 15% to 20% of the equipment cost. Thus, the total cost of each of our proposed network equal to network set-up cost plus network maintenance cost. The more detailed derivation of the set-up costs is explained in section 4.1. The maintenance cost of a node is assumed to be 15% of the cost of each node. Section 4.1 also analyzes the current and future WDM network and our proposed network total costs. In summary, the additional costs of a shared time-slot TDM wavelength optical WDM node when compared with the WDM node are the costs of OTSIs, input/output synchronizers, optical splitters/combiners, and Gigabit Ethernet cards, and difference in maintenance cost of each node. Similarly, the additional costs of a mini-slot TDM wavelength optical node when compared with the WDM node are the costs of OMSIs, input/output synchronizers for mini-slot streams, optical splitters/combiners for mini-slot streams, optical TDM multiplexers/de-multiplexers, and difference in maintenance cost of each node. In general, the implementation cost of the WDM node and the shared time-slot TDM wavelength optical WDM node is much lesser than the mini-slot TDM wavelength optical node. The reason is the mini-slot TDM wavelength optical node requires many more optical components.

#### 1.2.2.2 Analytical Model Aspect

It is very difficult to develop a mathematical model for performance analysis of shared time-slot TDM wavelength optical WDM networks due to the complexity in scheduling of time-slots. Instead, we propose an analytical model for time-slot wavelength network without sharing of time-slot. We use the analytical results to validate the corresponding simulation model developed for the network; the simulation model is subsequently used as a base for further simulation studies of related schemes.

There exists analytical models of WDM networks but they differ in their underlying assumptions, and have varying computation complexities and levels of accuracy. [95-99] present analytical models with limited wavelength conversion. [100-102] analyze the blocking performances of networks with no wavelength conversion and full wavelength conversion at each node. [103] focuses on success probability using wavelength converters in a network. The generalized reduced load approximation scheme for circuit-switched networks is first investigated in [104] and further developed by [105]. [106] extends the method in [105] to wavelength routing model for fixed routing and without WC. The main approach used in [106] for fixed routing is the Markov chain model with state dependent arrival rates. This paper reports the upper bound of the approximate probabilities in WDM without WC. The idea given in [106] is extended by [107] to derive an analytical expression to compute the blocking probability of networks with limited-range wavelength conversion for fixed routing. The approach used in [107] is also similar to the Markov chain model with state dependent arrival rates of [106]. However, the incoming wavelength can be converted to $x$ adjacent outgoing wavelengths, where $x$ is the degree of conversion. Let $\Pr(m_1,m_2)$ be defined as the probability of no common free wavelengths on links one and two. In [107], $\Pr(m_1,m_2)$ is obtained using a bipartite graph ($X$,$Y$), where the set of vertices $X$ and $Y$ represents the set of wavelengths available on the first and second links respectively. [108] extends the analysis of [102] to examine the blocking probabilities of a shared-wavelength TDM network with and without WC. The network blocking probabilities is obtained by solving the set of coupled nonlinear equations called Erlang's map. The independent link load assumption scheme is used in [108]. [109] shows less accuracy in one time-slot method using partitions of 0 slots free, 1 slot free, and >= 2 slots free. The reduced load model is not used in [109]. [110] presents a generalized framework for analyzing time-space switched optical networks. This paper uses a *z*-link path model where the first hop has *z*-l links and second hop consists of the last two links. Hence, the number of trunks free on the last link of the first hop is seen by the node *z* in the second hop. In this model, if the destination is not considered as the last node in a path, a four link path can be viewed as the first hop consisting of two links and the second hop consisting of the last link of the first hop and the third link. The Markovian correlation is assumed because the numbers of trunks free on the last link depends on the number of trunks free on the previous link. The authors of [110] do not show the accuracy of their model.

Using the partition based method, we extend the idea in [106] to propose an analytical model for TDM WDM network with OTSIs and without WC. We use the dependent link load assumption and the reduced load algorithm. Our partition based method does not use the z-link model and Markovian correlation assumption. We show the accuracy of the simulated results using the minimum fixed hop routing.

The next section describes the main contributions of our research.

## 1.3 Contributions and Organization of This Thesis

The key contributions of this thesis are:

(i) Proposed the shared time-slot wavelength router architecture with OTSIs and mini-slot router architecture heir corresponding traffic grooming schemes – time-slot TDM wavelength optical WDM and mini-slots TDM wavelength optical WDM. To our best of knowledge, this is the first attempt at demonstrating, via simulation, the technical feasibility of the mini-slot traffic grooming scheme. We show that an optical architecture that is capable of performing traffic grooming of both time-slots and mini-slots is feasible;

(ii) Demonstrated the behavior and effectiveness of our shared time-slot TDM wavelength optical WDM network and mini-slot TDM wavelength optical network through extensive simulations. Our shared time-slot TDM wavelength optical WDM network has the lowest blocking probability when compared with the traditional wavelength optical network without WC and conventional TDM WDM optical network. It is shown by simulation that the least cost routing method with at least a free time-slot [refer to pages 34 and 35] in a fiber link gives slight improvements in blocking probability when compared with the typical least cost method. Through extensive simulations, the effectiveness of fiber bandwidth utilization at the mini-slot level is demonstrated;

(iii) Evaluated the feasibility of realizing the shared time-slot TDM wavelength optical WDM network and mini-slot TDM wavelength optical network from the perspectives of the availability of optical components and the cost of implementation. The proposed network schemes are found to be feasible.

(iv) Proposed a partition based model for the analysis of the average network blocking probabilities in TDM wavelength optical network with OTSIs and without WC. To aid the analysis, we propose a schema that works for any number of partition patterns, regardless of the numbers of links, wavelengths in each link and time-slots in each wavelength. Our analytical model provides good accuracies when compared with the simulation results. Since the results of our model are shown to be close to the simulated results, network designers can use our model to predict the blocking probabilities of similar networks.

The rest of this thesis is organized as follows: Chapter 2 presents a shared time-slot TDM wavelength optical WDM network. Chapter 3 presents a mini-slot TDM wavelength optical WDM network. Chapter 4 compares the cost of the proposed networks and a conventional WDM network and highlights the future optical trends. Chapter 5 describes the initial study of an optical architecture that can perform traffic grooming with flexibilities of swapping mini-slots (channels) and time-slots of the same wavelengths of the same fiber at intermediate destinations. Chapter 6 presents the use of the partition approach to calculate the approximate blocking probabilities of the TDM wavelength optical network with OTSIs and without WC. Chapter 7 summarizes the key results, identifies possible future work, and concludes this thesis.

# CHAPTER 2

# Shared Time-slot TDM Wavelength Optical WDM Network[1]

WDM is a promising technology to accommodate the explosive growth in Internet and telecommunication traffic. Previous projects like the AON [111] and ACTS [112] have demonstrated that wavelength optical networks are feasible. A typical wavelength routed network consists of interconnected wavelength routers (Figure 2.1). The wavelength router is responsible for multiplexing and de-multiplexing wavelengths so that wavelengths at incoming ports can be routed to the desired output ports. Currently, WDM technology is widely employed in the backbone network. Recent advances in WDM technology have generated multiple magnitudes of raw bandwidth. Consequently, each wavelength typically operates at hundreds of Mbps or Gbps currently.

The wavelength bandwidth allocation problem has been investigated in [113]. However the proposed solutions do not tackle the issue of bandwidth wastage in each wavelength of the wavelength routed networks. To handle this issue, the TDM wavelength routed networks with scheduling of multi-rate connections has been proposed [76]. In each TDM frame, the number of time-slots is fixed. Each routing node behaves like a traditional TDM circuit switching node. Thus, the time-slots are pre-assigned during connection set-up. The main function of the routing node is to connect incoming

---

[1] A large part of this chapter appears in Journal of Optical Networking, "Framework for Shared Time-Slot TDM Wavelength Optical WDM Networks," Special Issue – Convergence, 2006. Printed by Optical Society of America (OSA). Also, a part of this chapter has been presented in 13th IEEE International Conference on Networks (ICON), "A Shared Time-Slot Router Architecture for TDM Wavelength Optical WDM Networks," Kuala Lumpur, Malaysia, 16th-18th Nov. 2005.

data in each time-slot into the desired output port, and the data transmission is all-optical. Hence, the bandwidth of each wavelength is more efficiently utilized, and the bottleneck of electronic data processing at the time-slot level is avoided.

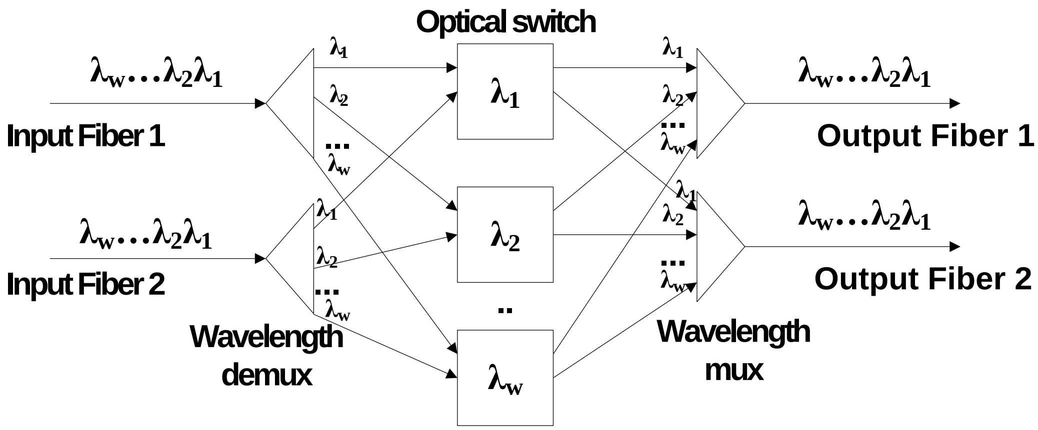


Figure 2.1: High level architecture of a wavelength router

[77,80-81,92,111] study the different aspects of TDM wavelength network. [111] shows that WDM tunable transceivers and a non-configurable wavelength router are feasible in a TDM wavelength routing network. [92] demonstrates that data packet encapsulated in a time-slot can be optically transferred. [77] studies the TDM wavelength routing network using TDM slots only. The goal of [77] is to maximize the overall network throughput. As expected, the network throughput increase causes the blocking probability to decrease. Gains in network throughput are seen to improve with the increase of number of fibers per link. The First-fit free time-slot and least loaded time-slot algorithms are also proposed in [77]. On the other hand, [81] proposes the time-domain wavelength interleaved networks (TWIN) to study the burst traffic collision [82] of time-slots at the core network. An example of such time-slots collision is shown in Figure 2.2. In this example, data sources A and B that arrived at port 1 and port 2 respectively, are contending for the same time-slot in wavelength $\lambda_z$ on the bursts at port 3.

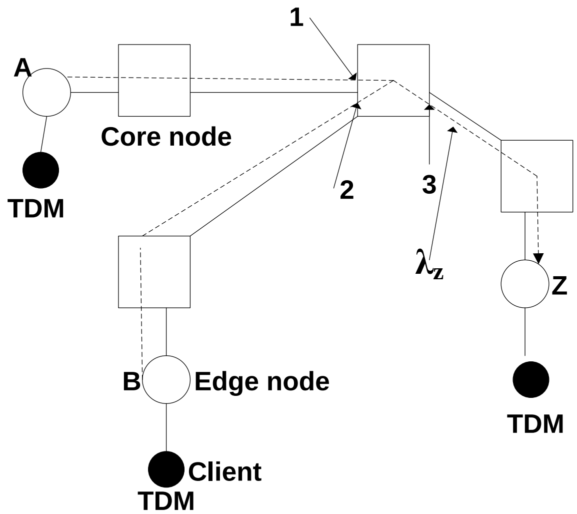


Figure 2.2: TWIN architecture of clients and core nodes

To prevent such burst collision, coordination between sources A and B is required. As a result, TWIN relies on complex scheduling algorithms to prevent such collisions; for example, the re-computation of schedule is carried out at the scheduler in each repetitive scheduling cycle. The distributed scheduling scheme [82] is better than a centralized network scheduler because the centralized network scheduler gives a slower response to traffic demand [114]. Furthermore, the distributed scheduling scheme allows independent scheduling and assigns time-slots for each node in the network as requests arrive. Then, [80] proposes a TDM wavelength routing architecture and studies its behavior by simulation. However, there are no OTSIs used at intermediate routers, and the connection requests are for at least one time-slot. All these [76-77,80-81,92, 111] do not address the sharing of a time-slot by many low speed connections in the TDM network.

In this chapter, we propose a network, shared time-slot TDM wavelength optical WDM network, which allows sharing of a time-slot by low speed connections like 10Mbps Ethernet. We also propose a shared time-slot wavelength router (STSWR), which is equipped with OTSIs. Each STSWR determines the route, the wavelength and the time-slot in the TDM frame for any connection to the network. In this network, all the successful connections going to the same destination router from the source router share the same time-slot. In order to avoid complex scheduling algorithms and time-slot contention at intermediate routers, the time-slots in our network are pre-assigned at each node using the OCS protocol. The implementation of the OCS protocol is similar to the mini-slot TDM optical network (see Section 3.2) except that the OCS protocol in our shared time-slot TDM wavelength optical WDM network allows the sharing of a time-slot in existing connections.

Next, we wish to illustrate the advantage of our shared time-slot scheme in effective bandwidth utilization when compared with a typical wavelength routed network using a very simple example (Figure 2.3). Assume that a connection from local workstation *b* to local workstation *c* is allocated time-slot 3 of $\lambda_1$ from STSWR 1 to STSWR 2. From STSWR 2 to STSWR 3, this connection is allocated time-slot 4 of $\lambda_1$. Another connection from local workstation *a* to local workstation *d* is sharing time-slot 3 of $\lambda_1$ from STSWR 1 to STSWR 2, and time-slot 4 of $\lambda_1$ from STSWR 2 to STSWR 3 with the first connection. In this example, the time-slot is interchanged at STSWR 2. Thus, two connections with unexpired connection durations that originate from the same STSWR and traveling along the same route to the destination STSWR share a time-slot from STSWR1 to STSWR 2 and another time-slot from STSWR2 to STSWR 3. Even if one of the connection durations has expired, the assigned time-slots for the route are not released until the last connection duration has expired. In comparison a typical wavelength routed network requires two wavelengths for these connections (Figure 2.1). Hence, there is a tremendous wastage of fiber bandwidth if the connection requests are for low speed connections.

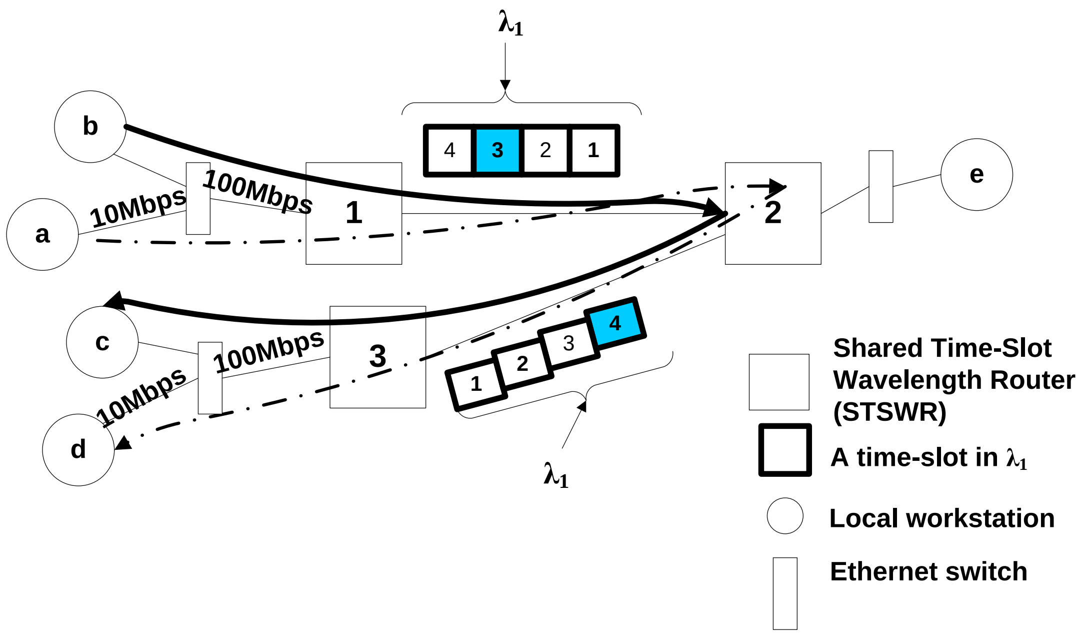


Figure 2.3: Conceptual diagram of the proposed shared time-slot wavelength optical data transport network

The rest of this chapter is organized as follows. In section 2.1, the network operations and STSWR architecture of the shared time-slot TDM wavelength optical WDM network are explained. In section 2.2, the algorithm for time-slot sharing at the source STSWR is presented. In section 2.3, the routing algorithms to study the behavior of the shared time-slot TDM wavelength optical WDM network are explained. The algorithm for time-slot sharing presented in section 2.2, and the routing algorithms explained in section 2.3 are used in our simulation study. In section 2.4, the simulated results are analyzed. In section 2.5, the shared time-slot TDM wavelength optical WDM network is extended to include the slot-by-slot fast WCs (SSWCs) in the STSWR architecture. In section 2.6, the main points of this chapter are summarized.

## 2.1 Network Operations and Router Architecture

To illustrate the workings of our proposed network, we assume that the low speed connections to each STSWR (Figure 2.4) are 10Mbps switched Ethernet connections, and they are connected to a 100Mbps Ethernet switch. This switch is connected to one of the local access controller unit (LACU) ports in an STSWR. Each LACU port can either be 100Mbps, 1Gbps or 10Gbps Ethernet interface. The Ethernet frame format and maximum size for each frame are the same for 10Mbps, 100Mbps, 1Gbps, and 10Gbps Ethernet. A higher speed interface port allows connection to a hierarchical star topology. Flooding of Ethernet frames can be easily contained within the domain of one hierarchical star topology because the OCS is employed in the network, and the data in each Ethernet frame is encapsulated in a pre-assigned time-slot. Thus, the problem of scaling Ethernet [115] does not occur.

According to the IEEE 802.3 frame format (Figure 2.5) [116], the maximum payload size is 1500 bytes for each Ethernet frame, which partly consists of the source station address and destination station address fields. Route computation is performed at each STSWR using the valid Internet Protocol (IP) address in the received Ethernet frame. The OSPF protocol of GMPLS is used by the STSWRs to exchange information about the network topology. The system is configured such that each STSWR is a default gateway for each local workstation that needs to access the LACU port, and the ARP procedure is assumed to be completed from the local workstation to the LACU port.

Upon receiving the Ethernet frame, the LACU removes the preamble and start of frame delimiter bits. The size of each Ethernet data frame is assumed to be 1518 bytes, excluding preamble and start of frame delimiter bits for 10Mbps and 100Mbps switched Ethernet. A 100Mbps switched Ethernet transmits 10 times more data frames per second

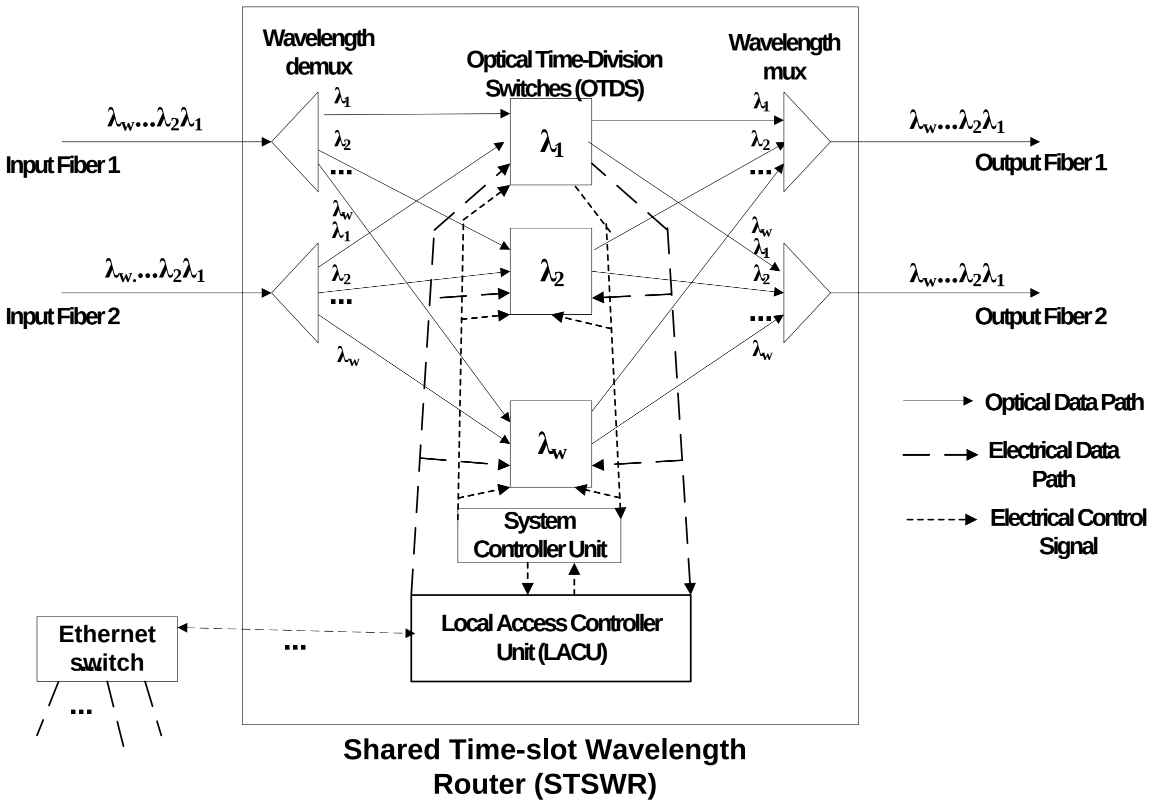


Figure 2.4: High level architecture of *2 x 2* STSWR

| | | | | | 46 to 1500 octets | | |
|---|---|---|---|---|---|---|---|
| 7 octets | 1 | 6 | 6 | 2 | >= 0 | >= 0 | 4 |
| Preamble | SFD | Destination Address | Source Address | Length | Data supplied by LLC | PAD | Frame Check Sequence |

Figure 2.5: IEEE 802.3 frame format

than a 10Mbps switched Ethernet. The destination station address field in the Ethernet frame contains the media access control (MAC) address of the LACU port in each STSWR. For a new connection request, the LACU communicates with the system controller unit for route computation using the destination IP address encapsulated in the Ethernet frame. Once the route is computed, a time-slot of a wavelength is assigned hop-by-hop along the computed route. When successfully completed, data is forwarded hop-by-hop along the route via the respective time-slot of each hop to the correct destination's local access buffer unit (LABU).

The LACU forwards the data in its electronic buffer to the electronic buffer of the correct LABU (Figure 2.6). An E/O conversion is later performed in the LABU so that data can be optically sent in the time-slot of a wavelength. The data in each Ethernet frame is encapsulated in each time-slot of a wavelength. Assume each TDM frame is transmitted at every 125μs, and each time-slot is capable of transmitting at 100Mbps. The intermediate STSWR forwards the time-slot of a wavelength to an adjacent STSWR based on the pre-assigned time-slot in a wavelength. Each intermediate STSWR does not perform any E/O and O/E when transferring data at the time-slot level. The bandwidth of each wavelength is divided into fixed-length time-slots and accessed via slot-based cyclic TDM mode. At the destination STSWR, an O/E conversion is performed on the time-slot of a wavelength. The relevant electronic data is stored in the buffer of LABU for later forwarding to the Ethernet switch through the LACU. Based on the destination IP address, the destination local workstation MAC address is determined and inserted into the destination station address field at the LACU. The MAC address of the LACU port is inserted into the source station address field. The LACU inserts the preamble and start of frame delimiter bits before forwarding the data to the Ethernet switch. Upon receiving the Ethernet frame, the Ethernet switch forwards it to the correct local workstation.

The architecture of a *2 x 2* STSWR is presented in Figure 2.4. The idea of this architecture is taken from [80] and can easily be expanded into a *W x W* STSWR if there are *W* input fibers and *W* output fibers [80]. At each input port, a wavelength de-multiplexer is used to separate the *w* wavelengths into *w* individual optical lines. The routing of incoming time-slots is carried out in a *2 x 2* optical time-slot switches (OTDS), where the same wavelength, for example, $\lambda_1$ is concentrated. Each output port of the OTDS is connected to a different *W x 1* wavelength multiplexer. Thus, a *W x W* STSWR, which has *W* outputs of the OTDS, is connected to *W W x 1* wavelength multiplexers respectively. The optical signals are combined in the wavelength multiplexer and passed to the correct output port. The intermediate STSWR does not perform any O/E for the time-slot that passes through it. This makes an all-optical data path. In order to ensure the input-ports and output-ports of each OTDS are connected according to the assigned time-slots, this connectivity information is stored after the time-slots and routes are computed. The control signals at each time-slot are generated by the electronic system controller unit using the stored information. This unit also performs tracking and calibration of the local timing signal for packet synchronization. In addition, the access of LACU and LABU is controlled by this unit. In order to access the STSWR, the local workstations need to interface with the LACU (Figure 2.4). The LACU not only handles the requests from these stations to establish light-paths, but also Ethernet data frames from or to the local workstations. According to the established light-paths, the LACU communicates with the LABU of the correct OTDS to retrieve or store the data in its buffer.

Figure 2.6 illustrates the *2 x 2* architecture of OTDS for $\lambda_1$. If there are *W* inputs and *W* outputs, the OTDS architecture is *W x W*. The main function of the OTDS is to make sure that time-slots are interchanged appropriately in an OTSI for each wavelength of a port. The architecture of the input and output packet synchronizers and the experimentation on them are presented in [92]. The data that are stored in each time-slot excluding its synchronization bits can be referred to as a packet. The packets should be transmitted as slotted time-slot streams as illustrated in Figure 2.7. Each time-slot is separated by a guard band. Guard bands between time-slots and increase in the slot duration are used to lessen the effects of slow system reconfiguration [117]. The optical input synchronizer, which is controlled by the system controller unit, synchronizes each time-slot in the OTDS to the local timer before entering the optical time-slot switches (OTSSs). The optical selective splitter (OSS) is controlled by the system controller unit, and it is used to select the data to the LABU or input to the correct OTSI in the OTSSs, where time-slot switching takes place. The FDLs are built in an OTSI to accommodate the simultaneous incoming time-slots that contain data; OTSI provides the flexibility of inter-changing time-slots [88-90]. In the OTSSs, the system controller unit configures the connectivity between the input ports and output ports according to the assigned time-slots. Since each connection is circuit switched, the possibility of two slots needing to be switched to the same output slot at an intermediate STSWR does not occur. It is assumed that each STSWR has fully system reconfigurable capability and is able to reconfigure after every time-slot. Due to the internal delay at the OTSI, the optical output synchronizer aligns the packets to eliminate jitter. After the alignment, the aligned packets exit the OTDS and enter the wavelength multiplexers. The time-slot to the

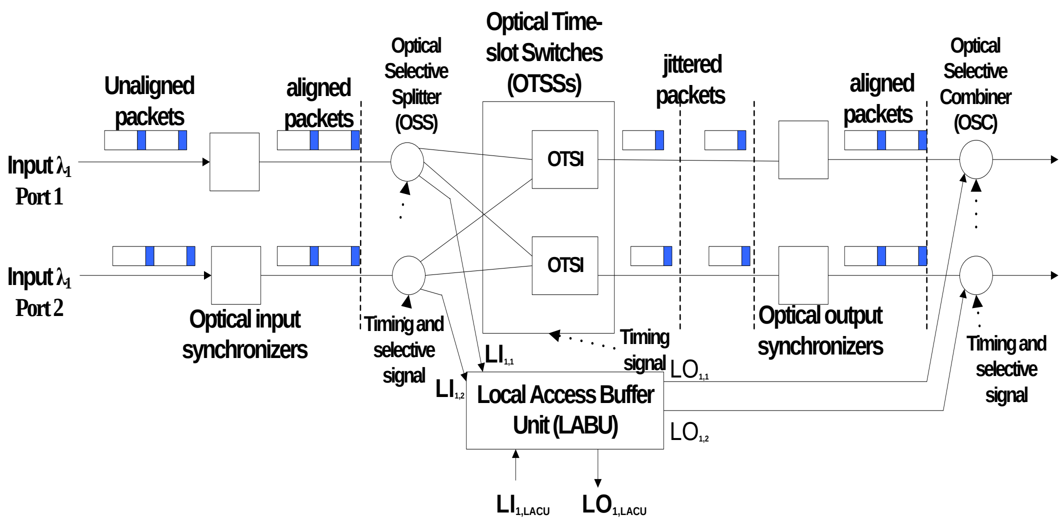


Figure 2.6: *2 x 2* architecture of OTDS $\lambda_1$

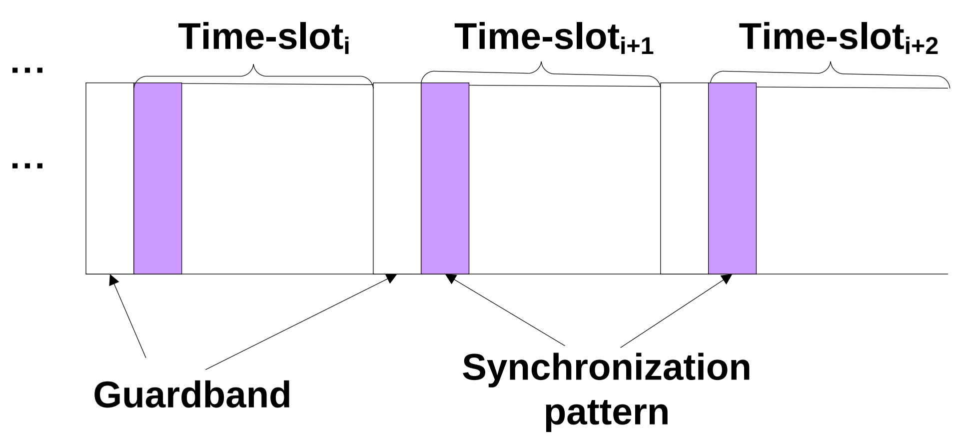


Figure 2.7: Time-slot streams

destination STSWR enters the LABU. An O/E conversion is performed on the time-slot and the relevant electronic data is stored in the buffer. The data is later forwarded to the LACU. Based on destination IP address, the destination local workstation MAC address is determined and inserted into the destination station address field at the LACU. The

MAC address of the LACU port is inserted into the source station address field. The LACU inserts the preamble and start of frame delimiter bits before forwarding the data to the Ethernet switch. The other main function of the LABU is to store outgoing data from the local workstations. Communication between the LABU and LACU is through the Port $LI_{1,LACU}$ and Port $LO_{1,LACU}$. After the E/O conversions in the LABU, the optical selective combiner (OSC), which is also controlled by the system controller unit, is used to add optical time-slots to the appropriate optical lines. The electronically controlled optical gates are used to implement the OSSs and OSCs. Materials for reducing crosstalk in switching components, multiplexers and de-multiplexers are found in [118-120].

## 2.2 Algorithm Pseudo-codes

### 2.2.1 A Shared Time-Slot Algorithm at a Source STSWR

We design a simple algorithm to determine the sharing of a time-slot for traffic with unexpired connection duration and travel along the same route from the same source STSWR to the destination STSWR. For a new route to the destination STSWR, the well-known First-Fit strategy is used for finding a free time-slot of a wavelength at each hop of the route. The maximum number of connections sharing a time-slot simultaneously at the source STSWR can be increased or decreased. This depends on the average data traffic volume, average connection duration and transmission rate of a time-slot. Assume that the minimum hop fixed routing (MHFR) strategy is used, and the connection requests are processed on a first-come-first-serve basis. At the source STSWR, the pseudo-codes of the algorithm work as follows:

Input: A new connection request from an Ethernet workstation

Output: (1) A free STSWR list is set and the first slot is used

(2) A successful connection is found

(3) Relevant information is stored for the first link of a new route

(4) A connection request is blocked because of no time-slot available in a wavelength

(5) The source and destination IP addresses are inserted into the IP-connection list

```
found=0
i=0
while (i < MAX_Wavelength && !found) do
    j=0
    while (j < MAX_Time-Slot && !found) do
        if (destination field in wavelength[i].time_slot[j] != request destination STSWR
        address)
        /* Assume Minimum Hop Fixed Routing */
            j++
        else
            if (wavelength[i].time_slot[j] list is not full)
            /* Assume maximum slot in a list is 10 */
                found=1
                Sequential search for an empty slot in wavelength[i].time_slot[j] list
                Mark the empty slot as used
                Increment successful_connection by 1
                Insert source and destination IP addresses into the IP-connection list
                /* This list is used to check for existing IP connections at the interface ports in the
                LACU */
                Add this connection request and relevant information to the simulator event list
                /* Release the connection request when the connection duration has expired */
            else
                j++
    if (!found)
        i++
if (!found)
/* A new route to the destination STSWR can be created */
    First-Fit strategy is used for finding a free time-slot of a wavelength at source STSWR
    if (found)
        /* Assume wavelength[x].time_slot[y] list is found as free */
        Relevant information is stored for the first link of a new route
```

Insert source and destination IP addresses into the IP-connection list
Insert the destination STSWR into the destination field of wavelength[x].time_slot[y] list
Mark the first slot of wavelength[x].time_slot[y] list as used
else
Connection request is blocked

### 2.2.2 An Algorithm for Releasing a Successful Connection in a Destination STSWR List

/* The connection duration of a successful connection has expired */

Input: Relevant information to release the successful connection
Output: (1) Mark occupied slot in the destination STSWR list as empty
(2) The destination STSWR list is set as not full
(3) The release of the established connection for the entire route is initiated
(4) The destination STSWR list is reused
(5) The source and destination IP addresses are deleted from the IP-connection list
/* Assume wavelength[x].time_slot[y] list */
Mark the occupied slot in wavelength[x].time_slot[y] list as empty
Set the wavelength[x].time_slot[y] list as not full
Delete source and destination IP addresses from the IP-connection list
If (released connection is the only connection in the wavelength[x].time_slot[y] list)
Mark the destination field in the wavelength[x].time_slot[y] list as empty
Initiate the release of the established connection for the entire route

## 2.3 Routing Methods

There are three routing methods used in our simulation study. The first routing method is MHFR. This method results in low blocking probability in the sense that a smaller number of hops would increase the chances of finding a free time-slot of a wavelength on all fiber links traversed by the route.

The second routing method is centralized least-cost routing (LCR) [121]. In LCR, a routing center is responsible for collecting the traffic status of each link. When a new network status update is received, the central controller performs the cost computation for all routes and distributes the least-cost paths to each switching node as a reference for route selection. Let $D^i(n^j)$ denote the cost of adding a type *i* call over link *j* at link state *n*. A route cost $D_R^i$ is then computed by $D_R^i = \sum_{j \in R} D^i(n^j)$. The least cost route, $R_{\min}$ is the one that has the minimum cost. Thus, $D_{R_{\min}}^i = R \in \overset{Min}{P}(s,d)\{D_R^i\}$, where $P(s,d)$ is the set of all the alternate routes from source *s* to destination *d*. We assume that the total fiber link capacity (TFC) between two nodes to be the fixed number of time-slots in a wavelength multiplied by the number of wavelengths in a fiber. The cost of each fiber link increases as the total number of free time-slots in a fiber decreases. For each fiber link, the cost is computed by using the simple formula of total number of used time-slots (TTU) divided by total fiber link capacity which is $\frac{TTU}{TFC}$.

The third routing method is least-cost routing method with at least a free time-slot in a fiber link (LCR-FTL). A route is not selected if there is no available time-slot of a wavelength in a fiber link between two nodes. Using the current connected traffic distribution shown in Figure 2.8, a very simple example is used to illustrate the advantage of LCR-FTL. Assume that each fiber link has two wavelengths, and each wavelength consists of eight time-slots. Suppose a connection request comes from node A to node E. The LCR method selects route ABE based on previous discussions. However, this route is blocked because there is no free time-slot in the fiber link between node A and node B. The LCR-FTL method selects an unblocked route ACE with at least a free time-slot in the fiber link between two nodes. It should be noted that some routes selected by all three methods (MHFR, LCR, LCR-FTL) are identical. As for LCR and LCR-FTL, the route selected may not be the minimum hop route.

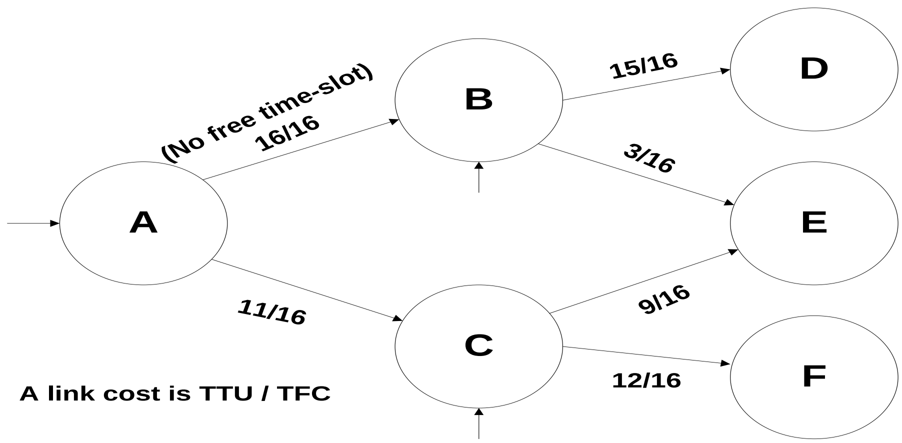


Figure 2.8: Example of current connected traffic distribution

## 2.4 Simulation and Result Discussion

Simulation conducted in this study is done using Optimum Network Performance (OPNET) based on the well-known NSFNET (14 nodes, 21 links) topology shown in Figure 2.9. Each node is an STSWR. The dedicated connection from each local workstation to the Ethernet switch is 10Mbps. The connection from the Ethernet switch to the LACU port is 100Mbps. Connection requests at a local workstation are generated independently from other local workstations according to a Poisson distribution [122] of arrival rate. Let $T_b$ denote the sum of blocked connections in the network G and $T_c$ denote the sum of all connection requests generated into the network G. Then the blocking probability in the network G is $\frac{T_b}{T_c}$. All blocked connections are terminated and never return. There is no queuing of blocked connections for retransmissions. These two assumptions relate to a real-life network environment where we need to request for a new connection if the previous request is blocked by the network. The first 1000 connection requests in each simulation run are deleted to obtain a steady state. The connection duration follows a negative exponential distribution [123]. No connection is blocked for data transfer once the time-slot of a wavelength is assigned for that connection. The network topology is fixed and never changes during the entire simulation time. Assume that each fiber consists of two wavelengths unless otherwise stated, and each TDM frame consists of eight time-slots. Each data point is the average of the results of many runs with different seeds. This helps to reduce the margin of errors and obtain 95% confidence intervals.

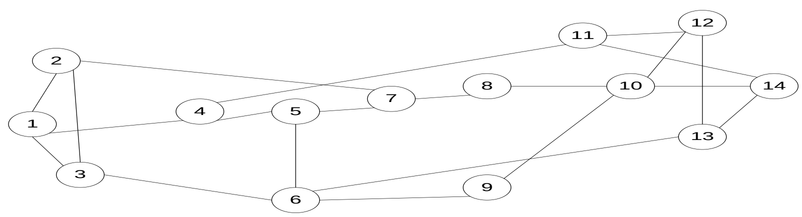


Figure 2.9: NSFNET topology

Simulation results are generated for (i) the proposed TDM wavelength network with shared time-slot (S-TS-48) scheme, the non-shared time-slot (NS-TS-48) scheme, and a conventional wavelength routed network without WC (Wav-No-Conv-48) [94] for an average connection duration of 48 seconds, (ii) the proposed TDM wavelength network with shared time-slot (S-TS-24) scheme, the non-shared time-slot (NS-TS-24) scheme, and a conventional wavelength routed network without WC (Wav-No-Conv-24) for an average connection duration of 24 seconds, (iii) the proposed TDM wavelength network in S-TS-48 with OTSI and without OTSI, (iv) an increasing the number of wavelengths in a fiber on the proposed TDM wavelength network with S-TS and an average connection duration of 40 seconds, (v) the blocking probability performance of the proposed TDM wavelength network with S-TS using different routing methods, namely MHFR, LCR and LCR-FTL, and (vi) the blocking probability of some individual routes as the traffic load between two routers is increased. Offered load in Erlangs is defined as the average connection arrival rate multiplied by the average connection duration. Each connection request is assumed to be 10Mbps. As the offered load in Erlangs increases, the blocking probability for each set of simulation result also increases. The reason is that more connection requests are generated when bandwidth availability is scarce. Figures 2.10 and 2.11 present the simulated results of shared time-slot scheme, non-shared time-slot scheme and conventional wavelength routed network scheme. All three schemes do not use WC. Figure 2.10 presents the results of the blocking probability versus the offered load in Erlangs for S-TS-48, NS-TS-48, and Wave-No-Conv-48. From the graph, S-TS-48 has a lower blocking probability than that of NS-TS-48 because more connections are sharing the bandwidth of a time-slot in a wavelength, and given the bandwidth requirement of each connection is smaller than the total bandwidth of a time-slot in a wavelength. The same conclusion is drawn for S-TS-24 and NS-TS-24 in Figure 2.11. An analysis of the simulation results in Figures 2.10 and 2.11 shows that on average connections with a shorter duration have lower blocking probability. The reason is that as connections are released faster, more connections can share the bandwidth of a time-slot in a wavelength. In Figure 2.10, Wave-No-Conv-48 has the highest blocking probability because each established connection occupies an entire wavelength which is a tremendous wastage of bandwidth.

Figure 2.12 presents simulation results of either using or not using OTSIs at intermediate STSWRs for the shared time-slot scheme. It shows the results of blocking probability versus offered load in Erlangs for S-TS-48 with and without OTSIs. For S-TS-48 without OTSI, the OTSSs are replaced by slot-by-slot switches as the delay of one time-slot in the same wavelength from one network node to another is used. It is obvious that S-TS-48 with OTSIs has a lower block probability than S-TS-48 without OTSIs. This shows the benefit of having OTSIs at intermediate STSWRs if the higher cost of OTSIs is acceptable. Hopefully with the advancement of optical technology, the FDLs in an OTSI will be replaced with inexpensive optical buffers. This will reduce the cost of fiber and implementation complexity.

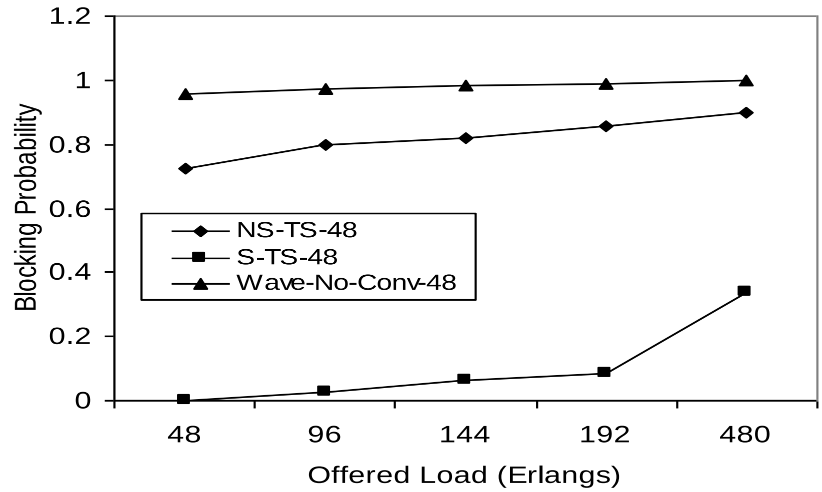


Figure 2.10: Blocking probability versus offered load for average connection duration of 48 seconds

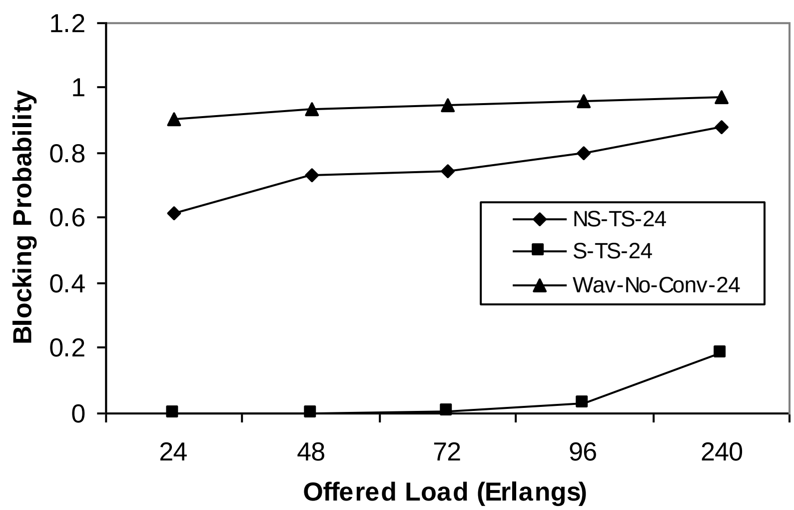


Figure 2.11: Blocking probability versus offered load for average connection duration of 24 seconds

Figure 2.13 shows the results of blocking probability versus offered load in Erlangs for increasing wavelengths in the shared time-slot scheme with average connection duration of 40 seconds (S-TS-40). As the number of wavelengths increases from two to six, it is obvious that the blocking probability decreases because more time-slots are available for sharing between established connection requests. Figure 2.14 shows the simulated results of using MHFR, LCR, and LCR-FTL in the proposed network of STSWRs. It presents the results of blocking probability versus offered load in Erlangs for S-TS-40 with the MHFR, LCR and LCR-FTL methods. The LCR blocking probability is only slightly lower than MHFR, even though the LCR method is able to adapt to the availability of time-slots in a network because the shared

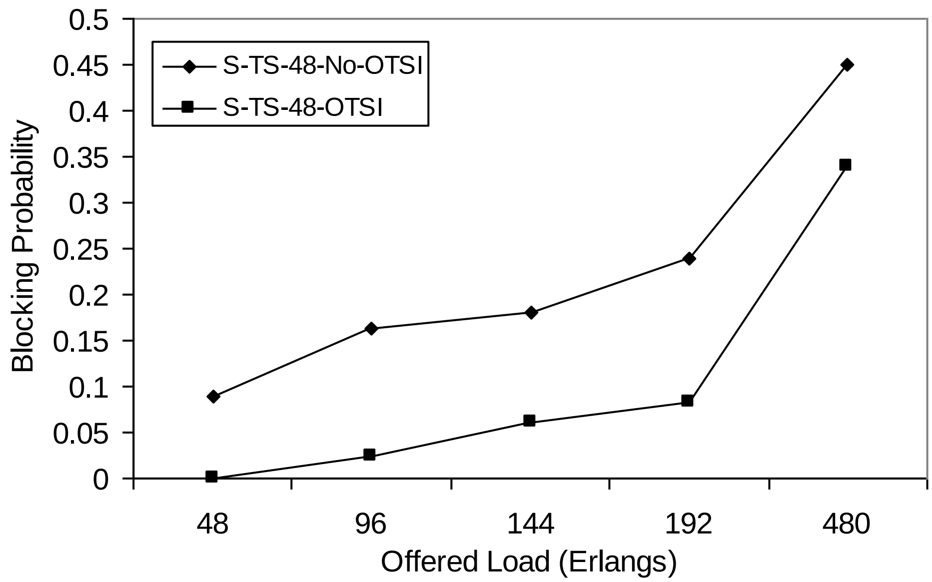


Figure 2.12: Blocking probability versus offered load with and without OTSIs

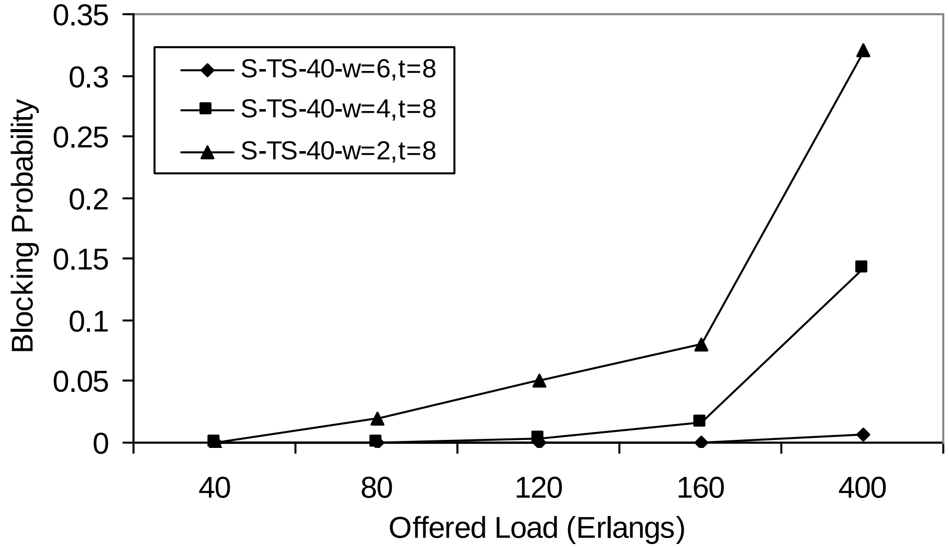


Figure 2.13: Blocking probability versus offered load for increasing wavelengths in a fiber

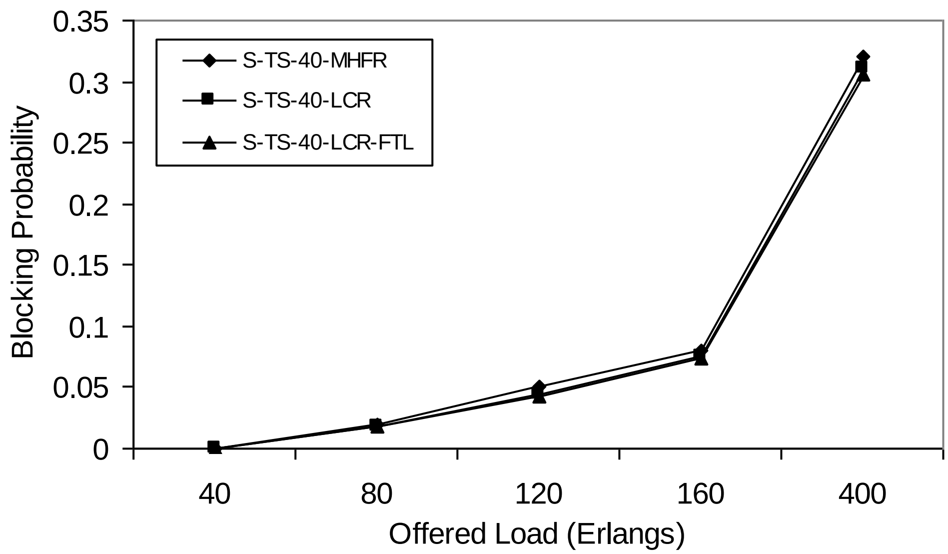


Figure 2.14: Blocking probability versus offered load for MHFR, LCR and LCR-FTL

time-slot of a route is not released until the last connection duration has expired. If a shared time-slot is released, a new route with the most availability of time-slots is determined for the next connection request from this source STWSR to the same destination STWSR. The blocking probability of LCR-FTL is as low as LCR or very slightly lower than LCR. When a shared time-slot is released, the LCR-FTL is capable to determine a route that has at least a free time-slot in a fiber link between two nodes.

Table 2.1 shows the blocking probability of some individual routes in the NSFNET topology (Figure 2.9) as the traffic load of these routes is increased. The average connection duration is 28 seconds, and the offered load is 280 Erlangs. Generally, the blocking probability for 80% of the traffic going from the same source router to the same destination router is the same or slightly higher than the traffic of 50%. This shows the effectiveness of the shared time-slot scheme for heavy volume data traffic going to the same destination router from the same source router.

Table 2.1: Blocking probability of some individual routes as the traffic load between these routes are increased

| Routes | Blocking probability for 80% traffic | Blocking probability for 50% traffic |
|---|---|---|
| 1 -> 2 | 0.04 | 0.04 |
| 11 -> 12 | 0.093 | 0.09 |
| 3 -> 6 -> 9 | 0.145 | 0.141 |
| 7 -> 8 -> 10 -> 14 | 0.23 | 0.21 |

## 2.5 A Shared Time-Slot TDM Wavelength Optical WDM Network with Slot-by-Slot Fast Wavelength Converters and OTSIs

[95-97,123-127] investigated the behavior of using WCs in WDM networks. However, the cost of a WC is still very high. One of the ways to reduce the cost of using WCs in fiber links switching networks is through sharing. [123, 128-129] have proposed different architectures of sharing these converters, namely dedicated, shared-per-link, and shared-per-node.

Figure 2.15 depicts the dedicated wavelength convertible switch architecture. Each node has two input and two output fiber links, and three wavelengths per fiber. The major components of each node are wavelength de-multiplexers, optical switches, WCs and wavelength multiplexers. A de-multiplexer is dedicated to each input fiber; a multiplexer is dedicated to each output fiber. In addition, a WC is available for every wavelength. Thus, for a node with $X$ input links, $X$ output links and $W$ wavelengths per fiber, there are $X$ number of $W$ x 1 wavelength multiplexers and de-multiplexers, a $XW$ x $XW$ non-blocking optical switch and $XW$ number of WCs. The wavelengths in each input fiber are de-multiplexed into individual wavelength. Assume that each wavelength contains a message. Then each wavelength is switched by the optical switch to one of the output ports connected to an output link. After that the wavelength may be converted by the WC. Finally, the message in each wavelength is multiplexed into an aggregate message and forwarded to the output fiber link. Since there is a WC dedicated for each wavelength, no connection request is blocked because of the unavailability of WCs. For example, if at a node, wavelength $w_i$ is available on its input link and $w_j$ is available on its output link, there will be a free converter at the node that can be used for a connection. This helps to reduce the blocking probability of connection requests. However, this architecture requires a lot of WCs which increases the cost of a switch. In some real situations, the number of connections that require WCs at a node is much less than $XW$ at any one time. A cost-effective solution is to use fewer WCs and to allow their sharing among different connections. In such a case, the shared-per-link or shared-per-node architecture switch is considered.

Figure 2.16 presents the share-per-link wavelength convertible switch architecture which uses one optical switch only. A WC bank (WCB) is dedicated to each output fiber link and is only shared by the wavelengths traversing to that particular output fiber link. If every WC bank has $k$ WCs, the optical switch is a $XW$ $x$ ($XW + Xk$) non-blocking switch. First, the de-multiplexed wavelengths are fed into the optical switch. Then the wavelengths are directed to the WCB for wavelength conversion or to the multiplexer associated with the output fiber link. All the wavelengths are multiplexed together by the

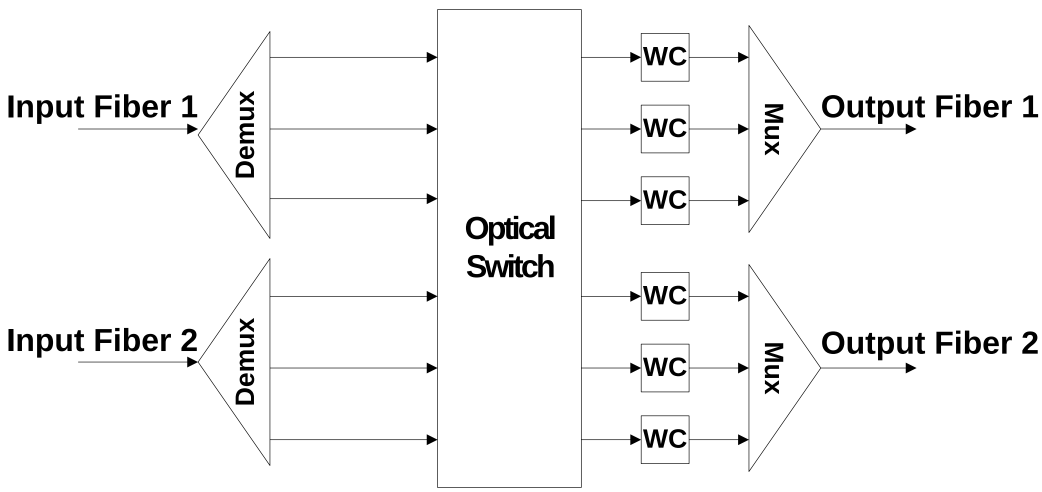


Figure 2.15: Dedicated WC switch architecture

multiplexer before they are forwarded to the output fiber. In this architecture the sharing efficiency is medium because a WCB serves an output fiber only. The WC cost is lower than the architecture presented in Figure 2.15 because fewer number of WCs are used. However, the optical switching complexity is higher than the architecture in Figure 2.15 .

Figure 2.17 depicts the share-per-node wavelength convertible switch architecture which uses two optical switches and a WCB. If there is $k$ WCs in the WCB, the first optical switch is a $DW$ $x$ ($DW + k$) nonblocking switch, and the second switch is a $k$ $x$ $Dk$

nonblocking switch. The arriving wavelength is first demultiplexed into individual wavelengths. These wavelengths are then fed into the optical switch. A wavelength which requires conversion is fed to the WCB. Otherwise, it is fed directly to the multiplexer associated with the desired output link. The main purpose of the second optical switch attached to the WCB is to direct the converted wavelength to the multiplexer associated with the desired output link. All the wavelengths are multiplexed by the multiplexer

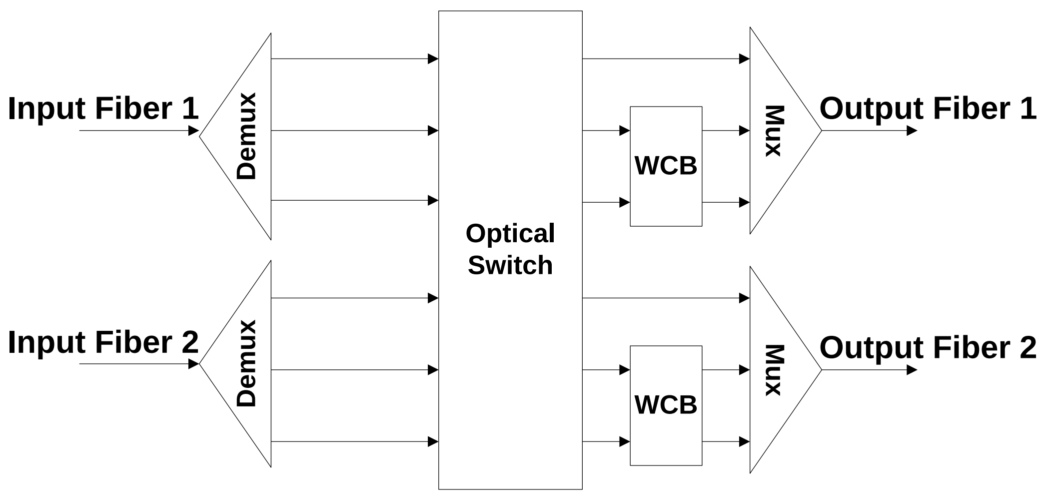


Figure 2.16: Share-per-link switch architecture

before they are sent to the output fiber. In this architecture, the sharing efficiency is high because the WCs are effectively shared. However, the optical switching complexity of this architecture is higher than the previous two architectures.

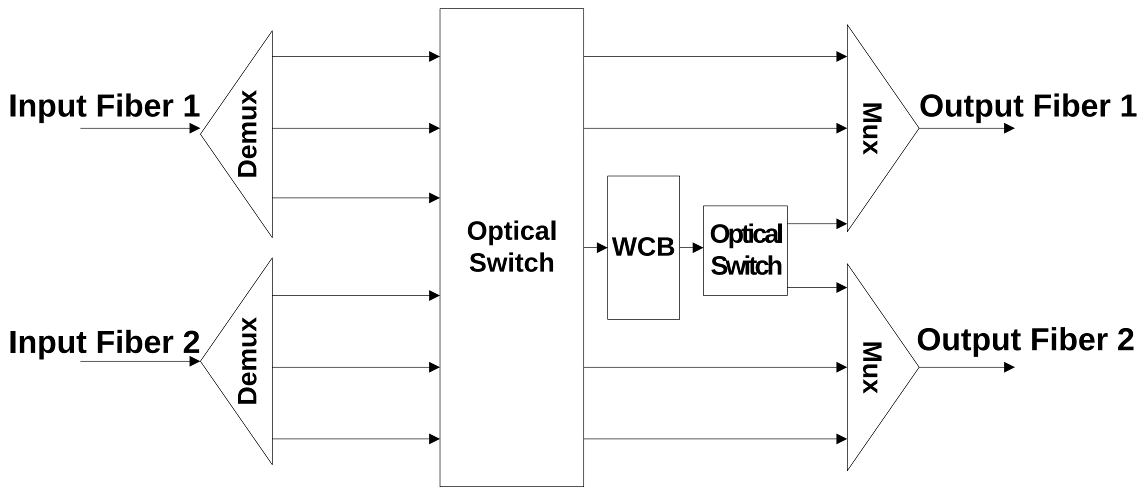


Figure 2.17: Share-per-node switch architecture

These three architectures differ in their blocking performance, complexity and cost. Table 2.2 below compare these attributes for each architecture.

Table 2.2: Comparisons of different wavelength convertible switching node architecture

| Optical Switch | Blocking Performance | Sharing Efficiency | Switching complexity |
|---|---|---|---|
| **Dedicated** | Low | Low | Low |
| **Share-per-link** | Medium | Medium | Medium |
| **Share-per-node** | High | High | High |

Currently, there is no work being done using OTSIs and SSWCs in shared time-slot TDM wavelength optical WDM network. In order to have a shared time-slot TDM wavelength optical WDM network with SSWCs, the *2 x 2* STSWR high level architecture is proposed (Figure 2.18). It is assumed that the number of SSWCs in the SSWC component is equivalent to the number of wavelengths in a fiber, and each SSWC can cover all these wavelengths. In this architecture, the time-slot in a wavelength is assigned at each hop of a route, and an SSWC component [130] is able to convert a time-slot in a wavelength to a time-slot in another wavelength. This is illustrated in Figure 2.19 through the conversion of $\lambda_1 t_1$ to $\lambda_2 t_1$ . Figure 2.20 shows another STSWR architecture with such SSWCs. In this architecture, source routing is required. By using the hop-by-hop method, the benefits of the SSWC for the outgoing fiber link cannot be realized if the OTSI is full. The time-slot in a wavelength for each hop is determined at the source STSWR. There are constraints in using time-slots in a wavelength for the architecture shown in Figure 2.20. For example, if $\lambda_1$ has no empty time-slots in the next router *j*, the SSWC component is able to swap the current $\lambda_1 t_1$ to the available $\lambda_2 t_1$ in the current router *i*. In this situation, $\lambda_1 t_1$ is not used from current router *i* to the next router *j* that contains the SSWCs even though it is empty. Figure 2.21 depicts an STSWR architecture that consists of an SSWC component with *k* such SSWCs dedicated to each output fiber. The value of *k* is less than number of wavelengths in a fiber and is greater than one. In this architecture, an SSWC component is only accessed by connections traversing that particular fiber link. The wavelength that arrives early will be circulated using the FDLs in the OTDS while waiting for the rest of the wavelengths to arrive. Meanwhile, Figure 2.22 presents the architecture of an SSWC component to be shared by all the input fibers to an STSWR. This SSWC component can also contain *k* such SSWCs, and the output wavelengths from the SSWC component is switched to the correct output fiber by an optical switch. Moreover, this SSWC can also be constructed to cover only certain number of wavelengths in a fiber.

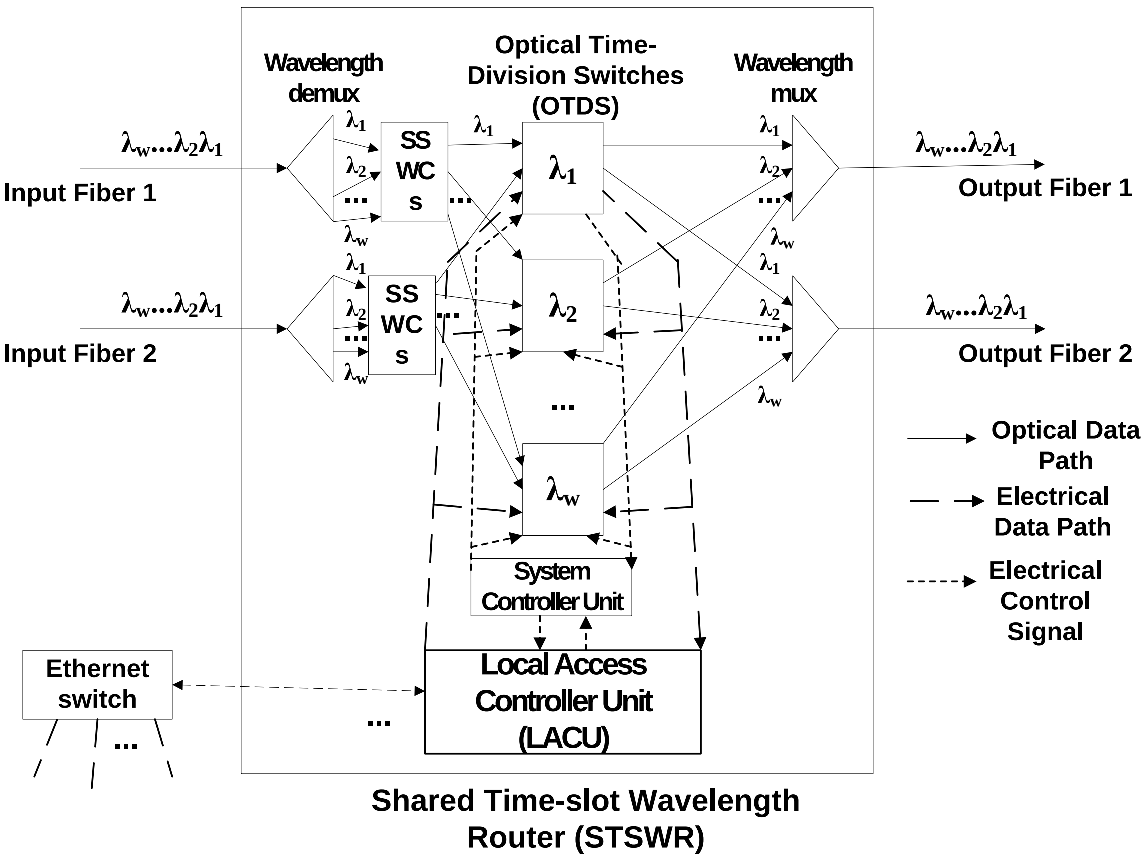


Figure 2.18: High level architecture of *2 x 2* STSWR with SSWC components before OTDSs

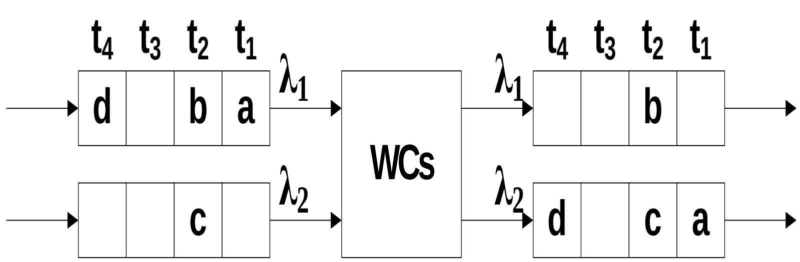


Figure 2.19: Detailed illustration of swapping time-slots in an SSWC component

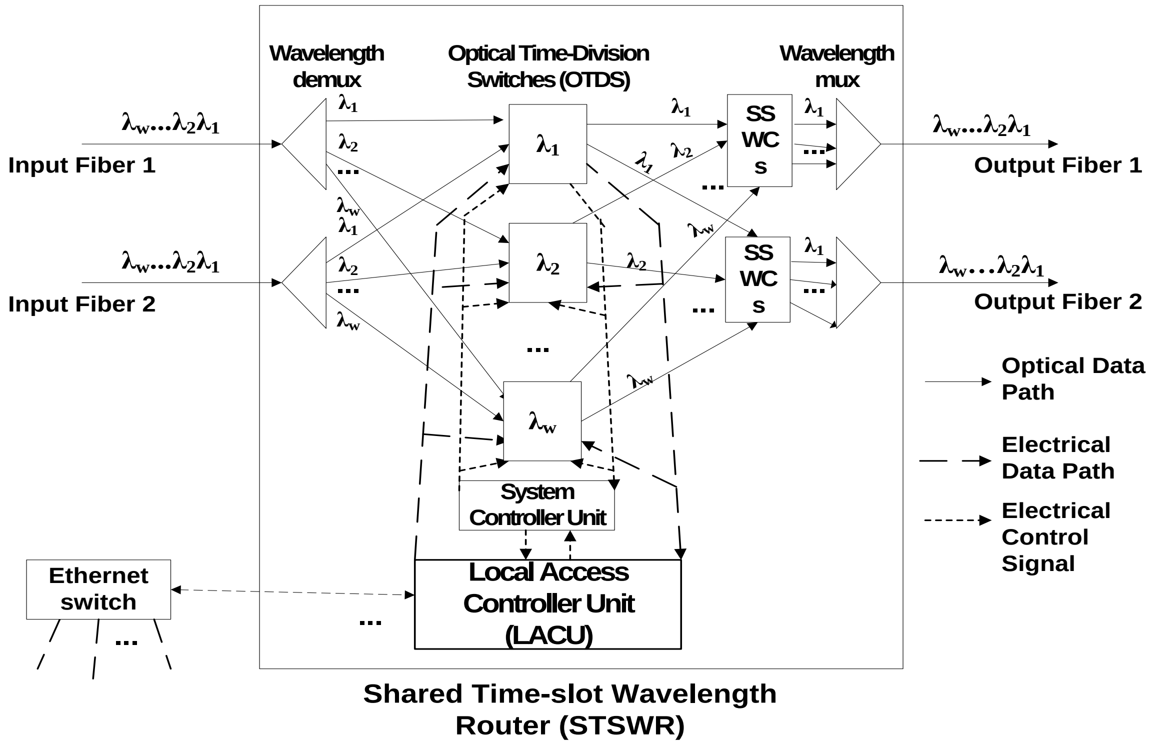


Figure 2.20: High level architecture of *2 x 2* STSWR with SSWC components after OTDSs

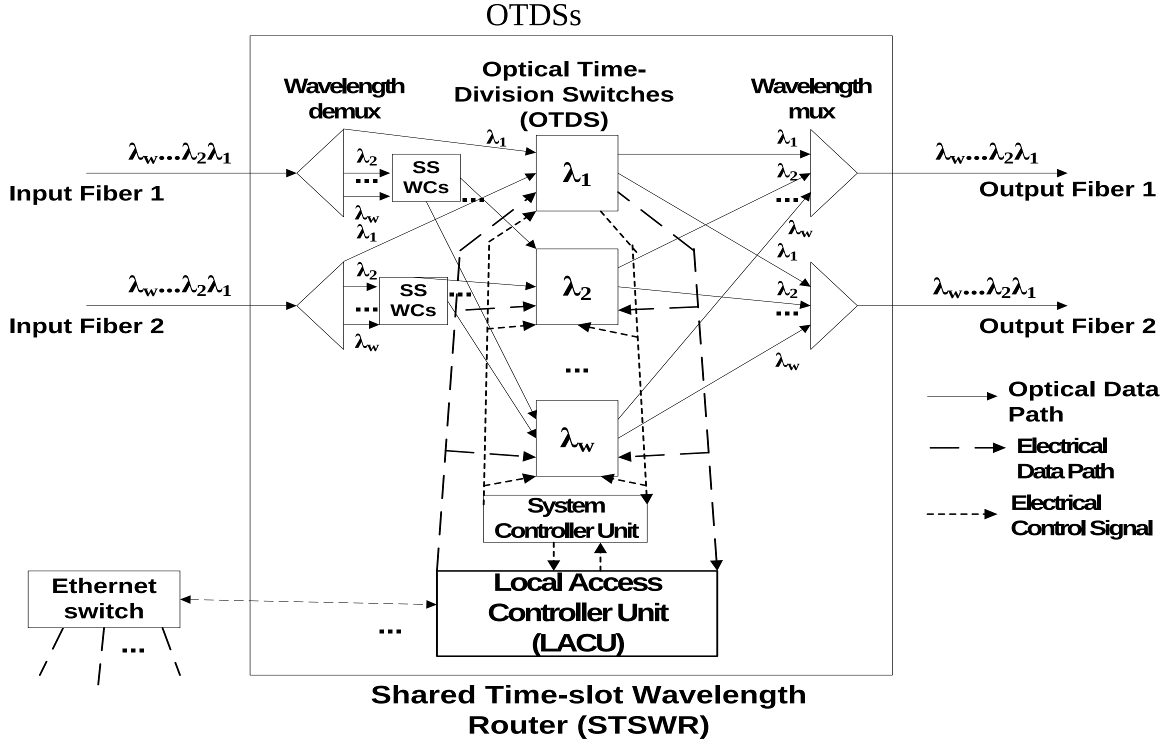


Figure 2.21: High level architecture of *2 x 2* STSWR with SSWC components that contains *k* SSWCs each

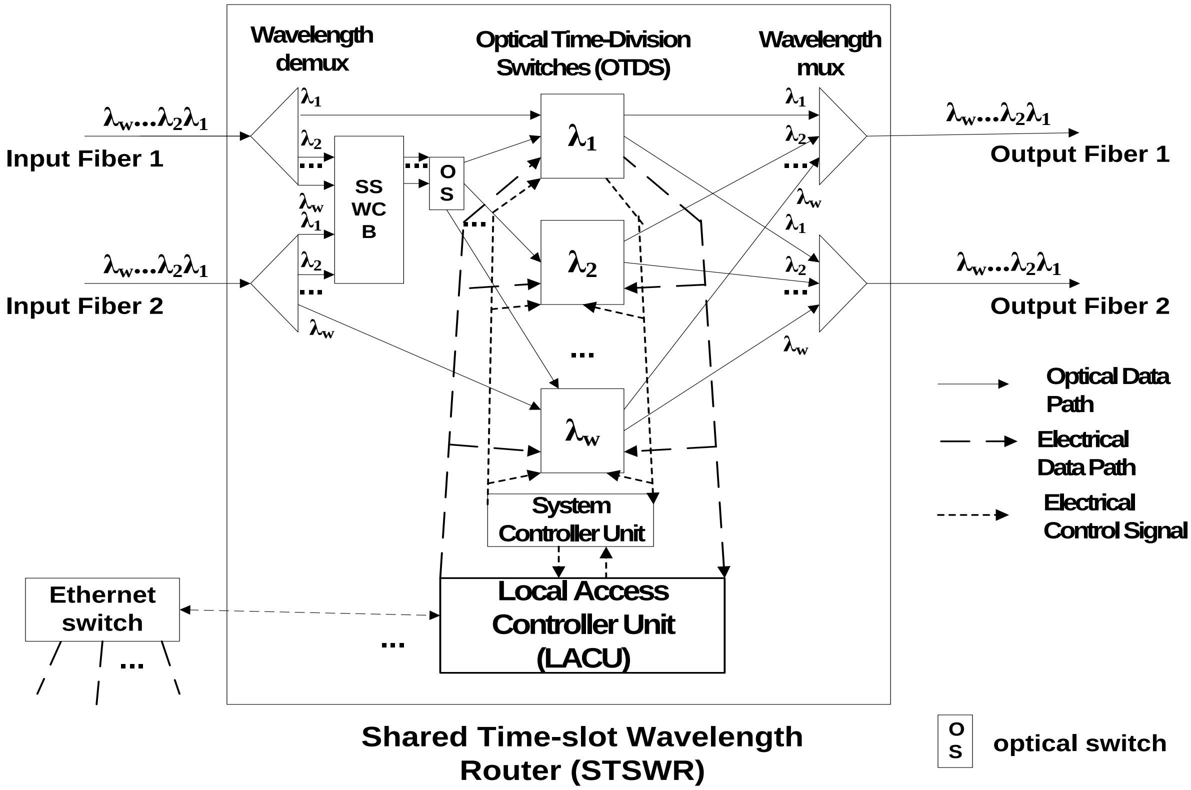


Figure 2.22: High level architecture of *2 x 2* STSWR with an SSWCB shared by all input fibers

## 2.6 Summary

In this chapter, we have proposed a framework for a shared time-slot TDM wavelength optical WDM network. Each STSWR is capable of allowing the bandwidth of a time-slot in a wavelength to be shared by many successful connections that travel along the same route from the same source STSWR to the destination STSWR. The shared time-slot of a route is not released until the connection durations of all the connections that are sharing this time-slot have expired. Each STSWR is equipped with OTSIs and performs OCS. Incoming data at the time-slot level is routed without any E/O and O/E conversions. OTSIs are employed for interchanging of time-slots at intermediateSTSWRs. Our shared time-slot scheme does not result in time-slot conflict at STSWRs because each time-slot in the network is assigned to one connection only.

The effectiveness and behavior of this network using our proposed shared time-slot scheme with three routing methods are demonstrated in terms of blocking probability by simulation. In addition, we have proposed a least cost routing method with at least a free time-slot in a fiber link. Finally, we have designed a few architectures (Figures 2.18, 2.21, and 2.22) for the STSWR with slot-by-slot fast WCs.

The next chapter discusses the architecture of a router in the mini-slot TDM optical network. The effectiveness and behavior of this network are demonstrated again by extensive simulations.

# CHAPTER 3

# Mini-slot TDM Optical WDM Network[2]

In the previous chapter, we presented the STSWR architecture. We investigated the effectiveness and behavior of the shared time-slot TDM wavelength optical WDM network by extensive simulations. In this network, the data is optically transmitted in time-slots.

In this chapter, we argue that it is feasible to transmit data in a mini-slot of a time-slot in a wavelength. We propose a network, mini-slot TDM optical WDM network to perform the transference of data stored in mini-slots. Each router, namely mini-slot time-slot wavelength router (MTWR) in this network is equipped with OMSIs. One of our objectives of dividing a time-slot into mini-slots is to study the performance of the mini-slot TDM optical WDM network as compared with the shared time-slot TDM wavelength optical WDM network. Moreover, the size of an OTSI is limited because of the timing constraints of how long the data can stay in a buffer (delay lines) [79]. In an optical network with OTSIs, this constraint limits the number of time-slots in a wavelength because each time-slot has to be operated by an OTSI. Furthermore, based on the current optical technology, it is more feasible to design a smaller size optical interchanger. The MTWR has to determine the route, wavelength, and mini-slot(s) of a time-slot in the TDM frame for any connection request. The three major components in MTWR to facilitate the flow of data optically in mini-slots are high speed optical gates, OMSIs, and

---

[2] A large part of this chapter will appear in Journal of Photonic Network Communications, "Mini-slot TDM WDM Optical Networks". Printed by Springer (USA). Also, a part of this chapter has been presented in 20th IEEE Advanced Information Networking and Application Conference (AINA), "A Mini-Slot Router Architecture for TDM Optical WDM Networks," Vienna, Austria, 18th-20th Apr. 2006.

input/output synchronizers. The first major component, the high speed optical gates have been reported to be feasible in [131-132]. The main purpose of the optical gates is to direct the optical signals. These gates are used in optical selective splitter or combiner components. In the next paragraph, we explain the feasibility of the other two components in the MTWR.

Solid-state switches can perform switching operations with a precision of 10ns or less [90]. To allow timing uncertainties due to possible jitter and drifting, a guard band of at least 10ns is allowed between each slot. To achieve reasonable data transmission efficiencies, time-slot durations should be at least 10 times the guard time [90]. Assume 10 gigabits per second for a wavelength, a TDM frame is transmitted in every 125μs, and 1μs per time-slot with a guard band of 100ns (Figure 3.1). A TDM frame can therefore contain roughly 104 time-slots, and the data size of each time-slot is 1500 bytes. If a time-slot consists of eight mini-slots, each mini-slot duration is 115ns with a guard band of 10ns (Figure 3.1). Since each mini-slot duration is 115ns, the changing state is performed every 115ns. This does not affect the optical transmission rate as a solid state optical switch can operate at a precision of 10ns or less. The basic building block of an OMSI consists of small solid state optical switch couplers. It comprises different stages, of which each stage is made up of an optical solid state switch. If the OMSI is in the cross state, the output will be the input delayed by a mini-slot time. This is done using the FDLs. If the switch is in the bar state, the mini-slots will be interchanged. If a mini-slot duration that carries more data bits is used, an increase in delay duration at an OMSI will be realized but a slower system reconfiguration is required at the routing nodes. Researchers [133] have experimented with optical input/output synchronizer that can handle time misalignments of up to 105.6ns. The phase variations during normal operation range from 10ns to 100ns. These variations are tracked at the dynamic section of the synchronizer using very fast switches without losing any packet. Thus, synchronizing the optical mini-slot packets of 115ns duration is viable.

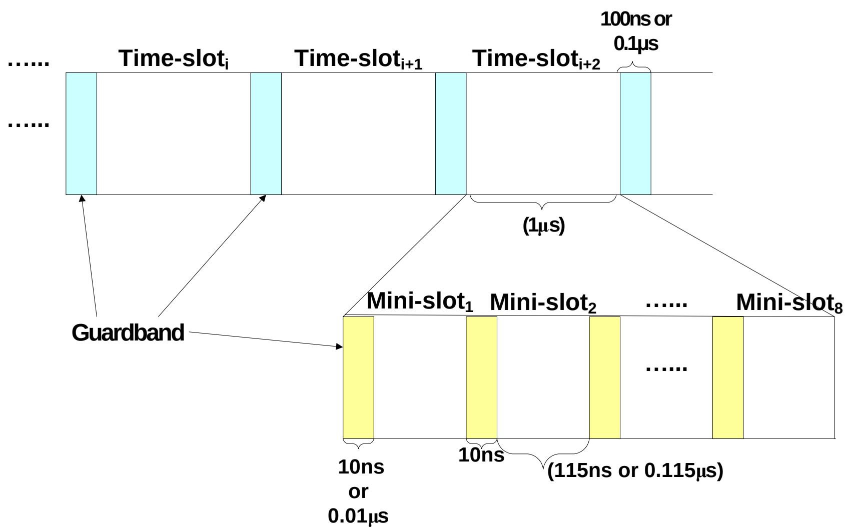


Figure 3.1: Time-slot and mini-slot durations

Next, a very simple example is used to illustrate the advantage of our mini-slot network in effective bandwidth utilization when compared with a typical wavelength routed network. Figure 3.2 shows such an example that assumes the following: (i) a connection request from the local access node is one mini-slot and (ii) each wavelength is divided into four fixed-length time-slots, and each time-slot is divided into four fixed-length mini-slots. A connection from local access node *b* to local access node *c* is allocated mini-slot 3 of time-slot 2 in $\lambda_1$ from MTWR 1 to MTWR 2. From MTWR 2 to MTWR 3, this connection is allocated mini-slot 4 of time-slot 2 in $\lambda_{1.}$

At the same time, another connection from local access node *a* to local access node *d* is allocated mini-slot 2 of time-slot 2 in $\lambda_1$ from MTWR 1 to MTWR 2. From

MTWR 2 to MTWR 3, this second connection is allocated mini-slot 3 of time-slot 2 in $\lambda_1$. At MTWR 2, mini-slot interchange takes place. Hence, two successful connections share a time-slot in a wavelength. In a typical wavelength routed network, two wavelengths are required for these two connections. Therefore, there is a tremendous wastage of fiber bandwidth for low speed connections.

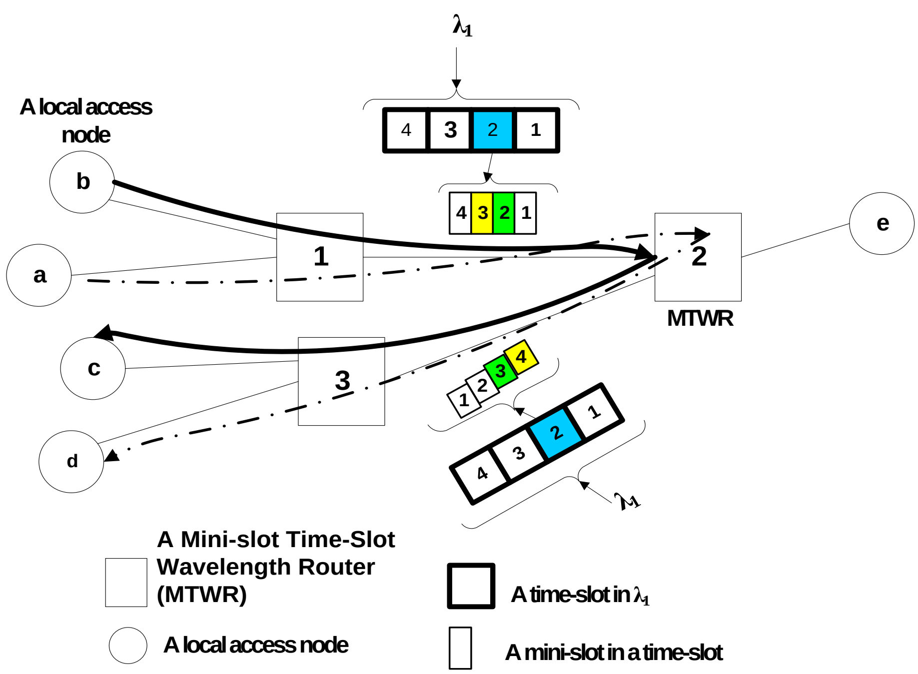


Figure 3.2: Conceptual mini-slot TDM wavelength network

The rest of the chapter is organized as follows. Section 3.1 explains the network operations and MTWR architecture of the mini-slot TDM optical WDM network. Section 3.2 briefly explains the OCS protocol implementation for this network. This OCS protocol is used in our simulation study. Section 3.3 discusses the simulation setup for the NSFNET topology, three by five mesh torus topology, and 40-node irregular topology. Section 3.4 presents the simulation results. Section 3.5 gives the summary of this chapter.

## 3.1 Network Operations and Router Architecture

Request of mini-slot(s) from the MTWR (Figure 3.3) can be from different Ethernet speed or SONET Synchronous Transport Signal (STS) connections. Assume the length of each mini-slot is 187.5 bytes (A time-slot data size of 1500 bytes divided by eight mini-slots). An 80 percent total bit rate efficiency gives 150 data bytes for a mini-slot. The other 20 percent (37.5 bytes) is used for guard band and synchronization bit pattern. According to the IEEE 802.3 frame format (Figure 2.5) [116], the payload size is

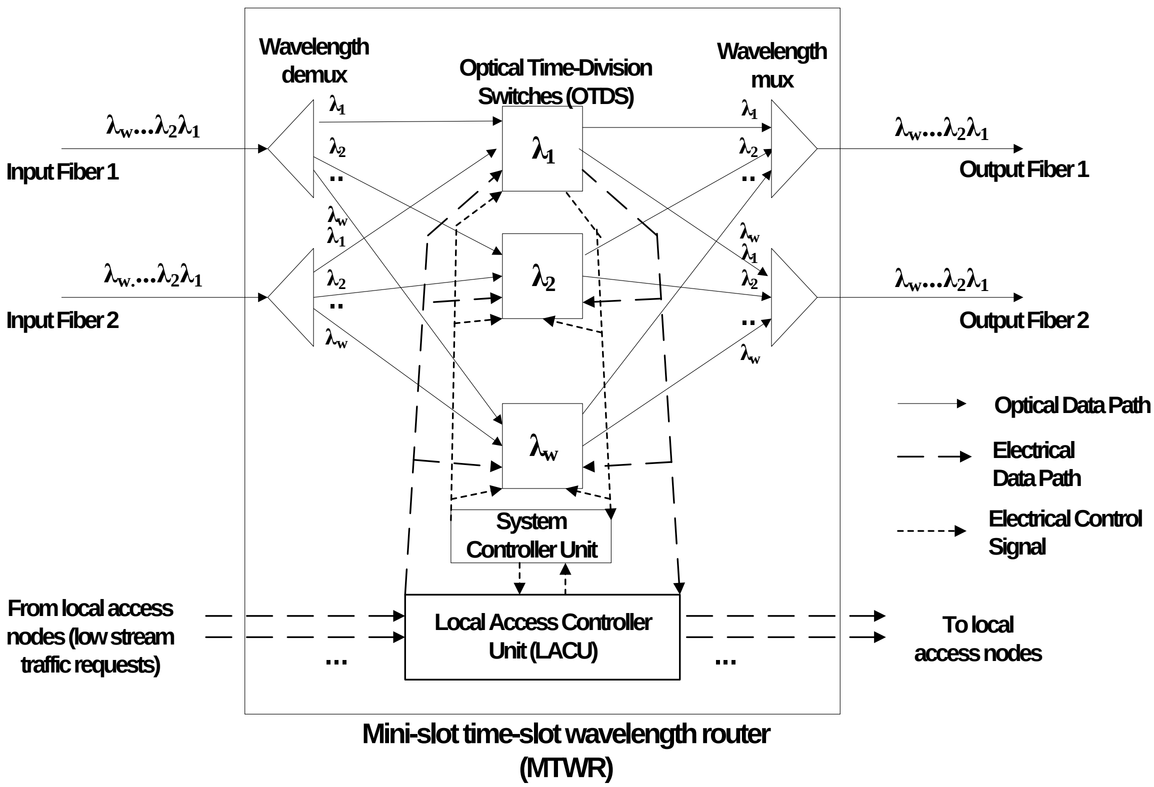


Figure 3.3: High level architecture of *2 x 2* MTWR

between 64 to 1500 bytes for each Ethernet frame. The fixed frame size of Ethernet fits well as the size of each frame is the same for 10Mbps, 100Mbps, 1Gbps, or 10Gbps. The higher speed Ethernet transmits more data frames per second than lower speed Ethernet but the frame size is the same. For 100Mbps Ethernet, more than one mini-slot can be requested. For 1 Gbps Ethernet, more than eight mini-slots can be requested. In this case, consecutive time-slots are allocated since each time-slot consists of eight mini-slots. It is noted that the data is still transmitted in mini-slots.

According to SONET STS-1 (STS-1) framing structure (Figure 3.4) [134], each row consists of 90 bytes. This can be fitted into one mini-slot. For the STS-1 which transmits 51.84 Mbps more than one mini-slot can be requested. As for the STS-3, an example of the STS-*N* frame structure (Figure 3.5) which transmits 155.52 Mbps, more than eight mini-slots can be requested. In such a case, consecutive time-slots are allocated. The length of each row (Figure 3.5) requires two mini-slots. Thus, more complex electronic processing is required at the source router for splitting each row into two so that the data from the access node can fit into two mini-slots. At the destination router, the data in the two consecutive mini-slots are combined into one row of the STS-3 format before the frame is sent to the destination access node.

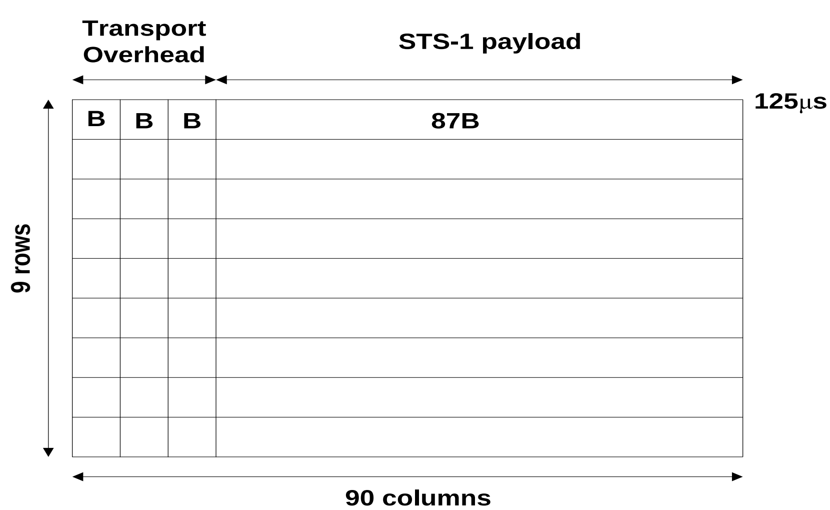


Figure 3.4: Structure of an STS-1 frame

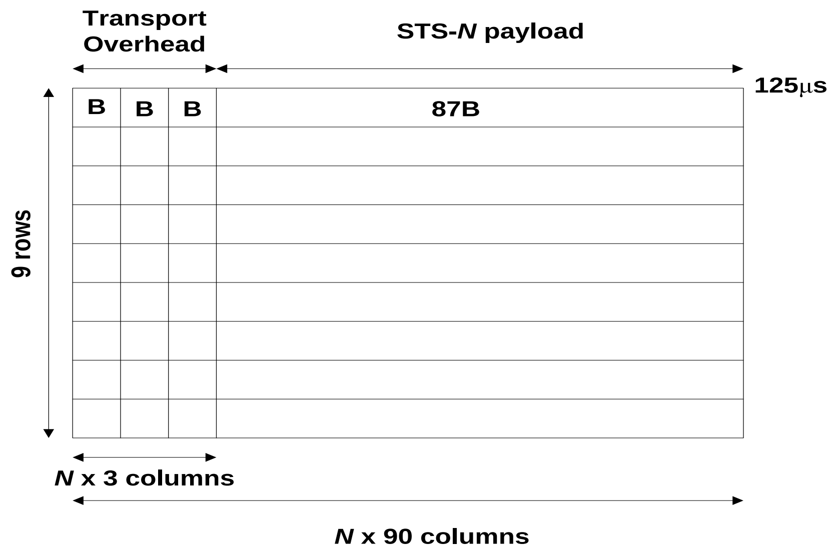


Figure 3.5: Structure of an STS-*N* frame

For simplicity, we assume that the request for mini-slot(s) are from different Ethernet connections, and each connection can request for one to eight mini-slots for data transfer. If a connection request is for more than one mini-slot, the available mini-slots are assigned consecutively at the source MTWR and of the intermediate MTWR(s). This is to ease implementation. Each local access node is connected to a port in the LACU. This is shown in Figure 3.3. When data is first received from the local access node, the LACU communicates with system controller unit for route computation, and the mini-slot(s) of a time-slot in the TDM frame of a wavelength is pre-determined along the pre-computed route before data transfer can begin. Once the route is computed, the mini-slot(s) of a time-slot in a wavelength is assigned hop-by-hop along the computed route. When the route is successfully completed, the LACU forwards the data to the electronic buffer of the correct LABU (Figure 3.3). The data is later converted into MTWR data format. It is assumed that the data contained in each frame from the local access node can be fitted into a mini-slot. An E/O conversion is later performed in the LABU so that data can be optically sent in the pre-allocated mini-slot of a time-slot in a wavelength. The intermediate MTWR forwards the pre-assigned mini-slot of a time-slot in a wavelength to an adjacent MTWR. Each intermediate MTWR does not perform any E/O and O/E when transferring data. The bandwidth of each wavelength is divided into fixed-length time-slots, and each time-slot is further divided into fixed-length mini-slots. A TDM frame consists of a fixed number of time-slots. At the destination MTWR, an O/E conversion is performed on the mini-slot of a time-slot in a wavelength. Then the electronic data is formatted according to the local access node data format. This is done in the LABU. The electronic data is stored in the buffer of the LABU for later forwarding to the local access node through the LACU.

Even though the architecture of a *2 x 2* MTWR shown in Figure 3.3 is almost identical to Figure 2.4, Figure 3.3 is presented for completeness in describing the working of the optical network with mini-slot routers. This architecture is easily expanded into a *W x W* MTWR if there are *W* input fibers and *W* output fibers [80]. At each input port, a wavelength de-multiplexer is used to separate the *w* wavelengths into *w* individual optical lines. The routing of incoming time-slots is carried out in a *2 x 2* optical time-division switches (OTDS), where the same wavelength, for example, $\lambda_1$ are concentrated. Each output port of the OTDS is connected to a different *W x 1* wavelength multiplexer. Thus, a *W x W* MTWR, which has *W* outputs of the OTDS, is connected to *W W x 1* wavelength multiplexers respectively. The optical signals are combined in the wavelength multiplexer and passed to the correct output port. The intermediate MTWR does not perform any O/E for the mini-slot that passes through it. This makes an all-optical data path. In order to ensure the input-ports and output-ports of each OTDS are connected according to the assigned mini-slot(s), this connectivity information is stored after the mini-slots and route are computed. The control signals at each mini-slot are generated by the electronic system controller unit using the stored information. This unit also performs tracking and calibration of the local timing signal for packet synchronization. In addition, the access of LACU and LABU is controlled by this unit. In order to access the MTWR, the local access nodes need to interface with the LACU (Figure 3.3). The LACU not only handles the requests from local access nodes to establish light-paths, but also the data frames from or to the local access nodes. According to the established light-paths, the LACU communicates with the LABU of the correct OTDS to retrieve or store the data in its buffer.

Figure 3.6 illustrates the *2 x 2* architecture of OTDS for $\lambda_1$ (The differences of this figure with Figure 2.6 are highlighted in the next paragraph). If there are *W* inputs and *W* outputs, the OTDS architecture will be *W x W*. The main function of the OTDS is to make sure that the mini-slots are interchanged appropriately in an OMSI for each wavelength of a port. The data that is stored in each mini-slot begins with synchronization bits and is followed by the packet. To apply the input/output synchronizers method discussed in [92] but at higher speed [133], the packets should be transmitted as slotted mini-slot streams. Each time-slot stream is optically de-multiplexed into individual time-slot. Each time-slot consists of a mini-slot stream, illustrated in Figure 3.7. Each mini-slot is separated by a guard band. It begins with synchronization bits, which are used for mini-slot alignment in an OTDS, and is followed by a packet. Each packet is synchronized to the local timing reference. This is done by the optical input synchronizer which is controlled by the system controller unit. The synchronizer detects the beginning of each incoming packet by recognizing the synchronization pattern and aligns the packet with the local timer before entering the optical mini-slot switches (OMSS). Each router is assumed to have fully system reconfigurable capability and is able to reconfigure after every mini-slot. The OSS is controlled by the system controller unit. It is used to select the data to the LABU or input to the correct OMSI in the OMSS. The OMSI in the OMSS provides the flexibility of inter-changing mini-slots. The mini-slot to the destination MTWR enters the LABU. An O/E conversion is performed on the mini-slot and the electronic data is stored in the buffer of LABU. The data from the mini-slot is formatted according to the local access station data format. The formatted data is later forwarded to the LACU. The LACU forwards the data to the correct local access node. The other mini-slot enters the OMSS, where mini-slot interchange can take place. FDLs are provided in each OMSI to accommodate the simultaneous incoming mini-slots that contain data. The number of OMSIs in the OMSS depends on the number of time-slots in each TDM frame as each time-slot requires one OMSI to exit slots in each TDM in the same output fiber. The function of the LABU is to store the incoming data destined for the MTWR or outgoing data from the local access node. The communication between the LABU and LACU is through the Port $LI_{1,LACU}$ and Port $LO_{1,LACU}$ . In the OTDS, the system controller unit configures the connectivity between the input ports and output ports based on the assigned mini-slot(s). Due to the internal delay by the OMSI, the optical output synchronizer aligns the packets to eliminate jitter. After the alignment, the aligned stream packets of a time-slot are multiplexed into time-slot streams before exiting the OTDS and entering the wavelength multiplexers. The OSC is used to add optical mini-slot(s) in the optical lines after E/O conversions in the LABU. The OSC is also controlled by the system controller unit. The electronically controlled optical gates are used to implement the OSSs and OSCs. Materials for reducing or avoiding crosstalk in switching components, multiplexers and de-multiplexers are found in [118-120].

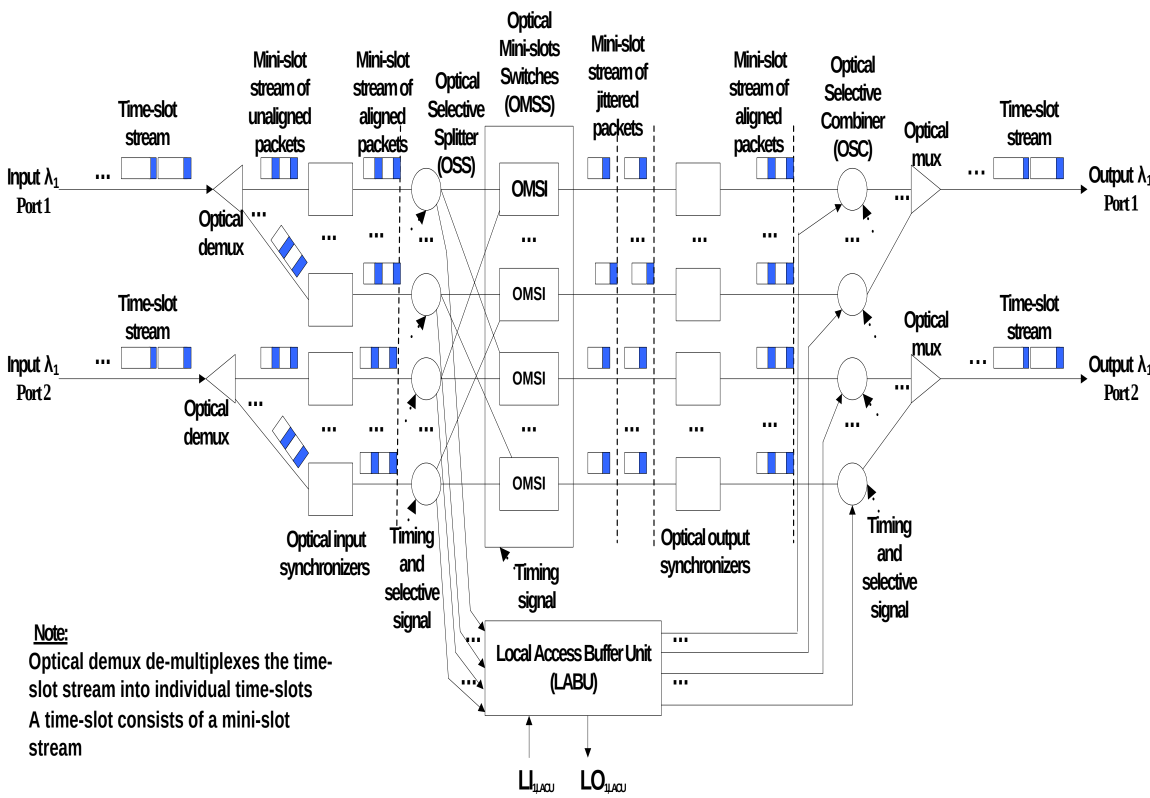


Figure 3.6: *2 x 2* architecture of OTDS for $\lambda_1$

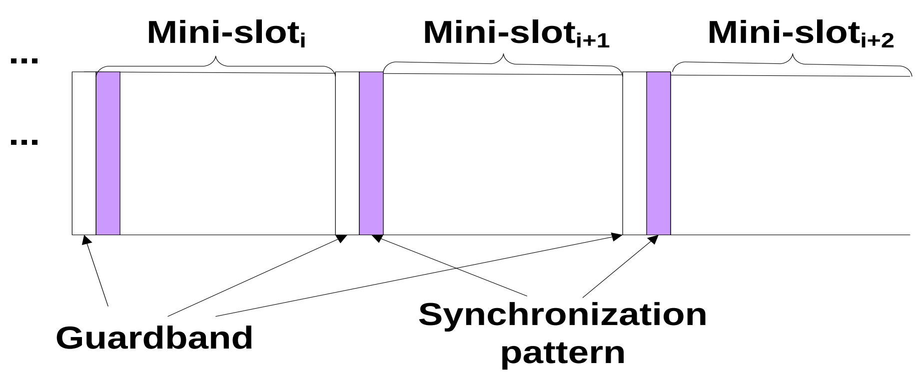


Figure 3.7: Mini-slot stream (This figure is the same as Figure 2.7 except the guardband, synchronization pattern, and each mini-slot duration are smaller)

An STSWR in Figure 2.4 provides Ethernet access. But a MTWR (Figure 3.3) allows mini-slot requests from Ethernet or SONET connections. Table 3.1 highlights the differences in terms of data transfer and optical components between Figures 2.6 and 3.6.

Table 3.1: Differences between Figures 2.6 and 3.6

| | **Figure 2.6** | **Figure 3.6** |
|---|---|---|
| **Data transfer** | Data is transported in time-slots. | Data is transmitted in mini-slots of a time-slot. |
| **Optical components** | (i) OTSIs<br>(ii) lower speed input and output synchronizers<br>(iii) lower speed optical selective splitters and optical combiners | (i) OMSIs<br>(ii) optical time-slot multiplexers and de-multiplexers<br>(iii) higher speed input and output synchronizers<br>(iv) higher speed optical selective splitters and optical combiners |

## 3.2. High Level OCS Implementation

The main purposes of the OCS protocol are to manage a connection request so that connection set up, data transfer, disconnecting a successful connection, and rejecting a connection request can take place. The OCS protocol provides the following phases: (i) connection establishment, (ii) connection confirmation, (iii) data transfer, (iv) disconnection, and (v) connection reject. For the connection establishment phase, the well-known First-Fit method is used.

Figure 3.8 illustrates the connection establishment, connection confirmation, data transfer, and disconnection phases between two workstations. The connection establishment phase is initiated at a source workstation by sending a connection request packet to a source router. This packet is routed through the network to the destination workstation. Then the connection confirmation phase begins. The connection confirmation packet travels from the destination workstation back to the source workstation through the same forward route. Once the packet reaches the source workstation, the optical data transfer phase is started. Data is transmitted from the source workstation to the destination workstation via the established route. The disconnection phase is initiated at the source workstation once the successful connection duration has expired. The mini-slot(s) is(are) released at each router till the destination router. At this point, the destination router informs the destination workstation about the disconnection.

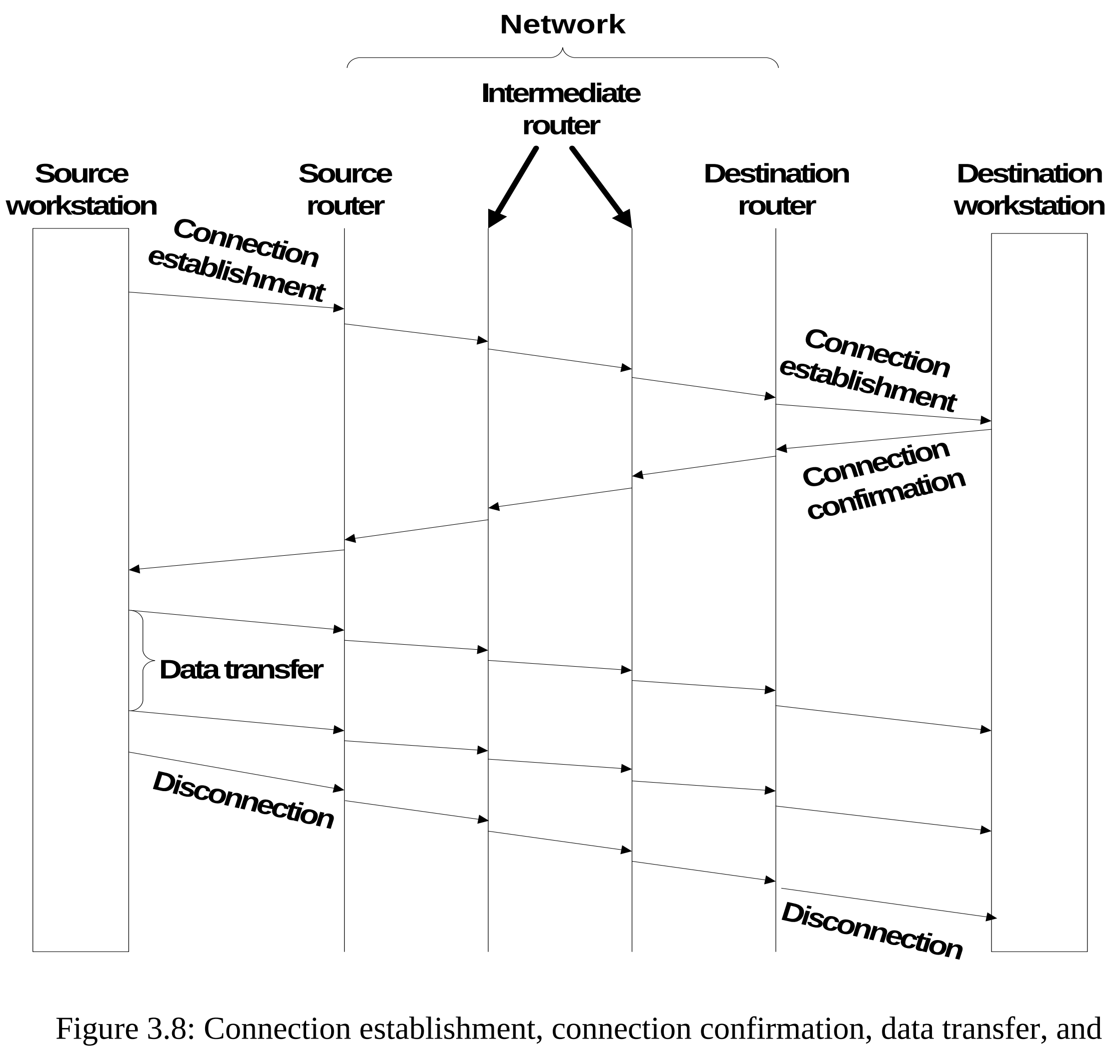


Figure 3.8: Connection establishment, connection confirmation, data transfer, and disconnection phases between two workstations

The First-Fit method is used for mini-slot assignment at the source and intermediate routers. The pseudo-codes for the First-Fit method at an intermediate router are shown as follows:

```
found=0
If the mini-slot(s) of the same time-slot of the same wavelength as previous node is not used
   found=1
Else
              Search for other mini-slot(s) in the same time-slot of the same wavelength
              If there is an available mini-slot(s)
                 found=1
If found
   Set the mini-slot(s) in the same time-slot of the same wavelength to not available
   Store all other relevant information
   Insert the current router address, outgoing mini-slot(s), the outgoing time-slot, the outgoing wavelength into
   the connection establishment packet
   Send the connection establishment packet to the next router of the route
Else
   Insert the source router address, incoming mini-slot(s), the incoming time-slot, the incoming wavelength into
   the reject packet
   Send the reject packet back to the previous router for the release of mini-slot(s), time-slot, wavelength
```

A connection reject phase is initiated at the source router (Figure 3.9) or at an intermediate router (Figure 3.10) of the optical backbone network. At an intermediate router, if there is an available mini-slot(s) in a time-slot of a wavelength, the connection request packet is forwarded to the next router. If there is no mini-slot(s) in a time-slot of a wavelength is available, a reject packet is created and is sent to the previous router, and the allocated mini-slot(s) is released at the previous router. This is continuously being done until the source router is reached. Then source router informs the source workstation about the unsuccessful connection request. If the connection request is initiated by the workstation (Figure 3.9) and there is no mini-slot(s) available, the connection request is rejected immediately and a reply is sent to the workstation from the source router.

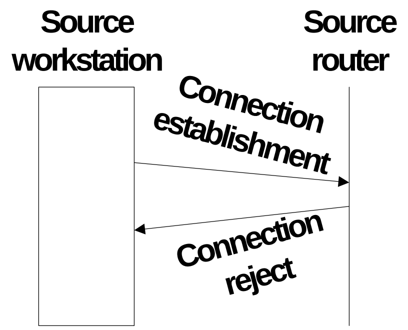


Figure 3.9: Connection reject initiated from the source router

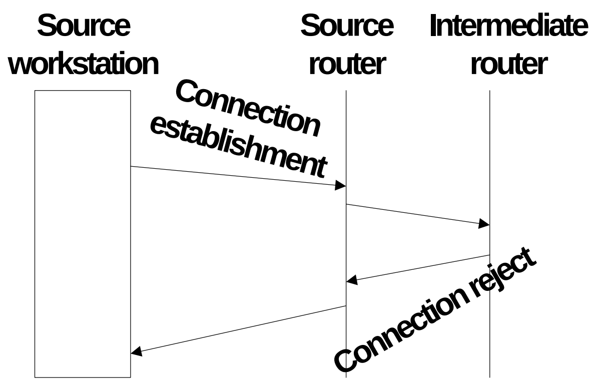


Figure 3.10: Connection reject initiated from an intermediate router

## 3.3 Simulation Setup

The simulation is done using OPNET based on the well-known NSFNET topology (Figure 2.9), a three by five mesh torus topology (Figure 3.11), and a 40-node irregular topology (Figure 3.12). The 40-node irregular topology is generated using the Waxman formula [135] with out-degrees of one to four. Each node is a MTWR. The following configurations are assumed in the simulation: (i) each wavelength has the transmission rate of up to 10Gbps, (ii) each TDM frame consists of 104 time-slots, and (iii) each time-slot consists of eight mini-slots. The TDM frame is transmitted at every 125μs. The three sets of bandwidth allocation under study are 1 to 2 mini-slots, 1 to 5 mini-slots, and 1 to 8 mini-slots. The bandwidth request for each set is randomly generated. For more than one mini-slot request, the algorithm allocates consecutive available mini-slots. The length of each mini-slot packet at MTWR is 187.5 bytes long including the overhead bits. Connection requests at the local access node *i* are generated into network *G*. Then the blocking probability in the network *G* is $\frac{T_b}{T_c}$. All blocked connections are terminated and never return. There is no queuing of blocked connections. These two assumptions relate to a real-life network environment where we need to request for a new connection if the previous request is blocked by the network. The first 1000 connection requests are deleted in order to reach a steady state. The connection duration follows a negative exponential distribution. No connection is blocked for data transfer once the mini-slot of a time-slot in a wavelength is assigned for that connection. The network topology is fixed throughout the simulation. The fixed shortest path routing method is used. Simulation runs are repeated multiple times with different seeds to reduce the margin of errors and obtained a 95% confidence interval for each run.

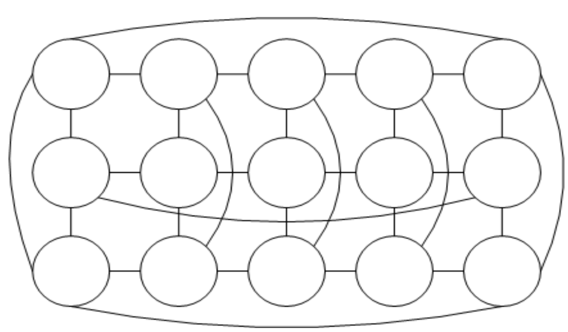

Figure 3.11: Three by five mesh torus topology

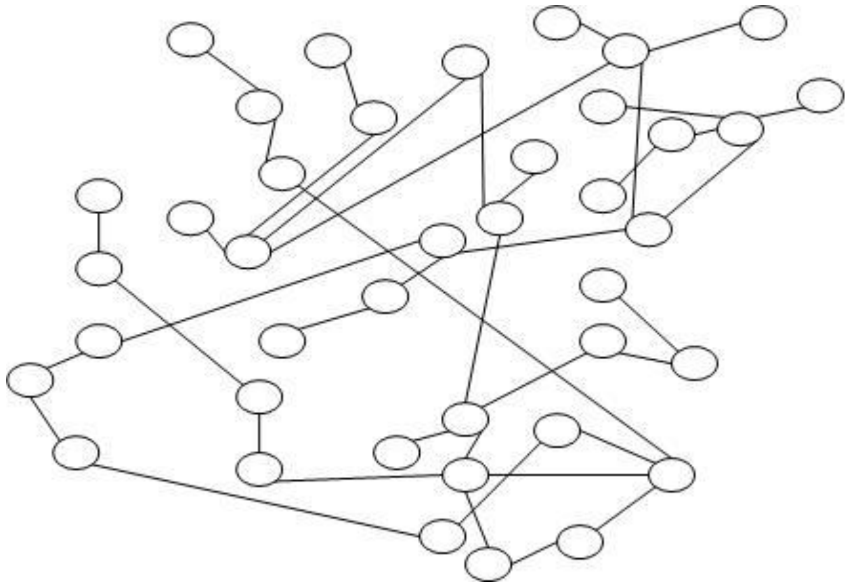

Figure 3.12: 40-node irregular topology

### 3.3.1 Simulation Results

Simulation results are generated for (i) proposed mini-slot TDM wavelength network with request from 1 to 2 mini-slots for each connection request (Mini-Slot-1to2), (ii) proposed mini-slot TDM wavelength network with request from 1 to 5 mini-slots for each connection request (Mini-Slot-1to5), (iii) proposed mini-slot TDM wavelength network with request from 1 to 8 mini-slots for each connection request (Mini-Slot-1to8), (iv) conventional wavelength routed network with no wavelength conversion (Wave-No-Conv) [94], and (v) increasing wavelengths in a fiber. [136] has experimented with data connection duration of 20 to 40 seconds in different sites at Lyon, France and [137] has done simulation of data connection duration that covers 8 to 44 seconds.

Let *W* denote wavelengths, *T* denote time-slots, and *MT* denote mini-slots. Table 3.2 tabulates the topologies used in generating simulation results shown in Figures 3.13 to 3.26.

For simplicity, TEB-SC is normalized into total number of established requested mini-slots, for example a successful connection requests for two mini-slots, and the total number of established requested mini-slots for this connection is two multiply by the number of hops. Offered load in Erlangs is defined as the connection arrival rate multiplied by the average connection duration. As the offered load in Erlangs increases, the blocking probability for each set of simulation results also increases. The reason is that more connection requests are generated when the bandwidth availability is scare. However, the TEB-SC decreases for each set of the simulation results because fewer connections are established. Figure 3.13 presents the results of the blocking probability versus the offered load in Erlangs for Mini-Slot-1to2, Mini-Slot-1to5,

Table 3.2: Topologies used in generating simulation results shown in Figures 3.13 to 3.26

| | NSFNET | 3 by 5 | 40-node |
|---|---|---|---|
| **Figure 3.13** | X | | |
| **Figure 3.14** | X | | |
| **Figure 3.15** | X | | |
| **Figure 3.16** | X | | |
| **Figure 3.17** | X | | |
| **Figure 3.18** | X | | |
| **Figure 3.19** | X | | |
| **Figure 3.20** | X | | |
| **Figure 3.21** | X | | |
| **Figure 3.22** | X | | |
| **Figure 3.23** | | X | |
| **Figure 3.24** | | X | |
| **Figure 3.25** | | | X |
| **Figure 3.26** | | | X |

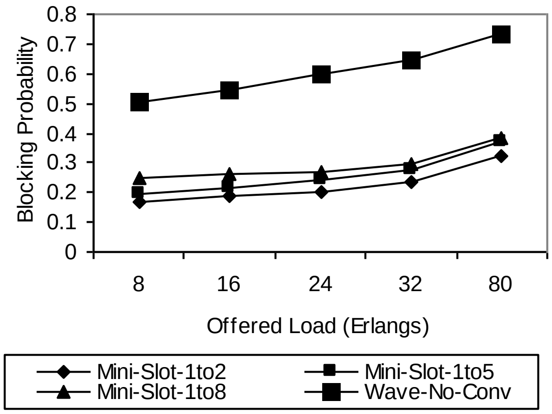


Figure 3.13: Blocking probability versus offered load for average connection duration of 8 seconds

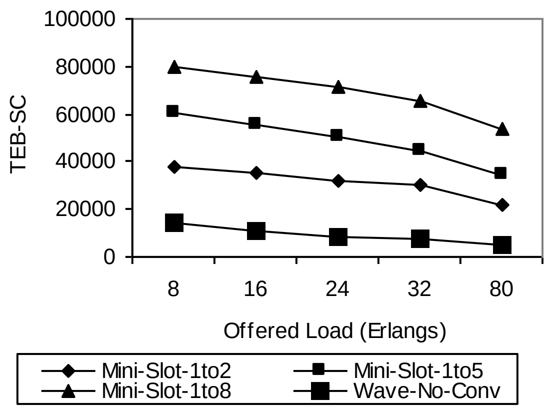


Figure 3.14: TEB-SC versus offered load for average connection duration of 8 seconds

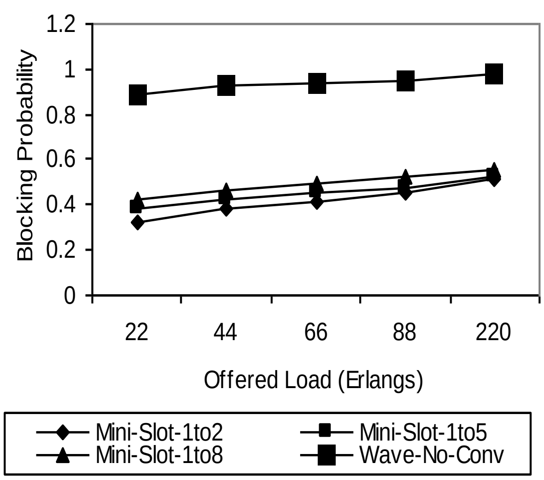


Figure 3.15: Blocking probability versus offered load for average connection duration of 22 seconds

Mini-Slot-1to8 and Wave-No-Conv, with an average successful connection of 8 seconds duration. It is obvious that Mini-Slot-1to2, Mini-Slot-1to5, and Mini-Slot-1to8 have a lower blocking probability than Wave-No-Conv. The reason is that the entire bandwidth in a wavelength is assigned to one successful connection in Wave-No-Conv but only a part of the bandwidth of a wavelength is assigned in the rest of the three systems. Mini-Slot-1to2 has the lowest blocking probability because each successful connection occupies the smallest part of the wavelength bandwidth. Thus, allowing more successful connections to share a wavelength bandwidth as compared with Mini-Slot-1to5 and Mini-Slot-1to8. Figure 3.14 shows the results of the TEB-SC versus offered load in Erlangs for Mini-Slot-1to2, Mini-Slot-1to5, Mini-Slot-1to8 and Wave-No-Conv. It is obvious that Wave-No-Conv has the lowest TEB-SC. The reason is the same as the explanation of Figure 3.13. The wavelength bandwidth can be assigned to only one successful connection in Wave-No-Conv but can be shared among different successful connections in Mini-Slot-1to2, Mini-Slot-1to5, and Mini-Slot-1to8. Mini-Slot-1to8 has the highest fiber bandwidth utilization because it has the highest TEB-SC even though its blocking probability is slightly higher than Mini-Slot-1to2 and Mini-Slot-1to5. The similar conclusion can be derived for an average connection of 22 seconds (Figures 3.15 and 3.16), 30 seconds (Figures 3.17 and 3.18), 44 seconds (Figures 3.19 and 3.20).

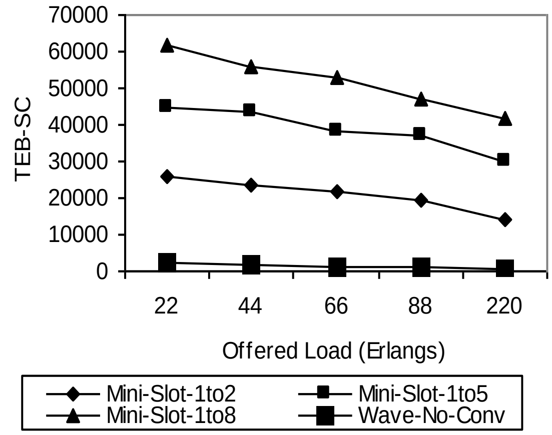


Figure 3.16: TEB-SC versus offered load for average connection duration of 22 seconds

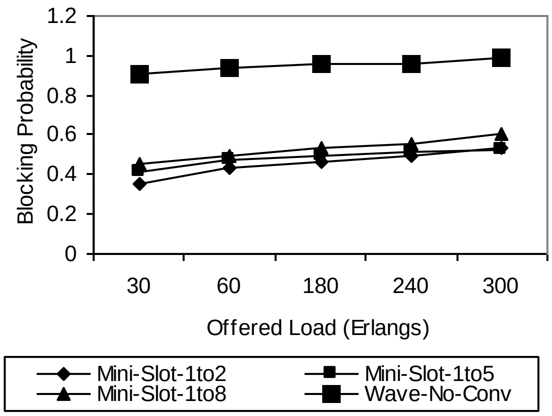


Figure 3.17: Blocking probability versus offered load for average connection duration of 30 seconds

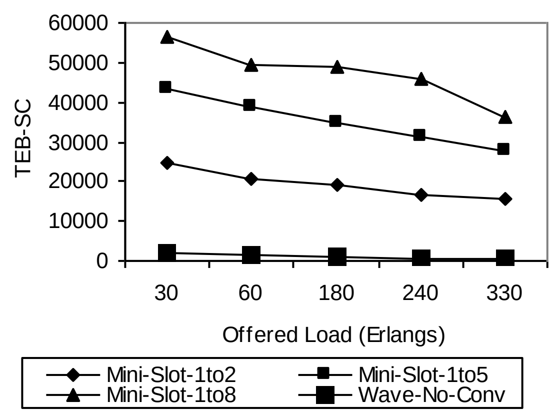


Figure 3.18: TEB-SC versus offered load for average connection duration of 30 seconds

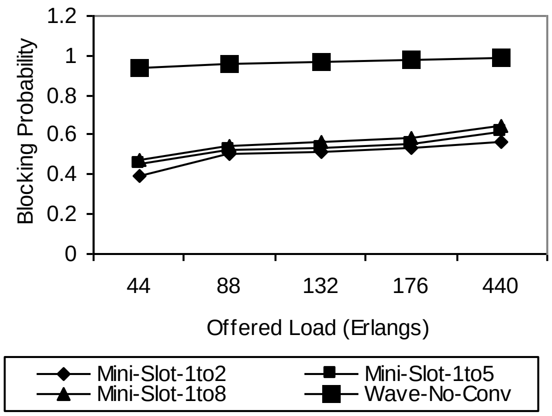


Figure 3.19: Blocking probability versus offered load for average connection duration of 44 seconds

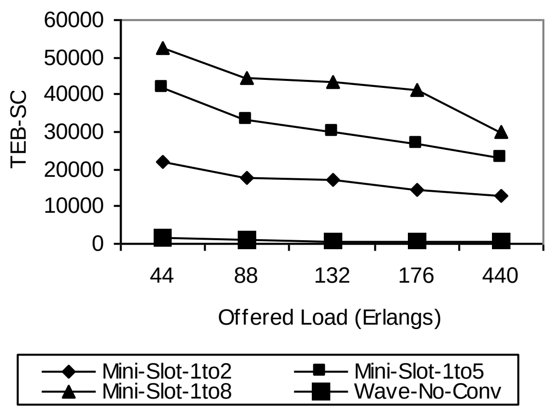


Figure 3.20: TEB-SC versus offered load for average connection duration of 44 seconds

Figure 3.21 shows the blocking probability versus offered load for increasing wavelengths in a fiber for average connection duration of 44 seconds. The mini-slot requests are from one to eight. As the number of wavelengths increases from two to six, it is obvious that the blocking probability decreases because more mini-slots are available for sharing between established connection requests.

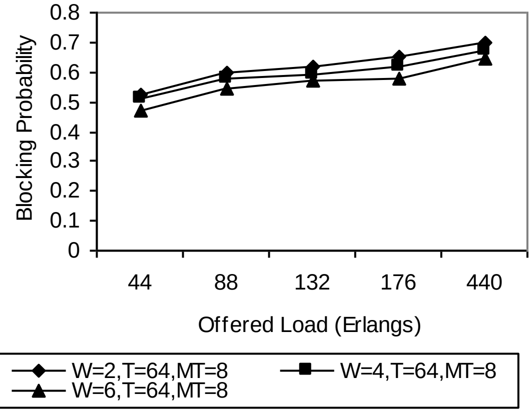


Figure 3.21: Blocking probability versus offered load for increasing wavelengths in a fiber for average connection duration of 44 seconds. Mini-slot requests are from one to eight

As the blocking probability decreases, the TEB-SC increases because more successful connections are established. This is shown in Figure 3.22. Figures 3.23 and 3.24 present the simulation results collected from the three by five mesh torus topology. The analysis of the results is similar to that of Figures 3.13 and 3.14. Figure 3.25 and Figure 3.26 show the simulation results collected from the 40-node irregular topology. An average successful connection duration is 22 seconds. The average number of hops for successful connections is 6.81. As the number of wavelengths increases from 8 to 32, the average blocking probability is higher but the TEB-SC decreases much more because the average number of hops for successful connections is 6.81. Because of the larger network size, the average number of hops between the source and destination has increased. It is a well-known fact that the blocking probability of a route increases as the number of hops for that route increases.

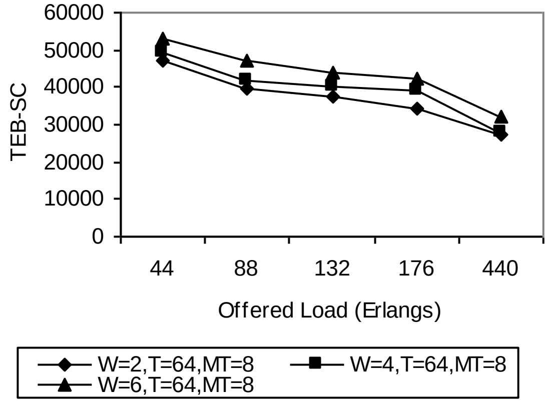


Figure 3.22: TEB-SC versus offered load for increasing wavelengths in a fiber for average connection duration of 44 seconds. Mini-slot requests are from one to eight

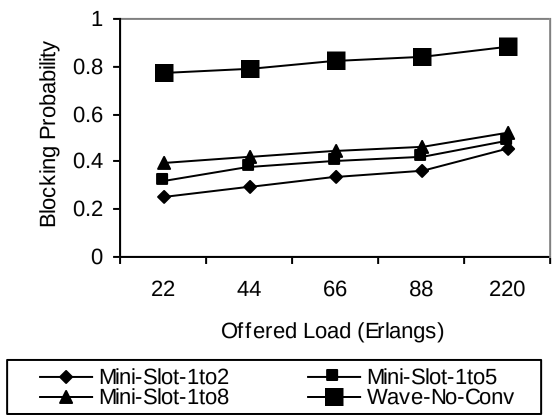


Figure 3.23: Blocking probability versus offered load for average connection duration of 22 seconds. (Three by five mesh torus topology)

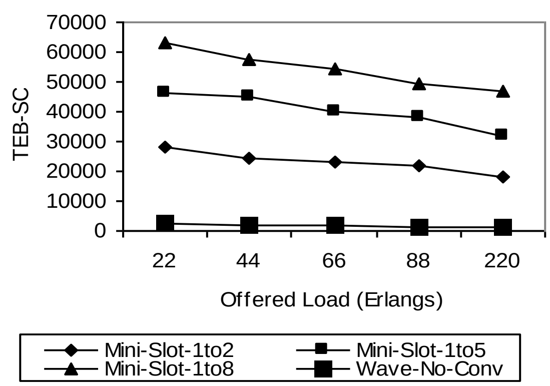


Figure 3.24: TEB-SC versus offered load for average connection duration of 22 seconds. (Three by five mesh torus topology)

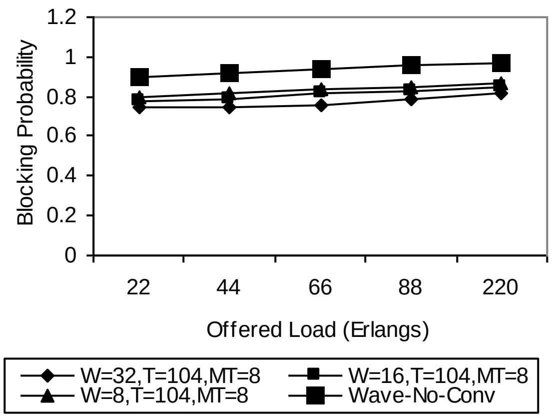


Figure 3.25: Blocking probability versus offered load for increasing wavelengths in a fiber for average connection duration of 22 seconds. Mini-slot requests are from one to two (40-node irregular topology)

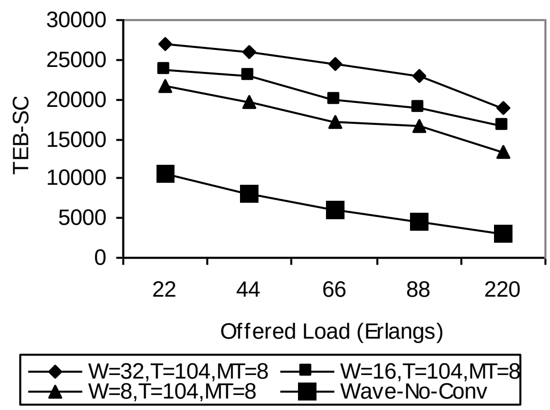


Figure 3.26: TEB-SC versus offered load for average connection duration of 22 seconds. (40-node irregular topology)

## 3.4 Performance Comparison of Shared Time-slot TDM Wavelength Optical WDM Networks and Mini-slot TDM Optical WDM Networks

The simulated results presented in Figures 3.27 and 3.28 are generated based on the NSFNET topology. In order to reach a steady state, the first 1000 connection requests are deleted. The connection duration follows a negative exponential distribution. The fixed shortest path routing method is used, and simulation runs are repeated multiple times with different seeds to reduce the margin of errors and obtained

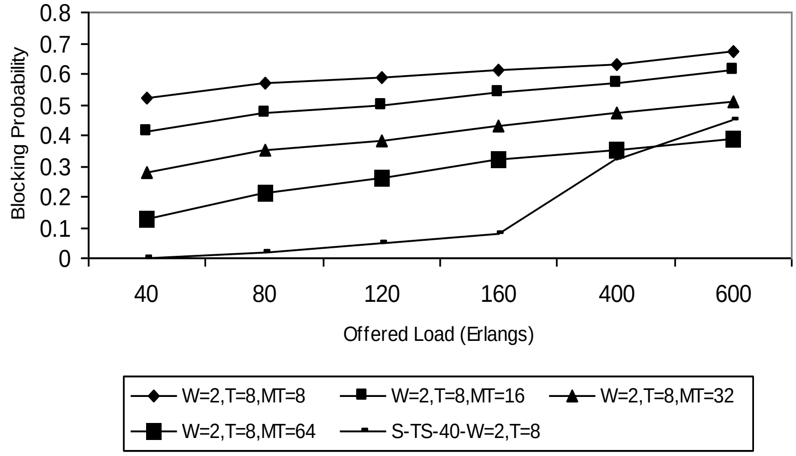


Figure 3.27: Comparison of shared time-slot and mini-slot schemes for *W*=2, *T*=8 and increasing mini-slots (NSFNET topology)

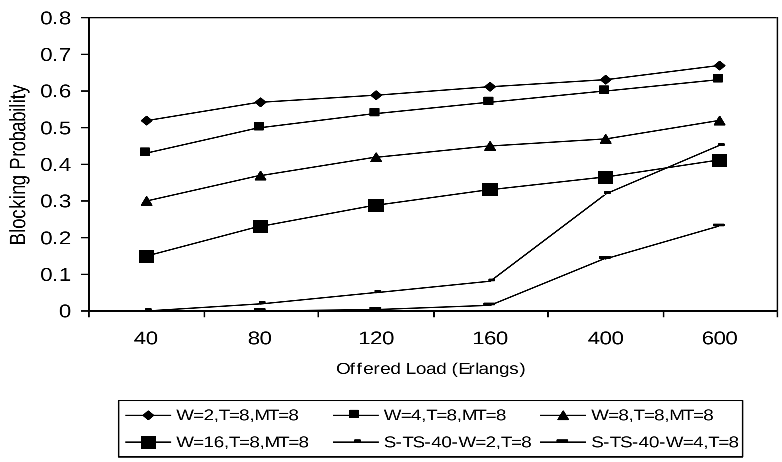


Figure 3.28: Comparison of shared time-slot and mini-slot schemes for increasing wavelengths (NSFNET topology)

a 95% confidence interval for each run. The average duration for successful connections is 40 seconds. For both proposed networks, the transmission speed of a time-slot is 100Mbps. The maximum number of successful connections to share a time-slot is 10. Each connection request for the mini-slot network is from 1 to 2 mini-slots.

Figure 3.27 presents the simulated results of the mini-slot TDM optical WDM network for increasing mini-slots and the shared time-slot TDM WDM optical wavelength network of *W*=2,*T*=8. Figure 3.28 compares the simulated results of both proposed networks for vary of wavelengths. Figure 3.28 does not show the blocking probability of the shared time-slot network ($W$=8,$T$=8) which is zero from 40 to 400 Erlangs but has a blocking probability of 0.02 at 600 Erlangs.

Generally, Figures 3.27 and 3.28 showed that the shared time-slot network has a lower blocking probability than the mini-slot network. The reason is that in the shared time-slot network, an existing connection between a source/destination router pair may admit a new connection request for sharing a timeslot if the total number of requests for sharing the timeslot has been less than 10. However, in the mini-slot network an existing route is removed once the connection duration is lapsed. The next connection request from the same source router to the same destination router may not be successful if there are no free mini-slots. Moreover the number of successful connections reduces with the increasing number of mini-slots requested per connection request. For example, if every connection requests for two mini-slots, the maximum number of successful connections in eight mini-slots is four compared with a maximum of 10 successful connections sharing a time-slot in the shared time-slot scheme.

Interestingly, the blocking probability of the shared time-slot scheme increases rapidly at higher offered load. Thus, at the offered load of 600 Erlangs, the blocking probability of the shared time-slot scheme ($W$=2,$T$=8) is higher than the mini-slot scheme of $W$=2,$T$=8,$MT$=64 (Figure 3.27) and $W$=16,$T$=8,$MT$=8 (Figure 3.28).

## 3.5 Summary

A mini-slot TDM WDM optical network with MTWRs has been proposed. Each MTWR is capable of transmitting data optically at the mini-slot(s) of a time-slot in a wavelength with the support of an electronic system controller. At the intermediate

MTWR, the incoming data is routed without any E/O and O/E conversions. No wavelength conversion is employed in the proposed router architecture. This helps to reduce the cost during implementation. The OCS is performed at each MTWR.

Simulation results show that for lower bandwidth requests, transferring data using the mini-slots of a time-slot in a wavelength gives higher fiber bandwidth utilization than the conventional wavelength routed network with no wavelength conversion. This leads to lower blocking probability and more successful connections. The reason is obvious. More smaller slots are available to handle lower bandwidth connection requests. As the number of wavelengths in a fiber increases, the blocking probability decreases because more mini-slots are available for successful connections. However, at present, these benefits come with the high cost and high complexity of developing an OMSI using FDLs. Hopefully, with the advancement of optical technology, the FDLs can be replaced with inexpensive optical buffers and implementation complexity can be reduced. At present, implementation of this proposed network at high speed is a real challenge and very high speed electronics are required. Our simulation results do not provide any concrete evidence on the effect of network size to the network performance because the link connections of the three networks vary.

Generally, our simulations show that the shared time-slot network has a lower blocking probability than the mini-slot network except for two cases at the offered load of 600 Erlangs.

The next chapter discusses the cost analysis of the proposed networks and future optical trends.

# CHAPTER 4

# Cost Analysis of Proposed Networks and Future Optical Trends

Chapters 2 and 3 describe the architectures of the STSWR and MTWR respectively. In addition, the behavior of the shared time-slot TDM wavelength optical WDM network and that of mini-slot TDM wavelength optical network are investigated using extensive simulations.

The next section of this chapter describes the proposed cost model and the cost analysis performed between a typical WDM network and the proposed networks. Section 4.2 briefly discusses the existing technologies like SONET/SDH and Ethernet that can connect to the core WDM network. Some possible future trends of optical networks are also presented in this section. The main points of this chapter are highlighted in the last section of this chapter.

## 4.1 Total Network Costs

### 4.1.1 Proposed Cost Model

The WDM network set-up cost model consists of the link provisioning cost ($C_{lp}$), the mux-demux cost ($C_{mux\text{-}demux}$), the trans-recv cost ($C_{trans\text{-}recv}$), and the cross-connect cost ($C_{cc}$). The $C_{lp}$ may include the fiber cable cost, optical regenerators, dispersion compensation components, digging cost, and leasing cost for each node. The maximum number of wavelengths in each fiber is a very important design parameter because it decides the number of regenerators and dispersion components required. For long haul networks, regenerators are required. However, the use of regenerators adds noise to the signal. The noise is reduced by using dispersion compensation components like forward error correction.

Consider the case for a conventional WDM network. $C_{lp} = N_f * C_f + N_r * C_r + N_{dc} * C_{dc}$, where $N_f$ is the number of kilometers used, $C_f$ is the cost of fiber for each meter, $N_r$ is the number of optical regenerators used, $C_r$ is the cost of an optical regenerator, $N_{dc}$ is the number of dispersion compensation components used, and $C_{dc}$ is the cost of a dispersion compensation component. Since a lot of fibers have already being laid in the ground [94], the cost of laying fibers, use of optical regenerators, and dispersion compensation components are assumed to be zero ($C_{lp} = 0$) in our case. $C_{mux-demux}$ includes the optical multiplexers and de-multiplexers. Thus, $C_{mux-demux} = N_{mux} * C_{mux} + N_{demux} * C_{demux}$, where $N_{mux}$ is the number of multiplexers used, $C_{mux}$ is the cost of a multiplexer, $N_{demux}$ is the number of de-multiplexers used, and $C_{demux}$ is the cost of a de-multiplexer. The $C_{trans-recv}$ includes the tunable transmitters and receivers. Thus, $C_{trans-recv} = N_{trans} * C_{trans} + N_{recv} * C_{recv}$, where $N_{trans}$ is the number of tunable transmitters used, $C_{trans}$ is the cost of a tunable transmitter, $N_{recv}$ is the number of tunable receivers used, and $C_{recv}$ is the cost of a tunable receiver. The number of wavelengths in each fiber determines the size of each switch. $C_{cc} = N_{oxc} * C_{oxc}$, where $N_{oxc}$ is the number of switches used, and $C_{oxc}$ is the cost of each switch. The cost of a switch increases with the number of cross-points. The maintenance cost of each node is assumed to be 15% multiplied by the cost of each node (see Section 1.2.2.1). The total cost of a WDM network = WDM network set-up cost + WDM network maintenance cost.

Thus, the total cost of a WDM network (WDM-N) = $\sum_{n=1}^{N}(C_{\text{mux-demux}} + C_{\text{trans-recv}} + C_{\text{cc}}) +$ $C_{lp}$ + $\sum_{n=1}^{N}(15\% * \text{cost of each node})$, where $N$ is the number of nodes in the network and the number of optical components in each node is the same.

Consider the case for a shared time-slot TDM wavelength optical network. $C_{OTSI}$ includes the optical time-slot interchangers. Thus, $C_{OTSIs} = N_{OTSI} * C_{OTSI}$, where $N_{OTSI}$ is the number of OTSIs used, and $C_{OTSI}$ is the cost of an OTSI. $C_{\text{inp-outp-sync}}$ includes the input synchronizers and output synchronizers. Thus, $C_{\text{inp-outp-sync}} = N_{inp} * C_{inp} + N_{outp} * C_{outp}$, where $N_{inp}$ is the number of input synchronizers used, $C_{inp}$ is the cost of an input synchronizer, $N_{outp}$ is the number of output synchronizers used, and $C_{outp}$ is the cost of an output synchronizer. $C_{\text{spl-comb}}$ includes the optical selective splitters and optical selective combiners. Thus, $C_{\text{spl-comb}} = N_{spl} * C_{spl} + N_{comb} * C_{comb}$, where $N_{spl}$ is the number of optical selective splitters used, $C_{spl}$ is the cost of an optical selective splitter, $N_{comb}$ is the number of optical selective combiners used, and $C_{comb}$ is the cost of an optical selective combiner. $C_{Ethers'} = N_{Ether} * C_{Ether}$, where $N_{Ether}$ is the number of high speed Ethernet cards used, and $C_{Ether}$ is the cost of a high-speed Ethernet card.

Thus, the total cost of the shared time-slot TDM wavelength optical WDM network (STS-N) = $\sum_{n=1}^{N}(C_{\text{mux-demux}} + C_{\text{trans-recv}} + C_{\text{cc}}) + \sum_{n=1}^{N}(C_{\text{OTSIs}} + C_{\text{inp-outp-sync}} + C_{\text{spl-comb}} + C_{\text{Ethers'}}) +$ $C_{lp} + \sum_{n=1}^{N}(15\% * \text{cost of each node})$, where $N$ is the number of nodes in the network and the number of optical components in each node is the same.

Consider the case for a mini-slot TDM wavelength optical network. $C_{OMSIs}$ includes the OMSIs. Thus, $C_{OMSIs} = N_{OMSI} * C_{OMSI}$, where $N_{OMSI}$ is the number of OMSIs used, and $C_{OMSI}$ is the cost of an OMSI. $C_{inp\text{-}outp\text{-}sync\text{-}m}$ includes the input synchronizers and output synchronizers for mini-slots. Thus, $C_{inp\text{-}outp\text{-}sync\text{-}m} = N_{inp\text{-}m} * C_{inp\text{-}m} + N_{outp\text{-}m} * C_{outp\text{-}m}$, where $N_{inp\text{-}m}$ is the number of input synchronizers for mini-slots used, $C_{inp\text{-}m}$ is the cost of an input synchronizer for mini-slots, $N_{outp\text{-}m}$ is the number of output synchronizers for mini-slots used, and $C_{outp\text{-}m}$ is the cost of an output synchronizer for mini-slots. $C_{spl\text{-}comb\text{-}m}$ includes the optical selective splitters and optical selective combiners for mini-slots. Thus, $C_{spl\text{-}comb\text{-}m} = N_{spl\text{-}m} * C_{spl\text{-}m} + N_{comb\text{-}m} * C_{comb\text{-}m}$, where $N_{spl\text{-}m}$ is the number of optical selective splitters for mini-slots used, $C_{spl\text{-}m}$ is the cost of an optical selective splitter for mini-slots, $N_{comb\text{-}m}$ is the number of optical selective combiners for mini-slots used, and $C_{comb\text{-}m}$ is the cost of an optical selective combiner for mini-slots. $C_{mux\text{-}demux\text{-}m}$ includes the optical multiplexers and de-multiplexers for mini-slots. Thus, $C_{mux\text{-}demux\text{-}m} = N_{mux\text{-}m} * C_{mux\text{-}m} + N_{demux\text{-}m} * C_{demux\text{-}m}$, where $N_{mux\text{-}m}$ is the number of multiplexers for mini-slots used, $C_{mux\text{-}m}$ is the cost of a multiplexer for mini-slots, $N_{demux\text{-}m}$ is the number of de-multiplexers for mini-slots used, and $C_{demux\text{-}m}$ is the cost of a de-multiplexer for mini-slots.

Thus, the cost of the mini-slot TDM wavelength optical network (MS-N) =

$$\sum_{n=1}^{N}(C_{\text{mux-demux}} + C_{\text{trans-recv}} + C_{\text{cc}}) + \sum_{n=1}^{N}(C_{\text{OMSIs}} + C_{\text{inp-outp-sync-m}} + C_{\text{spl-comb-m}} + C_{\text{mux-demux-m}}) + \mathrm{C_{lp}} +$$

$$\sum_{n=1}^{N}(15\% * \text{cost of each node})$$, where $N$ is the number of nodes in the network and the number of optical components in each node is the same.

### 4.1.2 Major Component Costs

The prices and information of various optical components are according to the quotes from vendors and the current market prices and according to our best of knowledge. They are listed as follows:

2*x*2 optical wavelength switch = US$300 [138]

2 ports optical wavelength multiplexer/de-multiplexer (C-band) = US$200 [138]. The price is US$100 per port.

16 ports optical wavelength multiplexer/de-multiplexer (C-band) = US$1600 [138]

Tunable laser = US$5700 [138]

Modulator = US$5400 [139]

Tunable transmitter = tunable laser + modulator = US$11100 (Assume same price for tunable receiver)

1*x*3 optical selective splitter = US$75 [138] . The price is US$25 per outgoing port

2*x*1 optical combiner = US$50 [138]. The price is US$25 per incoming port

Gigabit Ethernet card = US$50 [140]

Optical input/output synchronizer = US$500 [141]. (Assume same price as SDH synchronizer because there is no known commercial product of optical synchronizer for time-slot stream of 1 μs per time-slot or mini-slot stream of 115ns per mini-slot. The experimented optical synchronizers of 1 μs per time-slot and 115 ns per mini-slot are shown to be possible in [92] and [133] respectively.)

Optical time-slot interchanger (OTSI) (8*x*8 time-slots) = US$500 [142]. (Assume same price as digital time-slot interchanger because there is no known commercial product of OTSI. The design and feasibility of OTSI in changing state within 1 μs is shown to be possible in [90].)

Optical mini-slot interchanger (OMSI) (8*x*8 mini-slots) = US$500 [142]. (Assume same price as digital time-slot interchanger because there is no known commercial product of OMSI. The feasibility of OMSI changing state within 115ns is shown to be possible in page 52.)

Optical TDM (OTDM) multiplexer/de-multiplexer per port is US$100. (Assume same price as optical wavelength multiplexer/de-multiplexer because there is no known commercial standalone product of OTDM)

### 4.1.3 Cost Analysis

The following shows the estimated cost per node of the respective node of WDM network, shared time-slot TDM wavelength optical WDM network, and mini-slot TDM wavelength optical network.

(i) The cost of a WDM node = $(C_{\text{mux-demux}} + C_{\text{trans-recv}} + C_{cc}) + C_{lp} +$ (15% * cost of each node)

For example, the cost of a WDM node of two wavelengths per fiber (Figure 2.1) in 2007 = (US$800 + US$88,800 + US$600) + 0 + (15% * US$90,200) = US$103,730

Thus, the cost of a 14-node WDM network = US$103,730 * 14 = US$1,452,220 (*W*=2 per fiber in Table 4.1)

(ii) The cost of a shared time-slot TDM wavelength optical WDM node

$= (C_{\text{mux-demux}} + C_{\text{trans-recv}} + C_{cc}) + C_{lp} + (C_{\text{OTSIs}} + C_{\text{inp-outp-sync}} + C_{\text{spl-comb}} + C_{\text{Ethers'}}) +$ (15% * cost of each node)

For example, the cost of a shared time-slot TDM wavelength optical WDM node (Figure 2.6 and Figure 2.7) of $W$=2,$T$=8 per fiber in 2007

= (US$800 + US$88,800 + US$600) + 0 + (US$2,000 + US$4,000 + US$500 + US$400) + (15% * US$97,100) = US$111,665

Thus, the cost of a 14-node shared time-slot TDM wavelength optical WDM network is = US$111,665 * 14 = US$1,563,310 ($W$=2,$T$=8 per fiber in Table 4.2)

(iii) The cost of a mini-slot TDM wavelength optical node

$$= (C_{\text{mux-demux}} + C_{\text{trans-recv}} + C_{\text{cc}}) + \mathrm{C}_{\text{lp}} + (C_{\text{OMSIs}} + C_{\text{inp-outp-sync-m}} + C_{\text{spl-comb-m}} + C_{\text{mux-demux-m}}) + (15\% * \text{cost of each node})$$

For example, the cost of a mini-slot TDM wavelength optical node (Figure 3.3 and Figure 3.4) of $W$=2,$T$=8,$MT$=8 per fiber in 2007

= (US$800 + US$88,800 + US$600) + 0 + (US$16,000 + US$32,000 + US$4,000 + US$6,400) + (15% * US$148,600) = US$170,890

Thus, the cost of a 14-node shared time-slot TDM wavelength optical WDM network = US$170,890 * 14 = US$2,392,460 ($W$=2,$T$=8,$MT$=8 per fiber in Table 4.3)

Based on the above estimation, we can compute the cost of the respective networks as follow, bear in mind the assumption of zero cost for link provisioning ($C_{lp}$) . We will use the 14-node topology as an example in calculating the total cost of each of the network. Each node is assumed to have two incoming and two outgoing fiber links. Assume that there are eight high speed Ethernet ports for each shared time-slot TDM wavelength optical WDM node. The cost of a 14-node network to be constructed with the respective network technology is obtained by first calculating the cost of each node of that technology (assuming all nodes of a network are identical) multiplied by 14. The results are presented in Table 4.1 (WDM network), Table 4.2 (Shared time-slot TDM wavelength optical WDM network), and Table 4.3 (Mini-slot TDM wavelength optical network), where *W* denotes wavelength, *T* denotes time-slot, and *MT* denotes mini-slot. For the mini-slot TDM wavelength optical network, eight time-slots are chosen because we can compare the costs with shared time-slot TDM wavelength optical WDM network.

The difference in price for the WDM network and the shared time-slot TDM wavelength optical WDM network is the summation of additional costs of OTSIs, input/output time-slot synchronizers, optical time-slot splitters/combiners, Ethernet cards, and maintenance costs for each node. However, for the WDM network and the mini-slot TDM wavelength optical network, the difference in price is the summation of additional costs of OMSIs, input/output mini-slot synchronizers, optical mini-slot splitters/combiners, TDM multiplexers/de-multiplexers, and maintenance costs for each node. A network with 16 wavelengths in WDM network or shared time-slot TDM wavelength optical WDM network is much more expensive than the same network with

Table 4.1: Total cost 14-node topology for WDM network

| **WDM network** | ***W*=2 per fiber** | ***W*=8 per fiber** | ***W*=16 per fiber** |
|---|---|---|---|
| **2007** | US$1,452,220 | US$5,808,880 | US$11,617,760 |
| **2008** | US$726,110 | US$2,904,440 | US$5,808,880 |
| **2009** | US$363,055 | US$1,452,220 | US$2,904,440 |
| **2010** | US$181,528 | US$726,110 | US$1,452,220 |

Table 4.2: Total cost 14-node topology for Shared time-slot TDM wavelength optical WDM network

| **Shared time-slot TDM wavelength optical WDM network** | ***W*=2,*T*=8 per fiber** | ***W*=8,*T*=8 per fiber** | ***W*=16,*T*=8 per fiber** |
|---|---|---|---|
| **2007** | US$1,563,310 | US$6,233,920 | US$12,461,400 |
| **2008** | US$781,655 | US$3,116,960 | US$6,230,700 |
| **2009** | US$390,828 | US$1,558,480 | US$3,115,350 |
| **2010** | US$195,414 | US$779,240 | US$1,557,675 |

Table 4.3: Total cost 14-node topology for mini-slot TDM wavelength optical network

| **Mini-slot TDM wavelength optical network** | ***W*=2,*T*=8, *MT*=8 per fiber** | ***W*=8,*T*=8, *MT*=8 per fiber** | ***W*=16,*T*=8, *MT*=8 per fiber** |
|---|---|---|---|
| **2007** | US$2,392,460 | US$9,569,840 | US$19,139,680 |
| **2008** | US$1,196,230 | US$4,784,920 | US$9,569,840 |
| **2009** | US$598,115 | US$2,392,460 | US$4,784,920 |
| **2010** | US$299,058 | US$1,196,230 | US$2,392,460 |

two or eight wavelengths. The reason is the very high price of each tunable transmitter or receiver. The mini-slot TDM wavelength optical network is much more expensive than the other two networks because it requires a lot more OMSIs, input/output synchronizers, optical splitters/combiners, and TDM multiplexers/de-multiplexers. As the number of wavelengths increases in the network, the price differences also increase for the three networks because of the very large number of OMSIs, input/output synchronizers, optical splitters/combiners, and TDM multiplexers/de-multiplexers require for implementation. The projected price difference of the three networks decreases because of the assumption that optical component costs decrease by half every year [143]. This is shown in Figure 4.1, Figure 4.2, and Figure 4.3.

In next section, the current state of the main existing technologies and inter-working of main existing technologies with the core WDM technology are briefly described, and the possible future trends in optical networks are predicted.

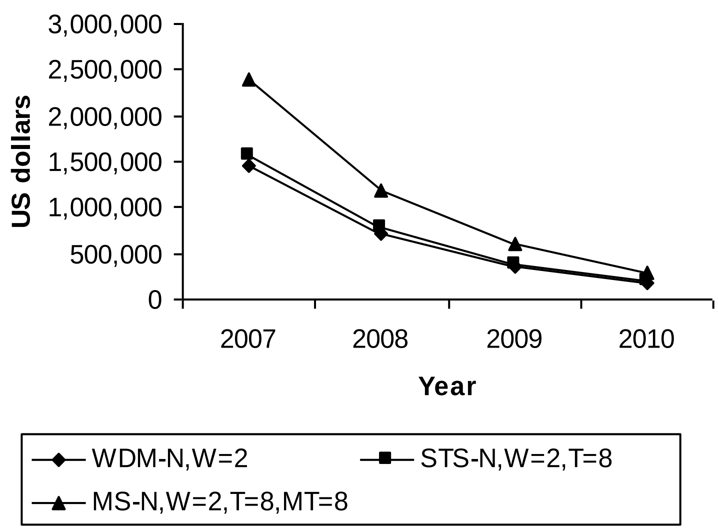


Figure 4.1: Cost comparison of WDM network ($W$=2), Shared time-slot TDM wavelength optical WDM network ($W$=2,$T$=8), and Mini-slot TDM wavelength optical network ($W$=2,$T$=8,$MT$=8). Each network has 14 nodes.

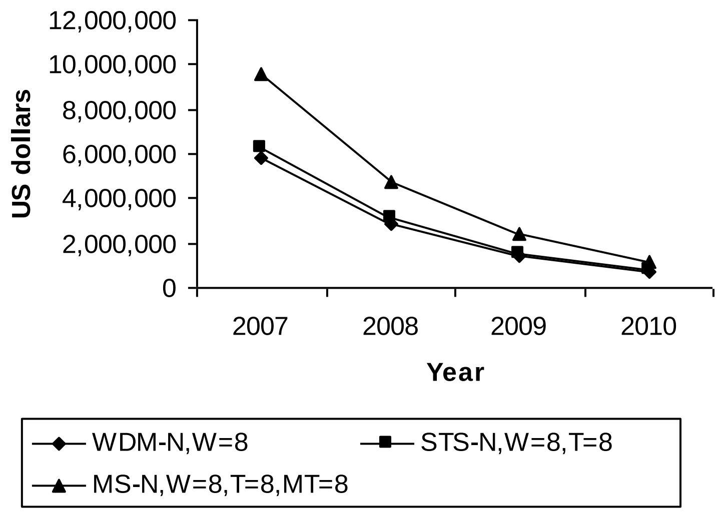


Figure 4.2: Cost comparison of WDM network (*W*=8), Shared time-slot TDM wavelength optical WDM network (*W*=8,*T*=8), and Mini-slot TDM wavelength optical network (*W*=8,*T*=8,*MT*=8). Each node has 14 nodes.

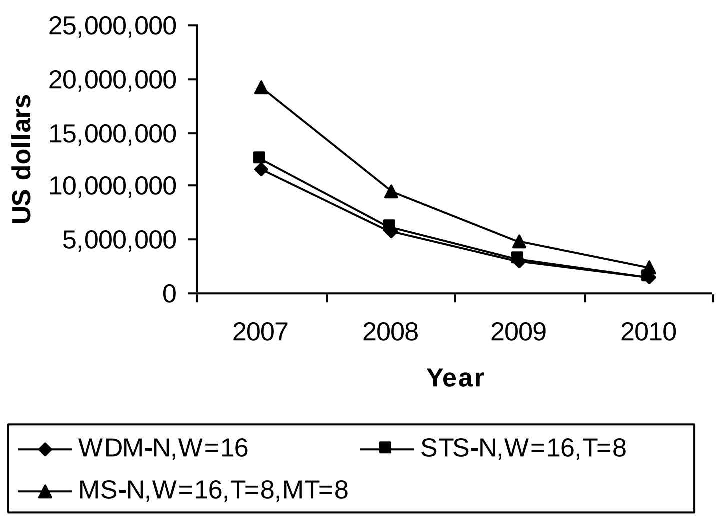


Figure 4.3: Cost comparison of WDM network (*W*=16), Shared time-slot TDM wavelength optical WDM network (*W*=16,*T*=8), and Mini-slot TDM wavelength optical network (*W*=16,*T*=8,*MT*=8). Each network has 14 nodes.

## 4.2 Existing Technologies

The existing technologies discussed in this section are as follows: SONET/SDH, Asynchronous Transfer Mode (ATM), Fiber Distributed Data Interface (FDDI), and Ethernet.

### 4.2.1 SONET/SDH

SONET/SDH will continue to play a role in optical networking because it is optimized for legacy voice traffic and has solid legacy voice support installation. It can provide operations, administration, maintenance, and provisioning (OAM&P) for optical networking. Moreover, SONET/SDH can carry ATM cells, IP packets, and other types of traffic. SONET channels without virtual circuits are the wrong size for carrying Ethernet traffic. Thus, a lot of bandwidth is wasted.

In long distance links, SONET/SDH is no longer the only option. WDM has many advantages over SONET/SDH configurations like optical amplifiers can be spaced 120km apart instead of using electrical regenerators spaced 40km apart in SONET/SDH configuration.

Most Metropolitan Area Networks (MANs) employ SONET/SDH rings [144]. Common services like T1, T3, OC-3, ATM, and Frame Relay dedicated can be connected to this ring configuration. Figure 4.4 presents an overview of this architecture. The SONET/SDH ring can then be connected to the WDM core network. With the emergence of WDM technology, it is natural to evolve from the traditional SONET/SDH rings to WDM SONET/SDH rings. Traffic grooming is performed to achieve high bandwidth utilization in SONET/SDH rings operating on a particular wavelength. Optical ADMs are used to add or drop wavelengths from the fiber. As data traffic continues to grow rapidly, its ‘bursty’ and unpredictable nature will become dominant in the MAN traffic. In order to deal with such “burstiness,” the MAN architecture should be flexible and exploit the full advantages of WDM technology. Thus, the next generation MANs may use WDM mesh topologies.

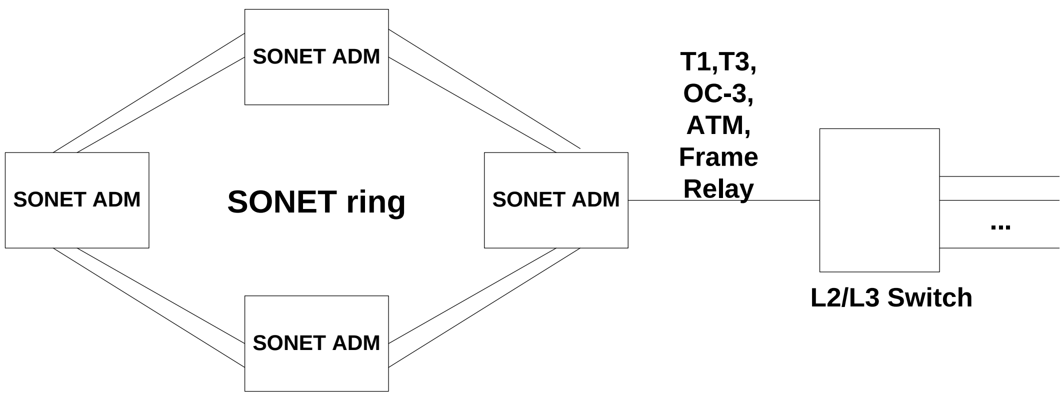


Figure 4.4: Overview of services to a SONET ring

At present, WDM technology is still too expensive for access networks. TDM is still more cost-effective and practical [143]. In order for WDM technology to be commercially viable for access networks, it must be able to provide significant benefits over existing access network solutions, and must be compatible with traditional access technologies like Ethernet and TDM technology.

### 4.2.2 ATM

ATM is popular for delivering Broadband Integrated Services Digital Network (B-ISDN). However, Internet has replaced B-ISDN services. For transport data unit, switching, and multiplexing, WDM is the dominant technology in the optical world. Thus, in the world of optical networking, ATM is being squeezed [85]. However, ATM is still popular with Virtual Private Network access for private organizations because of added security provided by ATM virtual circuits. The ATM switch can be connected to the SONET/SDH ring.

### 4.2.3 FDDI

FDDI is normally employed in the LAN backbone connecting sites over a MAN. FDDI mapping into SONET OC-3 (155.52 Mbps) requires 25Mbps of FDDI 4B/5B encoding overhead and uses 100Mbps for information transfer. The rest of the bandwidth is wasted. When a wavelength is used for FDDI traffic, only the optical coding of the assigned wavelength needs to be known. This requires less bandwidth overhead and the bandwidth not used is less. Assume each wavelength is running at 125Mbps. The user pays for 125Mbps of bandwidth but uses 100Mbps for information transfer. The FDDI service only occupies a wavelength in each fiber. The rest of the wavelengths are available for other services. Moreover, the WDM cross-connect nodes can even be customer owned and operated.

### 4.2.4 Ethernet

Vendors today have built WDM products with Ethernet interfaces and TDM modules [5,144,145]. Ten gigabit Ethernet (GbE) backbone is expected to be popular in the MANs for data traffic. It has the following advantages over the SONET:

- Ethernet inter-works very well with IP traffic, and IP traffic is fast growing in metro networks;

- SONET hardware is very expensive. It is estimated that Ethernet equipment costs less than 70% of SONET equipment;
- SONET access in the MAN is very wasteful of bandwidth for Ethernet LAN because a 10Mbps Ethernet bandwidth requires OC-1 (51.84 Mbps) or a 100Mbps Ethernet bandwidth requires OC-3 (155.52 Mbps). Hence, Metropolitan Ethernet is a perfect matched for standard LAN Ethernet access;
- Ethernet can be easily upgraded whereas increases in capacity in SONET is expensive, and time-consuming due to the need to manually configure of each multiplexer in the ring. SONET is not optimized for data traffic.

Currently, the advantages of SONET are that SONET is optimized for voice traffic and a lot of SONET ADM has already being installed in MANs. However, the next generation of SONET equipment [148] will provide more efficient data services, and easy migration. Moreover, this new class equipment will be backward compatible with legacy SONET systems. The SONET and Ethernet technologies are expected to compete fiercely in the MANs area.

As the demand for bandwidth in access networks increases, it is imperative to provide more bandwidth to the access networks. Today different solutions like digital subscriber loops and hybrid fiber coax [149] are used to support the demand for higher bandwidth. However, Ethernet Passive Optical Network (EPON) is emerging as a promising solution for the next generation access networks. There has been a lot of research being done in this area. EPON preserves the IEEE 802.3 frame format. EPON is an optimized architecture for fiber to home [149] and provides a low cost Ethernet residential access provided by the service providers. In short, EPON provides point-to-multipoint architecture, uses less expensive passive optical couplers, and the expensive optical line terminator (OLT) is shared by subscribers. Figure 4.5 illustrates an overview of the EPON architecture. The OLT may reside in the central office. The central office may link to core WDM technology, SONET rings in a MAN, or GbE in a MAN. There has been an EPON field trial environment in Taiwan [150]. Quality Of Service (QOS) in EPON has been studied in [151]. Performance of TDM over EPON is analyzed in [152]. Services provided by EPON are illustrated in [153]. Optical Ethernet is evolving very quickly in MANs [154].

Optical Ethernet is still new in long-haul networks. There are commercial 10 GeB Ethernet products that allow point-to-point duplex connections for the wide area network (WAN).

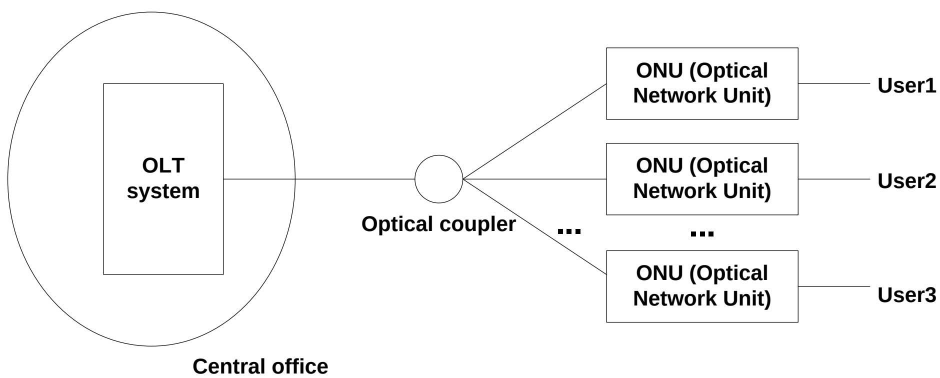


Figure 4.5: Overview of EPON architecture

### 4.2.5 Possible Future Trends in Optical Networks

Currently, there are existing WDM products that allow Ethernet access to TDM modules. The TDM modules support voice and Ethernet traffic. This trend and the cost reduction of the proposed shared time-slot TDM wavelength optical network in the near future (see Figures 4.1, 4.2, and 4.3) can pave the way for the actual implementation of this network.

EPON is going to be an emerging solution for the next generation access network. One possible future trend is EPON access to WDM network by encapsulating Ethernet data into TDM frames since there are already commercial WDM products that perform similar functions. The next generation SONET/SDH products will solve the shortcomings of the current SONET/SDH products. This will allow the SONET/SDH technology to compete with the GbE technology in the MANs area. The next generation MANs may use WDM mesh topologies. WDM will still be the dominant technology in the core networks. Optical Ethernet is still very new in MANs and WANs, but this trend may continue to evolve.

## 4.3 Summary

The cost model is used to determine the implementation costs of the two proposed networks. The differences in prices between a typical WDM network and the two proposed networks will become lesser in the future because of the prediction that the optical components costs will half every 12 months.

We have provided a brief overview of the existing technologies and competing technologies that can connect to the WDM backbone network. With regard to the possible of trends in optical networks, SONET/SDH will still remain dominant in the MANs but GbE is emerging fast in this area. In the access networks, traditional Ethernet is and will remain as the most popular for data transfer, but for voice traffic, TDM will still be a very dominant technology. WDM will remain the main technology for core networks. The availability of commercial WDM products with TDM modules that support voice and Ethernet traffic allow Ethernet access to WDM network by encapsulation of Ethernet frames into TDM format. In addition, EPON access to WDM network via TDM technology is one of the possible future trends because of the current availability of WDM products that allow Ethernet access.

The next chapter explains the workings of the flexible optical architecture that can perform traffic grooming at the time-slot and mini-slot levels. At present, the advantages of this architecture come with very high complexities and costs. Hopefully with the tremendous advancement of optical technology, commercial implementation of this architecture can become a reality one day.

# CHAPTER 5

# Flexible Optical Architecture[3]

This chapter briefly explains a flexible optical architecture in each node that can perform OCS traffic grooming at time-slots and mini-slots levels.

The shared time-slot TDM wavelength optical WDM node of chapter 2 provides limited flexibility of swapping time-slots in a wavelength of a fiber. It allows the time-slots interchange within the wavelength of a fiber. On the other hand, the mini-slot TDM wavelength optical node of Chapter 3 only allows the interchange of mini-slots within a time-slot in a wavelength of a fiber. It is therefore desirable to have a optical switch with a flexible architecture that can support both the time-slots and mini-slot operations.

This architecture allows switching of time-slots between different wavelengths in a fiber and switching of mini-slots between different time-slots within a wavelength and a fiber. Section 5.1 briefly explains the workings of the flexible optical architecture at each node. The major components of this architecture are a electronic system controller, multiplexing/de-multiplexing mini-slots (MDM), OTSIs, TS synchronizations blocks, mini-slot (MS) synchronization blocks, OMSIs, optical time-slot switches, and optical mini-slot switches. A main concern of this new proposed architecture is its technical feasibility of major components which is briefly explained in Section 5.2. Then we conclude this chapter.

---

[3] A part of this chapter has been presented in 4th Australian Network and Telecommunications Applications Conference (ANTAC), "Optical Architecture For Traffic Ungrooming and Grooming at Intermediate Destinations," Sydney, Australia, 8th-10th Dec. 2004.

## 5.1 Proposed Flexible Optical Architecture

Figure 5.1 presents the simplified grooming architecture consisting of a wavelength switch fabric and optical grooming (OG) fabrics. Wavelength switching with no WCs is performed in the wavelength switch fabric. Assume that each fiber has $W$ wavelengths ($\lambda$s), and each wavelength has one OG fabric. An OG fabric for one of the wavelengths in a fiber – wavelength one in fiber one ($F_1\lambda_1$) is discussed in Section 5.1.1.

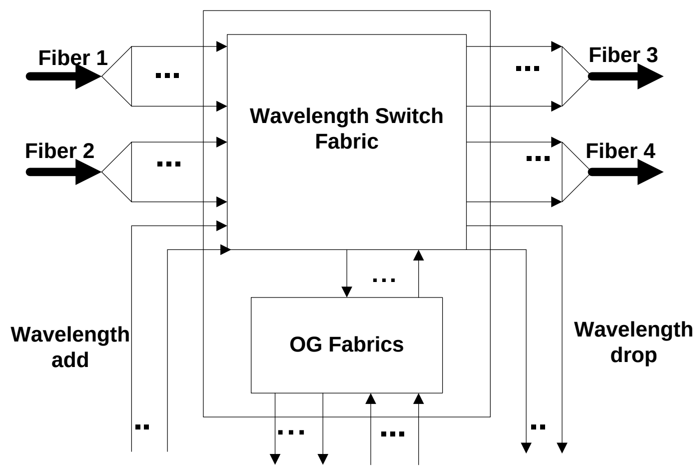


Figure 5.1: Simplified grooming architecture

### 5.1.1 $F_1W_1$ OG Fabric

This OG fabric (see Figure 5.2) provides optical multiplexing and de-multiplexing at finer granularity with OTSI. Assume that an OCS connection set-up is already successful. Thus, the required slot assignments are assigned at each node. It is also assumed that data is currently being optically transferred between nodes. When $F_1\lambda_1$ OG fabric receives a packet, this fabric separates the packet into a data portion and a control header. The data portion contains data to be transmitted, while the control header carries labels for correct data flow inside each node. The control header is passed to the electronic system controller which uses the labels stored in the control header to make switching decisions, control operations of OTSI and MDM, and manipulating optical crossbars. FDLs are used to provide necessary delay controls before the slots that contain the data reach all the components in the node.

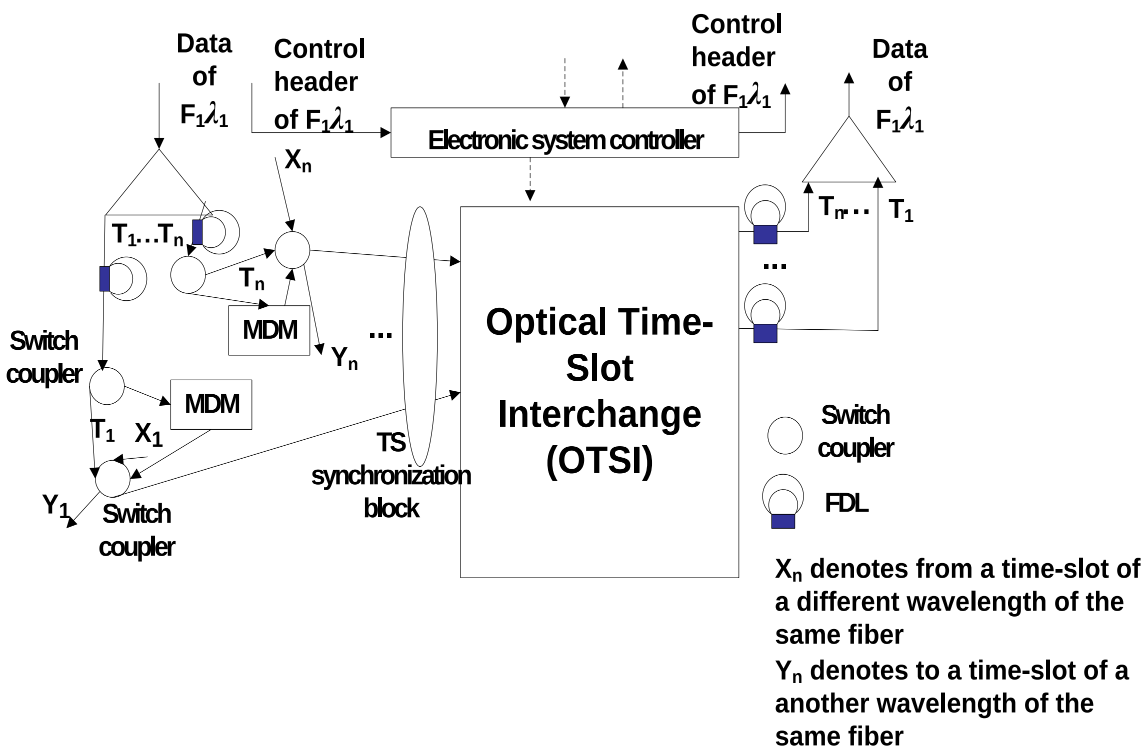


Figure 5.2: Simplified diagram of OG fabric for $F_1\lambda_1$

The data of $F_1\lambda_1$ is de-multiplexed into individual time-slots ($T_1 \ldots T_n$). As an example, time-slot, $T_n$ is used to illustrate rest of the data flow. The $T_n$ either flows to the MDM component or another path after the first switch coupler. If $T_n$ is to be de-multiplexed into mini-slots, it is sent to the MDM component. Otherwise, $T_n$ is directed to a different path. If the $T_n$ is for another wavelength in the same fiber, the $T_n$ is directed to path $Y_n$. A time-slot from a different wavelength of the same fiber arrives from path

$X_n$. After the MDM component, $T_n$ travels through another switch coupler to the TS synchronization block before it is fed into the OTSI. The incoming time-slots ($T_1 \ldots T_n$ ) from different switch couplers are multiplexed together into a time-slot stream in the synchronizing block, where the time-slot stream is synchronized before entering the OTSI. After the OTSI, the time-slots ($T_1 \ldots T_n$ ) are multiplexed to form the data portion of $F_1\lambda_1$. Before exiting the OG-fabric, a multiplexer combines the control header and data portion of $F_1\lambda_1$ back to $F_1\lambda_1$. Then the $F_1\lambda_1$ is fed to the wavelength switch fabric, where $F_1\lambda_1$ is switched to $F_3\lambda_1$.

### 5.1.2 MDM Component

In the MDM component (see Figure 5.3), the $T_n$ is optically de-multiplexed into mini-slots ($MS_1 \ldots MS_n$) and multiplexed them back to $T_n$. If the mini-slot, $MS_n$ in $T_n$ is required to sent to another time-slot of the same wavelength and fiber, it is directed to path $B_n$. In contrast, a mini-slot from another time-slot of the same wavelength and fiber arrives from path $A_n$. In the mini-slot synchronizer block, the mini-slots ($MS_1 \ldots MS_n$) are multiplexed together into a mini-slot stream, and the mini-slot stream is synchronized before entering the OMSI. The feasibility of performing OMSI and synchronizing of mini-slots is explained in chapter 3. After the OMSI, data is either added or dropped from the node using optical switch couplers. The existing mini-slots are multiplexed optically with incoming mini-slots into a time-slot. Then, the $T_n$ exits from MDM component .

### 5.1.3 Switching Time-slots between Different Wavelengths in a Fiber and Mini-slots between Different Time-slots Within a Wavelength and a Fiber

In order to realize the flexibility of switching time-slots between different wavelengths in a fiber and mini-slots between different time-slots within a wavelength of a fiber, the optical switches are used. Figure 5.4 is used to show the time-slots flow for a fiber that contains three wavelengths and *n* time-slots. Before the time-slots are fed into the optical time-slot switch, the time-slots are first multiplexed in the

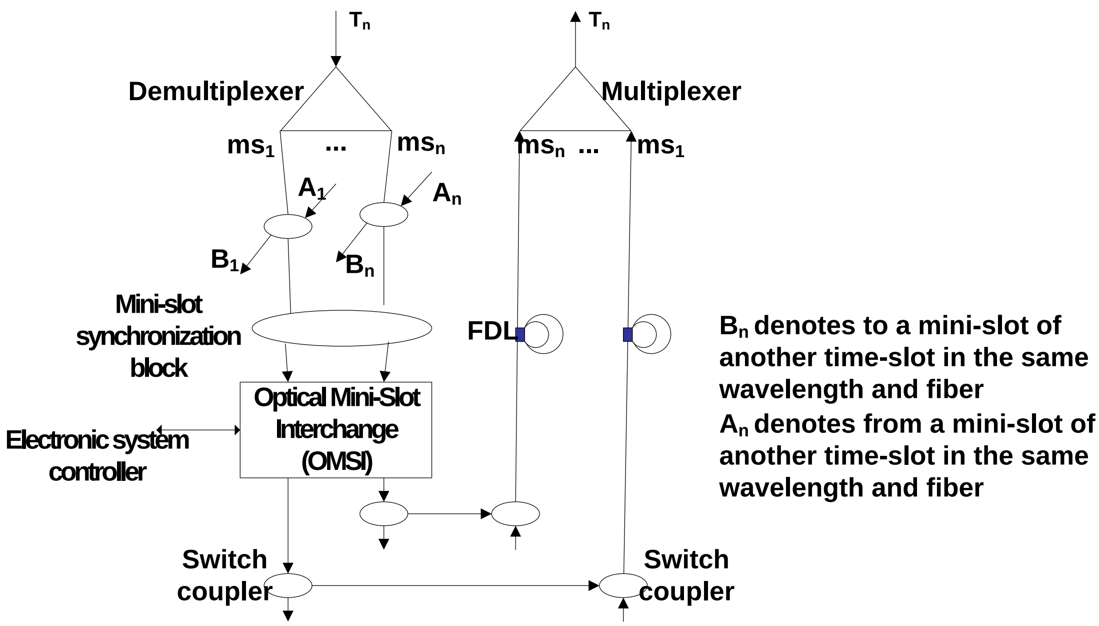


Figure 5.3: Multiplexing/De-multiplexing mini-slots (MDM) component

synchronization block into a time-slot stream, and then the stream is synchronized. After that the time-slot stream is de-multiplexed into individual time-slots in the synchronization block before entering the optical time-slot switch. Assume that there is some blocking between optical time-slot switches, and each time-slot requires one fiber line. Then the value $N$ of each time-slot switch ($N$ x $N$) is the number of time-slots in a wavelength plus the number of input time-slots from the other two optical time-slot switches. In a non-blocking situation, the value $N$ is the number of wavelengths in a fiber multiplied by the number of time-slots in a wavelength. In Figure 5.4, input fiber line $F_1\lambda_1T_n$ represents path $Y_n$ in Figure 5.2 to optical time-slot switch 1, while path $X_n$ in Figure 5.2 is represented by output fiber line $F_1\lambda_1T_n$ from optical time-slot switch 1 in Figure 5.4.

To provide such flexibility at the mini-slot level, optical mini-slot switches are used. Figure 5.4 can be used to demonstrate the mini-slot flow of different time-slots in the same wavelength and fiber except that optical mini-slot switches and mini-slot synchronization blocks are used and the flow is in mini-slot of a time-slot within a wavelength and a fiber.

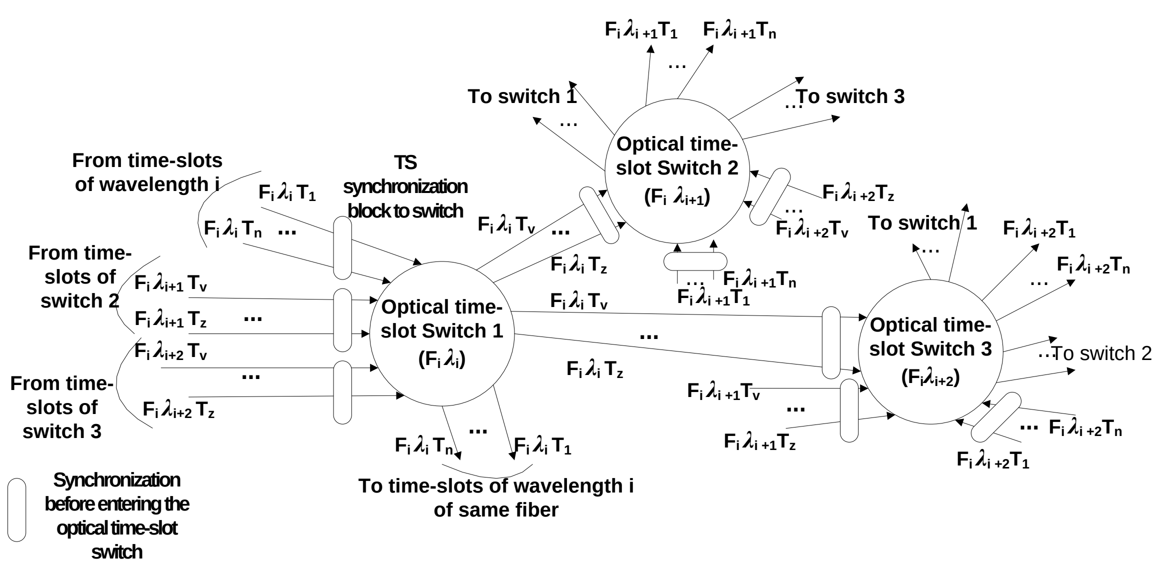


Figure 5.4: Time-slot flow between different optical time-slot switches with blocking

### 5.1.4 Three-stage Non-blocking Switching Architecture for Mini-slots

For interest a three-stage switching architecture is used to show non-blocking of switching mini-slots in different time-slots of different wavelengths in same or different fibers. Let $n$ denotes the number of input fibers to a switch, and $N$ denotes the total number of input fibers. Let $k$ denotes the number of $N/n$ cross $N/n$ middle stage optical switches. For this non-blocking case, the Clos formula [155], $k >= 2n - 1$ is used. In the example that follows, the value of $k = 2n$ is used as most switches can cater for $n$ inputs cross $2n$ outputs. The value of $N$ ($F$=1, $\lambda$=2, $T$=16 and $C$=16) is equal 2*16*16 or 512 for switching mini-slots between time-slots in different wavelengths of the same fiber. If $n$=16, $k = 2n = 32$, then the first stage consists of 32 ($N/n$) number of $n$ cross $k$ optical switches. The third stage consists of 32 ($N/n$) number of $k$ cross $n$ optical switches. Figure 5.5 illustrates this three-stage architecture fabric.

For switching mini-slots between time-slots in different wavelengths and fibers, the value of $N$ is much bigger. Let $F$=2, $\lambda$=4, $T$=16, and $C$=16. Then $N$ = 2*4*16*16 = 2048. If $n$ = 32 and $k$ = 64, the first stage will consist of 64 (=2048 / 32) number of 32 cross 64 optical switches. The second stage will consist of 64 optical switches of 64 cross 64. The third stage will consist of 64 optical switches of 64 cross 32. In order to reduce the number of cross-points in the Clos network, the time and space switching are to be combined [155].

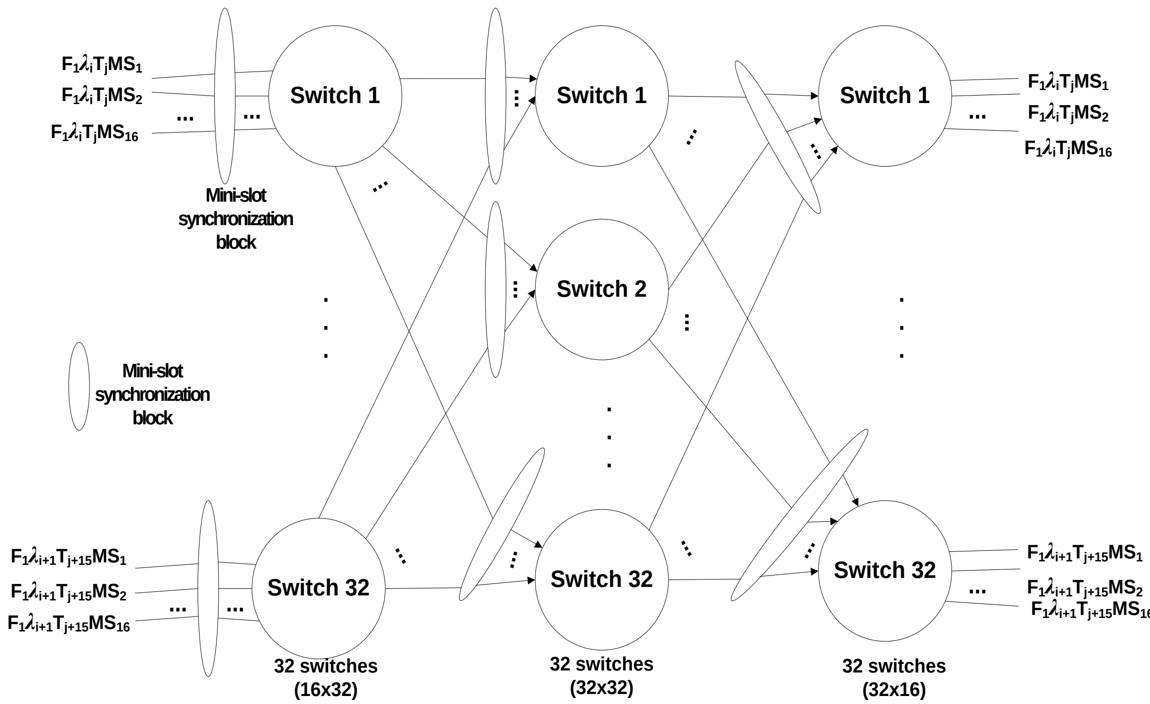


Figure 5.5: Three-stage architecture fabric (Non-blocking)

## 5.2 Technical Feasibility of Major Components and Conclusion

In this chapter, we briefly explain the workings of the flexible optical architecture and the flexibilities of this architecture are listed as follows:

- Switch between mini-slots in different time-slots of same wavelength and fiber
- Mini-slot interchange between mini-slots in the same time-slot, wavelength, and fiber
- Time-slot interchange between time-slots in same wavelength and fiber
- Switch between time-slots in different wavelengths of a fiber

Nevertheless, the technical feasibility of the major components that are used by the flexible optical architecture needs to be briefly addressed:

- Experiments on OTSIs are carried out in [90]. Furthermore, an OTSI has shown to be feasible in [91].
- Feasible development of an OMSI is shown in chapter 3 of this thesis.
- Synchronize optical time-slot packets has been demonstrated in [92] but Chapter 3 of this thesis has shown that synchronizing optical mini-slot packet is also possible.
- Feasible development of an optical MEMS time-slot switch is shown in [156], and use of a time-slot switch in a wavelength router is shown to be possible in [157]. In addition, [158] studies the time division multiplex and frequency division multiplex techniques to implement big size optical switches. An optical time-slot switch in OTDM architecture is similar to a wavelength switch in WDM architecture [157]. An optical mini-slot switch operates the same way as a time-slot switch except that the packet duration is shorter. As a solid state optical switch can operate at a precision of 10 ns or less, it does not affect the changing state of a mini-slot duration of at least 100 ns. The duration of 115 ns for a mini-slot is used as an example in the beginning of Chapter 3. Hence, optical mini-slot switch is possible to be built.

At this point, it is easy to deduce that the implementation of this architecture involves high complexities because there is no known commercial product of the components we have just discussed. The main complexities involve the synchronization, jitter, control logic, interchanging and switching of time-slots and mini-slots. To our best of knowledge, the implementation of this optical architecture has not been realized at the moment because optical technology is not mature enough and optical components are still costly. Thus, this chapter lays the foundation for further research in flexible optical architecture. Nevertheless, a much scaled down architecture version like the mini-slot router architecture is currently feasible. The mini-slot router architecture is capable of swapping mini-slots of the same time-slot, wavelength, and fiber or transfer a mini-slot of the same time-slot and wavelength between different fibers (see Figures 3.3 and 3.4).

In the next chapter, we present the analytical modeling of TDM wavelength optical networks. We use the partition based approach to calculate the approximate blocking probabilities of TDM wavelength optical network with OTSIs and without WC.

# CHAPTER 6

# Approximate Blocking Probabilities for TDM Wavelength Optical Network with OTSIs and without WC [4]

Chapter 2 describes the architecture and study the behavior of the proposed network namely, the shared time-slot TDM wavelength optical WDM network. Chapter 3 describes the architecture and study the behavior of the proposed network - the mini-slot TDM wavelength optical network. Chapter 4 compares the cost between the proposed networks and a typical wavelength network and highlights the future optical trend. Chapter 5 briefly explains the workings of the flexible optical architecture for traffic grooming at the time-slots and mini-slots level. This chapter focuses on the analytical modeling of wavelength optical network with OTSIs and without WC.

This thesis extends the proposal in [106] to TDM wavelength optical networks with OTSIs. The partition based method is used in our research to determine the blocking probability of transmission over two or more links. This method is chosen because it has never been applied to TDM WDM network with OTSIs and without WC using the reduced load approximation technique for fixed routing, and we hope to obtain some useful results from the analysis.

---

[4] A part of this chapter has been accepted in 15th IEEE International Symposium on Modeling, Analysis, and Simulation of Computer and Telecommunication Systems (MASCOTS), Istanbul, Turkey, 24th-26th Oct. 2007, “Average Network Blocking Probabilities for TDM WDM Optical Networks with OTSIs and without WC”. Also, a larger part of this chapter has been accepted to Journal of High Speed Networks, “Calculating the Approximate Blocking Probabilities in TDM Wavelength Optical Network with OTSIs and without WC”. Printed by IOS.

The rest of the sections in this chapter are organized as follows. Section 6.1 gives the partition based principles used in our research. Section 6.2 shows the way of deriving the mathematical expressions for our model. An algorithm is proposed to calculate the blocking probability of all links with available time-slots but have no WC. The use of the algorithm is illustrated using two very simple examples. Pseudo-codes for the two examples are provided in Section 6.3. Section 6.4 gives the mathematical equations and a reduced load algorithm to calculate the approximate average network blocking probabilities. Section 6.5 compares the simulation results with analytical results of blocking probabilities of various source-destination paths. Last but not least, Section 6.6 summarizes the main points of this chapter.

## 6.1 Partition Principles

A partition [159-160] of a positive integer $n$ is a collection of positive integers whose sum is $n$. Since the ordering is not important, a partition of $n$ can be regarded as a finite non-increasing sequence $n_1 >= n_2 >= n_3 >= n_4 >= \ldots >= n_k$ of positive integers such that $\sum_{i=1}^{k} n_i = n$. The table below shows the partitions of 1, 2, 3, 4, 5, and 6.

Table 6.1: Partitions of 1, 2, 3, 4, 5, and 6

| *N* | partitions of *n* | p(*n*) |
|---|---|---|
| 1 | 1 | 1 |
| 2 | 2 = 1+1 | 2 |
| 3 | 3 = 2+1 = 1+1+1 | 3 |
| 4 | 4 = 3+1 = 2+2 = 2+1+1 = 1+1+1+1 | 5 |
| 5 | 5 = 4+1 = 3+2 = 3+1+1 = 2+2+1 = 2+1+1+1 = 1+1+1+1+1 | 7 |
| 6 | 6 = 5+1 = 4+2 = 4+1+1 = 3+3 = 3+2+1 = 3+1+1+1 = 2+2+2 = 2+2+1+1 = 2+1+1+1+1 = 1+1+1+1+1+1 | 11 |

If $n = n_1 + n_2 + n_3 + n_4 + \ldots n_k$ is a partition of $n$, $n$ can be said as partitioned into $k$ parts of sizes $n_1, n_2, n_3, n_4, \ldots n_k$ respectively. For example, in the partition 5 = 2 + 2 + 1, there are 3 parts of sizes 2, 2, and 1 respectively. Another example by illustrating a partition of $n$ is to distribute $n$ identical objects into $n$ identical boxes with empty boxes allowed, as illustrated below.

**3 = 3 = 2 + 1 = 1 + 1 + 1**

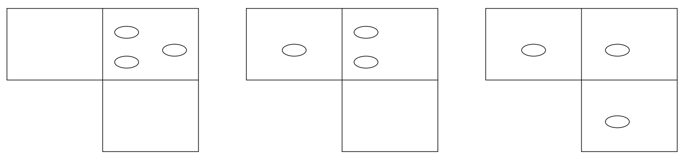

Now we applied the partition principle to calculate the number of blocking cases for the numerator in Section 6.2. For our case, the position of arrangement is important. A wavelength with at least one available time-slot is denoted by a plus (+) and with no available time-slot is denoted by a zero (0). A more detailed explanation of using this representation in deriving mathematical equations is given in Section 6.2. For the proposed algorithm, the number of wavelengths in a link that has at least one empty time-slot is represented by $k$ and the number of empty time-slots in a link is represented by $n$. In Section 6.3.2, the function Calculate_patterns() is used to illustrate the use of values $k$ and $n$.

## 6.2 Calculating Denominator and Numerator

Let $p_o^{(l)}(x_1, \ldots, x_r)$ be the probability not to have at least one empty time-slot at common wavelengths throughout the links $1, \ldots, r$ each having $l$ wavelengths with $s$ time-slots per wavelength, provided that there are $x_i$ empty time-slots over all wavelengths at link $i$, $i = 1,\ldots,r$ .

Let us consider the blocking probability $p_O^{(2)}(x_1, x_2)$ for two links, and each link has two wavelengths. Suppose $l = 2$. Let $N_{case}$ denotes the total number of unique cases of a link and $N\_xi_n$ denotes the number of arrangements for each unique case in link $xi$. The total number of arrangements in link $i$ for the number of empty time-slots $x_i$ is given by $T_{\text{arr}} = \sum_{n=1}^{Ncase} N\_xi_n$ if the number of empty time-slots in a wavelength is bounded by $s$. We shall use $T_{\text{arr}} = \sum_{n=1}^{Ncase} N\_xi_n$ for each link in the denominator. $T_{\text{arr}}$ can be determined by the following steps:

(1) Calculate the number of unique cases for each link. For each unique case, the number of empty time-slots in all the wavelengths of a link compared with the rest of the cases must not be the same regardless of the arrangement position;

(2) Determine the number of arrangements for each unique case. The numerator is the factorial of number of wavelengths ($l$) in a link. The denominator is the product of the factorial of each unique number of empty time-slots in each wavelength. If the same number of empty time-slots in each wavelength of a link occurs only once, we have 1! A 2! (two factorial) means that the same number of empty time-slots in each wavelength of a link occurs twice. Similar explanation is used for 3!, 4!, and so on;

(3) Add the number of arrangements for each unique case, and we shall obtain the value for $T_{\text{arr}}$ .

For example, let $l = 2$, $s = 2$, and $x_k$ = number of empty time-slots in link $k = 2$.

Step (1) | Step (2)

| Unique case one | Number of arrangements |
|---|---|
| $\begin{matrix} wav1 & wav2 \\ 1 & 1 \end{matrix}$ | $\frac{2!}{2!} = 1$ |

| Unique case two | Number of arrangements |
|---|---|
| $\begin{matrix} wav1 & wav2 \\ 2 & 0 \end{matrix}$ | $\frac{2!}{1!\,1!} = 2$ |

Finally, Step (3), we add the number of arrangements for unique cases one and two. Thus, $T_{\text{arr}}$ is three – [ 2 0], [0 2], and [1 1]. A [2 0] means that the number of empty time-slot in wavelength one is two and wavelength two is zero.

Another example, let $l$ = 2, $s$ = 2, and $x_{\text{i}}$ = number of empty time-slots in link $i$ = 3.

Step (1) | Step (2)

| Unique case one | Number of arrangements |
|---|---|
| $\begin{matrix} wav1 & wav2 \\ 2 & 1 \end{matrix}$ | $\frac{2!}{1!\,1!} = 2$ |

Finally, Step (3), we add the number of arrangements for unique case one. Thus, $T_{\text{arr}}$ is two – [ 2 1] and [1 2]. The cases [3 0] and [0 3] are not included because the number of time-slots for each wavelength ($s$) is two.

For the numerator, we used appropriate partitions of a matrix-based scheme (partition pattern) like the form $\begin{bmatrix} + & 0 \\ 0 & + \end{bmatrix}$, where zero at the place on row $i$ and column $j$ means $x_{ij} = 0$, whereas the plus sign implies that $x_{ij} > 0$.

There always exists empty time-slots at a common wavelength on the links if both $x_1 > 0$ and $x_2 > 0$, and at least one of them is greater than $s$. If $x_1 > s$, there will be empty time-slots at all wavelengths on the first link, and so a common wavelength with empty time-slots for both links. There are only two possible cases for not having empty time-slots at common wavelength across the links, when $0 < x_1 <= s$, and $0 < x_2 <= s$, i.e.

$$\begin{bmatrix} + & 0 \\ 0 & + \end{bmatrix} \text{ and } \begin{bmatrix} 0 & + \\ + & 0 \end{bmatrix}$$

The related blocking probability is then represented as $2\,(\sum_{n=1}^{Ncase} N\_x1n)^{-1}(\sum_{n=1}^{Ncase} N\_x2n)^{-1}$. Finally, we have

$$p_o^{(2)}(x_1, x_2) = \begin{cases} 1, & if \quad x_1 = 0 \; and/or \; x_2 = 0 \\ \dfrac{2}{(\sum_{n=1}^{Ncase} N\_x1n)(\sum_{n=1}^{Ncase} N\_x2n)}, & if \;\; 0 < x_1 <= s \; and \;\; 0 < x_2 <= s \\ 0, & otherwise \end{cases} \qquad (1)$$

Now, let us consider the blocking probability $p_o^{(2)}(x_1, x_2, x_3)$ for three links, each with two wavelengths. For the denominator, we shall use the formula $T_{\text{arr}} = \sum_{n=1}^{Ncase} N\_xi_n$ to determine the total number of arrangements for the number of empty time-slots in a link if the number of empty time-slots in a wavelength is bounded by $s$.

For the numerator, we calculate number of partitions which have no empty time-slots at common wavelengths using a matrix-based scheme (partition pattern) like the form $\begin{bmatrix} + & 0 \\ 0 & + \\ + & 0 \end{bmatrix}$, where zero at the place on row $i$ and column $j$ means $x_{ij} = 0$, whereas the plus sign implies that $x_{ij} > 0$.

Suppose that $0 < x_1, x_2, x_3 <= s$. The suitable partition patterns are represented as follows with the overall number of particular partitions put on the right of each group of related patterns.

$$\begin{bmatrix} + & 0 \\ + & 0 \\ 0 & + \end{bmatrix}, \begin{bmatrix} + & + \\ + & 0 \\ 0 & + \end{bmatrix}, \begin{bmatrix} 0 & + \\ + & 0 \\ 0 & + \end{bmatrix}, \binom{x_1+1}{1} = (x_1+1); \quad \begin{bmatrix} + & 0 \\ 0 & + \\ + & 0 \end{bmatrix}, \begin{bmatrix} + & + \\ 0 & + \\ + & 0 \end{bmatrix}, \begin{bmatrix} 0 & + \\ 0 & + \\ + & 0 \end{bmatrix}, \binom{x_1+1}{1} = (x_1+1);$$

$$\begin{bmatrix} + & 0 \\ + & 0 \\ 0 & + \end{bmatrix}, \begin{bmatrix} + & 0 \\ + & + \\ 0 & + \end{bmatrix}, \begin{bmatrix} + & 0 \\ 0 & + \\ 0 & + \end{bmatrix}, \binom{x_2+1}{1} = (x_2+1); \quad \begin{bmatrix} 0 & + \\ + & 0 \\ + & 0 \end{bmatrix}, \begin{bmatrix} 0 & + \\ + & + \\ + & 0 \end{bmatrix}, \begin{bmatrix} 0 & + \\ 0 & + \\ + & 0 \end{bmatrix}, \binom{x_2+1}{1} = (x_2+1);$$

$$\begin{bmatrix} + & 0 \\ 0 & + \\ + & 0 \end{bmatrix}, \begin{bmatrix} + & 0 \\ 0 & + \\ + & + \end{bmatrix}, \begin{bmatrix} + & 0 \\ 0 & + \\ 0 & + \end{bmatrix}, \binom{x_3+1}{1} = (x_3+1); \quad \begin{bmatrix} 0 & + \\ + & 0 \\ + & 0 \end{bmatrix}, \begin{bmatrix} 0 & + \\ + & 0 \\ + & + \end{bmatrix}, \begin{bmatrix} 0 & + \\ + & 0 \\ 0 & + \end{bmatrix}, \binom{x_3+1}{1} = (x_3+1).$$

Since the patterns in the first and third columns appear to be counted twice and each of the patterns has only one representative partition, the number of different partitions is $2(x_1 + 1) + 2(x_2 + 1) + 2(x_3 + 1) - 6 = 2(x_1 + x_2 + x_3)$. The related blocking probability is equal to $p_o^{(2)}(x_1, x_2, x_3) = \dfrac{2(x_1 + x_2 + x_3)}{(\sum_{n=1}^{Ncase} N\_x1n)(\sum_{n=1}^{Ncase} N\_x2n)(\sum_{n=1}^{Ncase} N\_x3n)}$.

Consider the case when $s < x_1 <= 2s$, and $0 < x_2, x_3 <= s$. The partition patterns and number of partitions are as follows:

$$\begin{bmatrix} + & + \\ + & 0 \\ 0 & + \end{bmatrix}, \begin{bmatrix} + & + \\ 0 & + \\ + & 0 \end{bmatrix} = 2(2s - x_1 + 1) .$$

For the case when $s < x_2 <= 2s$ and $0 < x_1, x_3 <= s$, the number of partitions is $2(2s - x_2 + 1)$. For the case when $s < x_3 <= 2s$ and $0 < x_1, x_2 <= s$, the number of partitions is $2(2s - x_3 + 1)$ . Finally, we get (2). When any two of the variables $x_1$, $x_2$, $x_3$ are greater than *s*, there is always a common wavelength with empty time-slots.

$$p_o^{(2)}(x_1, x_2, x_3) = \begin{cases} 1, & if \;\; x_i = 0 \text{ for at least one } i = 1,2,3 \\ \dfrac{2(x_1+x_2+x_3)}{(\sum_{n=1}^{Ncase} N\_x1n)(\sum_{n=1}^{Ncase} N\_x2n)(\sum_{n=1}^{Ncase} N\_x3n)}, & if \;\; 0 < x_1,x_2,x_3 <= s \\ \dfrac{2(2s-x_3+1)}{(\sum_{n=1}^{Ncase} N\_x1n)(\sum_{n=1}^{Ncase} N\_x2n)(\sum_{n=1}^{Ncase} N\_x3n)}, & if \;\; 0 < x_1,x_2 <= s \text{ and } s < x_3 <= 2s \\ \dfrac{2(2s-x2+1)}{(\sum_{n=1}^{Ncase} N\_x1n)(\sum_{n=1}^{Ncase} N\_x2n)(\sum_{n=1}^{Ncase} N\_x3n)}, & if \;\; 0 < x_1,x_3 <= s \text{ and } s < x_2 <= 2s \\ \dfrac{2(2s-x_1+1)}{(\sum_{n=1}^{Ncase} N\_x1n)(\sum_{n=1}^{Ncase} N\_x12n)(\sum_{n=1}^{Ncase} N\_x3n)}, & if \;\; 0 < x_2,x_3 <= s \text{ and } s < x_1 <= 2s \\ 0, & otherwise \end{cases} \quad (2)$$

An example to calculate the denominator for $p_o^{(2)}(x_1, x_2, x_3)$ is given below.

Let $l$ = 2, $s$ = 2, $x_1$ = number of empty time-slots in link 1 = 2, $x_2$ = number of empty time-slots in link 2 = 2, $x_3$ = number of empty time-slots in link 3 = 3.

First, we calculate the total number of arrangements for link $x_1$ .

| Step (1) | Step (2) |
|---|---|
| <u>Unique case one</u> | <u>Number of arrangements</u> |
| $wav1 \quad wav2$<br>$2 \quad\quad 0$ | $\frac{2!}{1!\,1!} = 2$ |

Unique case two | Number of arrangements

| <u>Unique case two</u> | | <u>Number of arrangements</u> |
|---|---|---|
| $wav1$ | $wav2$ | $\frac{2!}{2!} = 1$ |
| 1 | 1 | |

Finally, Step (3), we add the number of arrangements for unique cases one and two. Thus, $T_{\text{arr}}$ for link $x_1$ is three – [ 2 0], [0 2], and [1 1].

Second, we calculate the total number of arrangements for link $x_2$ . The calculation is the same as link $x_1$. Thus, $T_{\text{arr}}$ for link $x_2$ is also three – [2 0], [0 2], and [1 1].

Third, we calculate the total number of arrangements for link $x_3$ .

Step (1) | Step (2)

| <u>Unique case one</u> | | <u>Number of arrangements</u> |
|---|---|---|
| $wav1$ | $wav2$ | $\frac{2!}{1!\,1!} = 2$ |
| 2 | 1 | |

Finally, Step (3), the total number of arrangements for $T_{\text{arr}}$ is 2 because there is only one unique case.

Thus, the value of denominator is 3 multiply by 3 multiply by 2 $((\sum_{n=1}^{Ncase} N\_x1_n)\ (\sum_{n=1}^{Ncase} N\_x2_n)\ (\sum_{n=1}^{Ncase} N\_x3_n))$ which 18 when $0 < x_1, x_2 <= s$ and $s < x_3 <= 2s$ .

Now let us consider three wavelengths in each of the two links. The blocking probability of $p_o^{(3)}(x_1, x_2) = 1$, if $x_1 = 0$ and/or $x_2 = 0$. The blocking probability of $p_o^{(3)}(x_1, x_2) = 0$, if $x_1, x_2 > 0$ and at least one of the variables $x_1$ and $x_2$ is greater than $2s$.

For the denominator, we shall use the formula $T_{\text{arr}} = \sum_{n=1}^{Ncase} N\_xi_n$ to determine the total number of arrangements for the number of empty time-slots in a link if the number of empty time-slots in a wavelength is bounded by $s$.

For the numerator, we begin by assuming that $0 < x_1 <= s$ and $0 < x_2 <= s$. The suitable partition patterns are represented below together with overall number of particular partitions put on the right of each group of related patterns.

$$\begin{bmatrix} + & 0 & 0 \\ 0 & + & 0 \end{bmatrix}, \begin{bmatrix} + & 0 & 0 \\ 0 & 0 & + \end{bmatrix}, \begin{bmatrix} + & 0 & 0 \\ 0 & + & + \end{bmatrix}, \binom{x_2+1}{1} = (x_2 + 1);$$

$$\begin{bmatrix} 0 & + & 0 \\ + & 0 & 0 \end{bmatrix}, \begin{bmatrix} 0 & + & 0 \\ 0 & 0 & + \end{bmatrix}, \begin{bmatrix} 0 & + & 0 \\ + & 0 & + \end{bmatrix}, \binom{x_2+1}{1} = (x_2 + 1);$$

$$\begin{bmatrix} 0 & 0 & + \\ + & 0 & 0 \end{bmatrix}, \begin{bmatrix} 0 & 0 & + \\ 0 & + & 0 \end{bmatrix}, \begin{bmatrix} 0 & 0 & + \\ + & + & 0 \end{bmatrix}, \binom{x_2+1}{1} = (x_2 + 1);$$

$$\begin{bmatrix} + & + & 0 \\ 0 & 0 & + \end{bmatrix}, \qquad \binom{x_1-1}{1} = (x_1 - 1);$$

$$\begin{bmatrix} + & 0 & + \\ 0 & + & 0 \end{bmatrix}, \qquad \binom{x_1-1}{1} = (x_1 - 1);$$

$$\begin{bmatrix} 0 & + & + \\ + & 0 & 0 \end{bmatrix}, \qquad \binom{x_1-1}{1} = (x_1 - 1).$$

Note that each row in the above pattern table describes a general pattern type. The types are intended to determine the partition subsets which are mutually disjoint. For instance, three patterns in the first row define together a general partition pattern type " $x_1$ is fully assigned to $x_{11}$, whereas $x_2$ can be freely distributed among $x_{22}$ and $x_{23}$". If $x_2$ = 1, $x_2$ cannot be divided into two positive parts. In this case, there are two partitions with one part equal to zero. Both of them are represented through the first and second patterns. It is clear that the third pattern is not inapplicable in this case.

Since $x_1$ has a fixed assignment, the actual number of partitions is determined by the ways of distributing $x_2$ among two destinations, including two ways when one of the destinations gets zero, that is, $\binom{x_2+1}{1} = x_2 + 1$.

Note also that one pattern in the fourth row means "$x_1$ can be freely distributed among $x_{11}$ and $x_{12}$ provided that it can be divided into two positive parts, whereas $x_2$ is fully assigned to $x_{23}$". It is clear that this partition cannot be applied to the case when $x_1$ = 1.

Since the number of partitions is determined by the ways of distributing $x_1$ among two destinations provided that each destination does not get zero, the actual number of partitions is $\binom{x_1-1}{1} = (x_1 - 1)$. If $x_1 = 1$, the expected result is zero. Finally, the partition with $x_1 = 1$ and $x_2$ assigned to $x_{23}$ has already be counted with the second partition patterns in the first and second rows.

The number of partitions when $0 < x_1, x_2 <= s$ is equal to $3\binom{x_1-1}{1} + 3\binom{x_2+1}{1} = 3(x_1 + x_2)$ whereas the blocking probability takes the form $p_o^{(3)}(x_1, x_2) = \frac{3(x_1 + x_2)}{(\sum_{n=1}^{Ncase} N\_x1n)(\sum_{n=1}^{Ncase} N\_x2n)}$. The suitable partition patterns with the actual numbers of related partitions when $s < x_1 <= 2s$ and $0 < x_2 <= s$ can be represented as follows:

$$\begin{bmatrix} + & + & 0 \\ 0 & 0 & + \end{bmatrix}, \qquad (2s - x_1 - 1);$$

$$\begin{bmatrix} + & 0 & + \\ 0 & + & 0 \end{bmatrix}, \qquad (2s - x_1 - 1);$$

$$\begin{bmatrix} 0 & + & + \\ + & 0 & 0 \end{bmatrix} \quad (2s - x_1 - 1).$$

The number of partitions is equal to $3(2s - x_1 + 1)$, whereas the blocking probability takes the form $p_o^{(3)}(x_1, x_2) = \dfrac{3(2s - x_1 + 1)}{(\sum_{n=1}^{Ncase} N\_x1n)(\sum_{n=1}^{Ncase} N\_x2n)}$. By obvious symmetry, the blocking probability when $0 < x_1 <= s$ and $s < x_2 <= 2s$ takes the form $p_o^{(3)}(x_1, x_2) =$ $\dfrac{3(2s - x_2 + 1)}{(\sum_{n=1}^{Ncase} N\_x1n)(\sum_{n=1}^{Ncase} N\_x2n)}$.

Finally, it is easy to see that for $s < x_1, x_2 <= 2s$ the blocking probability is equal to 0 since there is at least one common wavelength with empty time-slots. The summary of results is presented in (3).

$$p_o^{(3)}(x_1, x_2) = \begin{cases} 1, & if \;\; x_1 = 0 \; and/or \;\; x_2 = 0 \\ \dfrac{3(x_1+x_2)}{(\sum_{n=1}^{Ncase} N\_x1n)(\sum_{n=1}^{Ncase} N\_x1n)}, & if \;\; 0 < x_1 <= s \; and \;\; 0 < x_2 <= s \\ \dfrac{3(2s-x_1+1)}{(\sum_{n=1}^{Ncase} N\_x1n)(\sum_{n=1}^{Ncase} N\_x2n)}, & if \;\; s < x_1 <= 2s \; and \;\; 0 < x_2 <= s \\ \dfrac{3(2s-x_2+1)}{(\sum_{n=1}^{Ncase} N\_x1n)(\sum_{n=1}^{Ncase} N\_x2n)}, & if \;\; 0 < x_1 <= s \; and \;\; s < x_2 <= 2s \\ 0, & otherwise \end{cases} \quad (3)$$

We give two examples to calculate the denominator for $p_o^{(3)}(x_1, x_2)$.

For the first example, let $l = 3$, $s = 2$, $x_1$ = number of empty time-slots in link 1 = 2, and $x_2$ = number of empty time-slots in link 2 = 2.

Step (1)

Unique case one

| $wav1$ | $wav2$ | $wav3$ |
|---|---|---|
| 2 | 0 | 0 |

Step (2)

Number of arrangements

$$\frac{3!}{1!\ 2!} = 3$$

Unique case two

| $wav1$ | $wav2$ | $wav3$ |
|---|---|---|
| 1 | 1 | 0 |

Number of arrangements

$$\frac{3!}{2!\ 1!} = 3$$

Finally, Step (3), we add the number of arrangements for unique cases one and two. Thus, $T_{\text{arr}}$ for link $x_1$ is six – [ 2 0 0], [0 2 0], [0 0 2], [1 1 0], [0 1 1], and [1 0 1]. A [1 1 0] means that the number of empty time-slot in wavelength one is one, wavelength two is one and wavelength three is zero. Similar calculations are performed for link $x_2$. Thus, $T_{\text{arr}}$ for link $x_2$ is also six. Hence, the value of denominator is 36 $\left( (\sum_{n=1}^{Ncase} N\_x1n)(\sum_{n=1}^{Ncase} N\_x2n) \right)$ when $0 < x_1 <= s$ and $0 < x_2 <= s$ .

For the second example, let $l = 3$, $s = 2$, $x_1$ = number of empty time-slots in link 1 = 3, and $x_2$ = number of empty time-slots in link 2 = 2.

First, we calculate the total number of arrangements for link $x_1$ .

Step (1)

Unique case one

| $wav1$ | $wav2$ | $wav3$ |
|---|---|---|
| 2 | 1 | 0 |

Step (2)

Number of arrangements

$$\frac{3!}{1!\ 1!\ 1!} = 6$$

Unique case two

| $wav1$ | $wav2$ | $wav3$ |
|---|---|---|
| 1 | 1 | 1 |

Number of arrangements

$$\frac{3!}{3!} = 1$$

Finally, Step (3), we add the number of arrangements for unique cases one and two. Thus, $T_{\text{arr}}$ for link $x_1$ is seven – [ 2 1 0], [0 2 1], [2 0 1], [1 2 0], [0 1 2], [1 0 2], and [1 1 1].

Second, we calculate the total number of arrangements for link $x_2$ .

| Step (1) | | | Step (2) |
|---|---|---|---|
| <u>Unique case one</u> | | | <u>Number of arrangements</u> |
| *wav*1 | *wav*2 | *wav*3 | |
| 2 | 0 | 0 | $\frac{3!}{1!\,2!} = 3$ |
| <u>Unique case two</u> | | | <u>Number of arrangements</u> |
| *wav*1 | *wav*2 | *wav*3 | |
| 1 | 1 | 0 | $\frac{3!}{2!\,1!} = 3$ |

Finally, Step (3), we add the number of arrangements for unique cases one and two. Thus, $T_{\text{arr}}$ for link $x_2$ is six – [ 2 0 0], [0 2 0], [0 0 2], [1 1 0], [0 1 1], and [1 0 1].

Thus, the value of denominator is 42 ($(\sum_{n=1}^{Ncase} N\_x1n)(\sum_{n=1}^{Ncase} N\_x2n)$) when $s < x_1 <= 2s$ and $0 < x_2 <= s$ .

By continually applying the partitions principle and the matrix-based scheme, the mathematical expressions of $l$ = 4,5,…for two links can be obtained. Similarly, the mathematical expressions of $l$ = 3 and number of links > 2, and $l$ > 3 and number of links >= 2 can also be obtained. However, as the number of wavelengths and links increases, this method has difficulty to obtain the mathematical expressions for large number of groupings. Thus, we propose a schema that is able to calculate the $p_O^{(l)}(x_1,\ldots,x_r)$ for any number of links, any number of wavelengths in each link, and any number of time-slots in each wavelength.

A flowchart is designed in Figure 6.1 to illustrate the schema. Generally, the number of nested *while* loops in the schema is determined by the number of links; for example, a two link route has two *while* loops (see Section 6.3.1), and a three link route has three *while* loops (see Section 6.3.2). The pattern that is used to determine blocking is a one row matrix for each link like [+ 0] for two wavelengths. A + in this case means there is at least one time-slot in wavelength one. A 0 in this case means that there is no time-slot empty in wavelength two. Blocking occurs if there is no + sign in the common wavelength of all the links. The pattern changes as the number of wavelengths in a link is altered. For example, the pattern can be [+ + 0] for three wavelengths in a link and [+ + + 0] for four wavelengths in a link. The minimum and maximum number of wavelength(s) required to store the number of empty time-slots is determined. Each condition such as $s < x_2 <= 2s$ can easily be tested using an if-then-else statement to obtain required patterns for a link. For example, the required patterns for number of $x_i$ empty time-slots distributed in three wavelengths of link $i$ with condition s $< x_i <=$ 2s are [+ + 0], [0 + +], [+ 0 +], and [+ + +]. These patterns are used to determine the blocking patterns for the numerator of our formula like in Section 6.3.1 Line 11 and Section 6.3.2 Line 35. In the same example, the total number of patterns for each link in the denominator is calculated using the formula $T_{\mathrm{arr}} = \sum_{n=1}^{Ncase} N\_xi_n$. Let $\alpha$ denote the total number of blocking patterns. Let $\beta$ denote the total number of blocking and non-blocking patterns. The value of $p_O^{(l)}(x_1, \ldots, x_r)$ is $\frac{\alpha}{\beta}$. In order to illustrate the workings of the schema, two simple examples are provided.

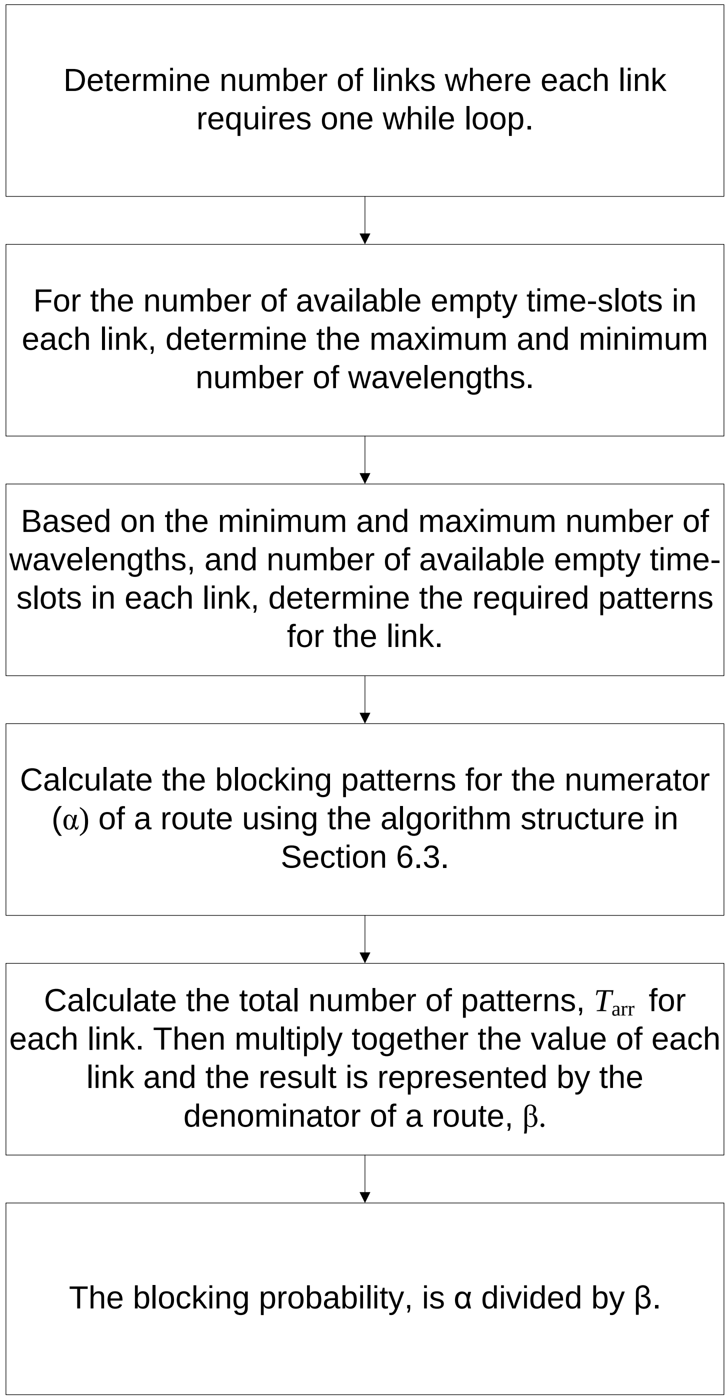


Figure 6.1: Flowchart of the schema

The first example is that for two links. Each link has two wavelengths, and each wavelength has two time-slots. The value of $s$ is two because each wavelength can contain two time-slots. The number of empty time-slots for each link is assumed to be two. The minimum number of wavelengths in each link that need to store the empty time-slots is one, and the maximum number of wavelengths in each link that need to store the empty time-slots is two. Hence, there are three different patterns in each link. They are [+ 0] where the empty time-slots are all in wavelength one, [0 +] where the empty time-slots are all in wavelength two, and [+ +] where there is one empty time-slot in wavelength one and another empty time-slot in wavelength two. By applying formula (1), the blocking probability, $p_o^{(2)}(x_1, x_2)$ is $\frac{2}{(\sum_{n=1}^{Ncase} N\_x1_n)(\sum_{n=1}^{Ncase} N\_x2_n)}$ which is equal to $\frac{2}{9}$, where the number of empty time-slots for each link is two and number of time-slots in a wavelength is two and number of wavelengths in a link is two. Thus, the value of $x_1 = 2$ and $x_2 = 2$ and $s = 2$ and $l = 2$. The value of the denominator is 9 because there are three possible patterns for each link which are [1 1], [2 0], and [0 2]. Thus, the total number of possible patterns for both links are 9 (3 multiply by 3).

Now, let us explain the workings of the schema to get the same blocking probability value of $\frac{2}{9}$. We use the formula from the schema pseudo-codes (see Section 6.3.1 Line 11), $\frac{blk}{(\sum_{n=1}^{Ncase} N\_x1_n)(\sum_{n=1}^{Ncase} N\_x2_n)}$. The denominator of this formula is the total number of blocking and non-blocking patterns for the two links. In this case, it is $(\sum_{n=1}^{Ncase} N\_x1_n)(\sum_{n=1}^{Ncase} N\_x2_n)$. The total number of arrangements for each link is calculated to be three. Thus, the total value of the denominator is nine (3 multiply by 3).

The numerator is the value of *blk*, a floating point variable. The value of *blk* is initialized to 0.0 . If the pattern in the first link is [+ 0], blocking will only occur if the second link is [0 +] (see Section 6.3.1 Line 6). Since the empty time-slots are stored in one wavelength for both links (see Section 6.3.1 Line 7), *blk* is incremented by one (see Section 6.3.1 Line 8). If the pattern in the first link is [0 +], blocking will only occur if the second link is [+ 0] (see Section 6.3.1 Line 6). Since the empty time-slots are stored in one wavelength for both links (see Section 6.3.1 Line 7), *blk* is incremented by one (see Section 6.3.1 Line 8). If the pattern in the first link is [+ +], no blocking will occur because there always exists a common wavelength in both links (see Section 6.3.1 Line 6). Thus, the final value of *blk* is two. In order to make the schema runs more efficiently, the pattern [+ +] can be omitted because we know that blocking will not occur.

The second example consists of three links. Each link has two wavelengths, and each wavelength has two time-slots. Thus, the value of *s* is two because each wavelength can contain two time-slots. The number of empty time-slots for each link is assumed to be two. The minimum number of wavelengths in each link that needs to store the empty time-slots is one and the maximum number of wavelengths in each link that need to store the empty time-slots is two. Hence, the number of patterns for each link is three. They are [+ 0] where the empty time-slots are all in wavelength one, [0 +] where the empty time-slots are all in wavelength two, and [+ +] where there is one empty time-slot in wavelength one and another empty time-slot in wavelength two. By applying formula (2), the blocking probability, $p_o^{(2)}(x_1, x_2, x_3)$, where $0 < x_1, x_2, x_3 <= s$ is $\frac{2(x_1 + x_2 + x_3)}{(\sum_{n=1}^{Ncase} N\_x1n)(\sum_{n=1}^{Ncase} N\_x2n)(\sum_{n=1}^{Ncase} N\_x3n)}$ which is equal to $\frac{12}{27}$, where the number of empty time-slots for each link is two. Thus, the value of $x_1 = 2$, $x_2 = 2$, and $x_3 = 2$. Now, let us explain the workings of the schema to get the same blocking probability value of $\frac{12}{27}$. We use the formula from the schema pseudo-codes (see Section 6.3.2 Line 35), $\frac{blk}{(\sum_{n=1}^{Ncase} N\_x1n)(\sum_{n=1}^{Ncase} N\_x2n)(\sum_{n=1}^{Ncase} N\_x3n)}$. The denominator of our formula is the total number of blocking and non-blocking patterns for the three links. In this case it is $(\sum_{n=1}^{Ncase} N\_x1n)(\sum_{n=1}^{Ncase} N\_x2n)(\sum_{n=1}^{Ncase} N\_x3n)$. The total number of arrangements for each link is calculated to be three. Thus, the total value of the denominator is 27. The numerator is the value of *blk*, a floating point variable. The value of *blk* is initialized to 0.0 . The integer variables Arr_r, Arr_r-1, and Arr_r-2 are set to one (see Section 6.3.2 Line 12). Figure 6.2 shows the 12 suitable partition patterns that allow a connection to be blocked. Each row in a partition pattern represents the pattern for each link. The first column represents wavelength one. The second column represents wavelength two. The first row represents the first link, the second row represents the second link, and so on.

$$\begin{bmatrix} + & O \\ + & O \\ O & + \end{bmatrix}\begin{bmatrix} + & O \\ O & + \\ O & + \end{bmatrix}\begin{bmatrix} + & O \\ O & + \\ + & O \end{bmatrix}\begin{bmatrix} O & + \\ + & O \\ O & + \end{bmatrix}\begin{bmatrix} O & + \\ O & + \\ + & O \end{bmatrix}\begin{bmatrix} O & + \\ + & O \\ + & O \end{bmatrix}$$

$$\begin{bmatrix} + & + \\ + & O \\ O & + \end{bmatrix}\begin{bmatrix} + & + \\ O & + \\ + & O \end{bmatrix}\begin{bmatrix} + & O \\ + & + \\ O & + \end{bmatrix}\begin{bmatrix} O & + \\ + & + \\ + & O \end{bmatrix}\begin{bmatrix} O & + \\ + & O \\ + & + \end{bmatrix}\begin{bmatrix} + & O \\ O & + \\ + & + \end{bmatrix}$$

Figure 6.2: Suitable partition patterns that causes blocking

Blocking will only occur for all the 12 cases in Figure 6.2 (see Section 6.3.2 Line 8). Since the empty time-slots are stored in one wavelength (see Section 6.3.2 Line 9) for all the three links in the first six cases (first row of Figure 6.2), *blk* is incremented by one for each case (see Section 6.3.2 Line 10). Thus the value of *blk* is six after evaluating the first six cases. For the next six cases (second row of Figure 6.2), there is a pattern [+ +], where one time-slot is stored in wavelength one, and another time-slot is stored in wavelength two. For the seventh ($\begin{bmatrix} + & + \\ + & 0 \\ 0 & + \end{bmatrix}$) case and eighth ($\begin{bmatrix} + & + \\ 0 & + \\ + & 0 \end{bmatrix}$) case, the empty time-slots in link one are stored in more than one wavelength (see Section 6.3.2 Line 13). The number of parts for [+ +] is two (see Section 6.3.2 Line 14). Since the number of *n* compositions represents the number of empty time-slots, the value of *n* is two. As the number of parts is equal to number of *n* compositions (see Section 6.3.2 Line 15), the value of Arr_r-2 remains one. For the second and third links, the empty time-slots are stored in only one wavelength so the values of Arr_r-1 and Arr_r still remain as one. Because Arr_r, Arr_r-1, and Arr_r-2 have the value one (see Section 6.3.2 Line 28), *blk* is incremented by one for each of the two cases (see Section 6.3.2 Line 29). Now, the value of *blk* is eight. For the ninth ($\begin{bmatrix} + & 0 \\ + & + \\ 0 & + \end{bmatrix}$) case and tenth ($\begin{bmatrix} 0 & + \\ + & + \\ + & 0 \end{bmatrix}$) case, the empty time-slots in link two are stored in more than one wavelength (see Section 6.3.2 Line 18). The number of parts for [+ +] is two (see Section 6.3.2 Line 19). Since the number of *n* compositions is the number of empty time-slots, the value of *n* is two. As the number of parts is equal to number of *n* compositions (see Section 6.3.2 Line 20), the value of Arr_r-1 remains one. For the first and third links, the empty time-slots are stored in only one wavelength so the values of Arr_r-2 and Arr_r still remain as one. Because Arr_r, Arr_r-1, and Arr_r-2 have the value one (see Section 6.3.2 Line 28), *blk* is incremented by one for each of the two cases (see Section 6.3.2 Line 29). Now, the value of *blk* is 10. Similar explanation applies for the last two cases. Finally, the final value of *blk* is 12.

Let a plus (+) represents a wavelength with at least one empty time-slot. In a different situation where the number of *k* parts is not equal to number of *n* compositions and k parts is greater than one, the number of patterns for that link can be computationally calculated by calling the function Calculate_patterns(*k*,*n*). If a link has two wavelengths with each has at least one empty time-slot ([+ +]) and the total number of empty time-slots is three, the value of *k* is two ($k = 2$) and *n* is three ($n = 3$) respectively. Assume that each wavelength contains a maximum of two time-slots ($s = 2$). The total number of patterns calculated is 2. The two cases are [2 1], where there are two empty time-slots in wavelength one and one empty time-slot in wavelength two and [1 2], where there are one empty time-slot in wavelength one and two empty time-slots in wavelength two. The cases [3 0] and [0 3] are not included because the number of time-slots in each wavelength should not be more than two.

## 6.3 Schema Pseudo-codes

The schemas in this section are applied in Section 6.4 and they are used to determine $p_o^{(l)}(x_1, \ldots, x_r)$.

### 6.3.1 Schema Pseudo-codes for Two Links and Each Link has Two Wavelengths and Each Wavelength has Two Time-Slots

Input: Number of empty time-slots in each link for *r* number of links (*r* is > 1)

Output: $p_o^{(l)}(x_1, \ldots, x_r)$ for a connection of *r* links

**<u>Line</u>**

(1) Determine minimum and maximum number of wavelengths required for the empty of time-slots in link *r*-1 and *r*. /* Number of empty time-slots must be >= 1. For two links, the value of *r* is 2. */

(2) while (pattern for matching is empty for link $r$-1) do { // Number of patterns is three for matching two wavelengths, where each wavelength has two time-slots on each link

(3) Get a pattern for link $r$-1 // Available patterns to be matched are [+ 0], [0 +], [+ +]

(4) while (pattern for matching is available for link $r$) do {

// Number of patterns for matching two wavelengths is three, where each wavelength has two time-slots on each link

(5) Get a pattern for link $r$ // Available patterns to be matched are [+ 0], [0 +], [+ +]

(6) if (no common wavelength exists in both links) // There is a blocking pattern

(7) if (the available time-slots in links $r$-1 and $r$ are in only one wavelength)

(8) blk=blk+1.0

(9) } // End of second while loop beginning at line 4

(10) } // End of first while loop beginning at line 2

(11) Calculate the blocking probability of $\frac{blk}{(\sum_{n=1}^{Ncase} N\_x1n)(\sum_{n=1}^{Ncase} N\_x2n)}$

### 6.3.2 Schema Pseudo-codes for Three Links and Each Link has Two Wavelengths and Each Wavelength has Two Time-Slots

Input: Number of empty time-slots in each link for $r$ number of links ($r$ is > 1)

Output: $p_O^{(l)}(x_1, ..., x_r)$ for a connection of $r$ links

**Line**

(1) Determine minimum and maximum number of wavelengths required for the empty of time-slots in links $r$-2, $r$-1, and $r$. /* Number of empty time-slots must be >= 1. For three links, the value of $r$ is 3. */

(2) while (pattern for matching is available for link $r$-2) do {

// Number of patterns is three for matching two wavelengths, where each wavelength has two time-slots on each link

(3) Get a pattern for link $r$-2 // Available patterns to be matched are [+ 0], [0 +], [+ +]

(4) while (pattern for matching is available for link $r$-1) do {

// Number of patterns is three for matching two wavelengths, where each wavelength has two time-slots on each link

(5) Get a pattern for link $r$-1 // Available patterns to be matched are [+ 0], [0 +], [+ +]

(6) while (pattern for matching is available for link $r$) do {

// Number of patterns for matching is three for two wavelengths, where each wavelength has two time-slots on each link

(7) Get a pattern for link $r$ // Available patterns to be matched are [+ 0], [0 +], [+ +]

(8) if (no common wavelength exists in the three links) // There is a blocking pattern

(9) if (available time-slots in links $r$-2 , $r$-1 and $r$ are in only one wavelength)

```
(10)                    blk=blk+1.0
(11)                else  {
(12)                    Arr_r = Arr_r-1 = Arr_r-2 = 1
(13)                    if (empty time-slots in link r-2 is in more than one wavelength) {
(14)                        Determine the number of k parts
/* Value of k is the number wavelengths that has at least one empty time-slot and n compositions
is the number of empty time-slots in link r-2  */
(15)                        if (k parts != number of n compositions)
(16)                            Arr_r = Calculate_patterns(k,n);
(17)                    } // End of if statement beginning at line 13
(18)                    if (empty time-slots in link r-1 is in more than one wavelength) {
(19)                        Determine the number of k parts
/* Value of k is the number wavelengths that has at least one empty time-slot and n compositions
is the number of empty time-slots in link r-1 */
(20)                        if (k parts != number of n compositions)
(21)                            Arr_r-1 = Calculate_patterns(k,n);
(22)                    } // End of if statement beginning at line 18
(23)                    if (empty time-slots in link r is in more than one wavelength) {
(24)                        Determine the number of k parts
/* Value of k is the number wavelengths that has at least one empty time-slot and n compositions
is the number of empty time-slots in link r */
(25)                        if (k parts != number of n compositions)
(26)                            Arr_r-2 = Calculate_patterns(k,n);
(27)                    } // End of if statement beginning at line 23
(28)                    if (Arr_r == Arr_r-1 == Arr_r-2 == 1)
(29)                        blk=blk+1.0
                        else
(30)                        blk = blk + (Arr_r * Arr_r-1 * Arr_r-2 )
(31)                } // End of if statement beginning at line 8
(32)            }   // End of third while loop beginning at line 6
(33)        }   // End of second while loop beginning at line 4
(34)    } // End of first while loop beginning at line 2
```

(35) Calculate the blocking probability of $\dfrac{blk}{(\sum_{n=1}^{Ncase} N\_x1n)(\sum_{n=1}^{Ncase} N\_x2n)(\sum_{n=1}^{Ncase} N\_x3n)}$

int Calculate_patterns($k$,$n$) {

/* $s$ is the maximum number of time-slots in each wavelength, $k$ is the number of wavelengths in each link that has at least one empty time-slot, and $n$ is the empty time-slots for that link. Let a plus (+) represents a wavelength that has at least one empty time-slot.*/

(1) Put a one in each wavelength that has a plus (+) since a plus (+) in a wavelength represents at least one empty time-slot). Assume that there are $x$ such wavelengths. This means that $k = x$.
(2) Calculate the number of unique cases for distributing $n - x$ empty time-slots in $k$ parts where each part is not more than $s - 1$ because we have already put a one in each wavelength that has a plus in it. For each unique case, the number of empty time-slots in $x$ wavelengths of a link compared with the rest of the cases must not be the same regardless of the arrangement position.
(3) For each unique case, calculate the number of ways of distributing $n - x$ empty time-slots in $k$ parts. The numerator is the factorial of $x$ wavelengths in a link. The denominator is the product of the factorial of each unique number of empty time-slots in $x$ wavelengths. If the number of empty time-slots in $x$ wavelengths of a link occurs only once, we have 1!. A 2! means that the number of empty time-slots in $x$ wavelengths of a link occurs twice. Similar explanation is used for 3!, 4!, and so on.
(4) Add the value for each unique case.
(5) Return the total value
}

## 6.4 Calculating Approximate Blocking Probabilities

### 6.4.1 Fixed Time-slot Wavelength Routing

Let us consider a network of arbitrary topology with $J$ links and $C$ time-slots on each link. The total number of time-slots ($C$) of each link is equivalent to the number of time-slots of each wavelength multiplied by the number of wavelengths per link. A route $R$ is a subset of links from $\{1,\ldots,J\}$. Calls arrive for route $R$ as a Poisson stream with rate $a_R$ . A call is accepted if it is assigned a time-slot in a wavelength $w_i$ on all links in route $R$. Let $X_j$ be the random variable denoting the number of idle time-slots on link $j$ in equilibrium. Let $X = (X_1,\ldots, X_J)$, $q_j(t) = \Pr[X_j = t]$; and $t = 0,\ldots,C$ be the idle capacity distribution. Suppose $X_1,\ldots, X_J$ are mutually independent random variables, then $q_j(t) = \prod_{j=1}^{J} q_j(t_j)$, where $t = (t_1, t_2, \ldots, t_J)$. Further suppose that there are $t$ idle time-slots on link $j$; the time until the next call is set up on link $j$ is exponentially distributed with $\alpha_j(t)$. This parameter is the call set-up rate on link $j$ when $t$ time-slots are free on link $j$. It follows that the number of idle time-slots on link $j$ can be viewed as a birth-and-death process as shown in Figure 6.3. Each state $m$ is the number of idle time-slots on link $j$. The death rate is $C$-$m$ at state $m$. By solving the Markov chain, we have

$$q_j(t) = \frac{C(C-1)\ldots(C-t+1)}{\alpha_j(1)\alpha_j(2)\ldots\alpha_j(t)} q_j(0), \qquad (4)$$

where $t = 1,\ldots,C$ and

$$q_j(0) = \left[1 + \sum_{t=1}^{C} \frac{C(C-1)\ldots(C-t+1)}{\alpha_j(1)\alpha_j(2)\ldots\alpha_j(t)}\right]^{-1}. \qquad (5)$$

The call set-up rate on link $j$ when there are $t$ idle time-slots on link $j$, $\alpha_j(t)$, is obtained by combining the contributions from the request streams to routes of which link $j$ is a member.

$$\begin{aligned} \alpha_j(t) &= 0, \quad \text{if } t = 0 \\ &= \sum_{R: j \in R} a_R \Pr[X_R > 0 \mid X_j = t], \qquad (6) \quad t = 1,\ldots,C. \end{aligned}$$

If the route consists of one link, the probability term Pr( . ) under the summation sign in (6) will be equal to 1. If the route consists of two links, let $R = \{i,j\}$. The term Pr( . ) can be further simplified by conditioning it on the set of disjoint events $\{X_i = l \mid l = 0,\ldots,C\}$.

$$\begin{aligned} &\Pr[X\{i,j\} > 0 \mid X_j = t] \\ &= \sum_{l=1}^{C} \Pr[X_i = l \mid X_j = t] \Pr[X_R > 0 \mid X_j = t,\ X_i = l] \\ &= \sum_{l=1}^{C} q_i(l)(1 - p_0(t,l)) \qquad (7) \end{aligned}$$

where $p_0(t,l)$ may be given by (1) or (3) or the proposed schema.

Similarly, for a three-hop route $R = \{i,j,k\}$, and routes more than three hops, the probabilities can be obtained. For a three-hop route with two wavelengths per link, $p_0(l,t,n)$ is given by (2) or the proposed schema.

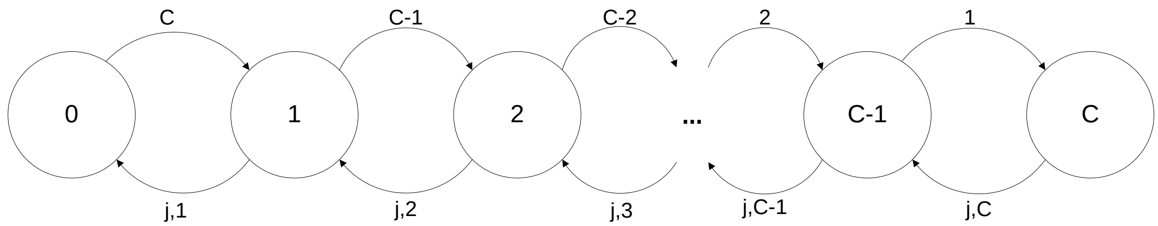


Figure 6.3: Birth-and-death process for idle time-slots distribution on link *j*

### 6.4.2 Blocking Probability for Route *R*

The blocking probability for calls to route *R* is

$$
\begin{aligned}
L_R &= \Pr[X_R = 0] \\
&= q_i(0), \qquad \text{if } R = \{i\}, \\
&= \sum_{l=0}^{C}\sum_{t=0}^{C} q_i(l)q_j(t)\,p_0(l,t)\,, \text{ if } R = \{i,j\}, \\
&= \sum_{l=0}^{C}\sum_{t=0}^{C}\sum_{n=0}^{C} q_i(l)q_j(t)q_k(n)\,p_0(l,t,n)\,, \text{ if } R = \{i,j,k\}, \\
&= \sum_{l=0}^{C}\sum_{t=0}^{C}\sum_{n=0}^{C}\sum_{m=0}^{C} q_i(l)q_j(t)q_k(n)q_r(m)\,p_0(l,t,n,m)\,, \text{ if } R = \{i,j,k,r\}. \quad (8)
\end{aligned}
$$

Similarly, the blocking probabilities for routes with more than four hops can be calculated.

### 6.4.3 Algorithm for Calculating Approximate Blocking Probability

The following reduced load algorithm calculates the approximate blocking probabilities for the traffic on all the routes and average network blocking probability.

Step 1) For all routes *R*, let $\overline{L_R} = 0$.
For $j = 1,\ldots,J$, let $\alpha_j(0) = 0$, and let $\alpha_j(m)$ be chosen arbitrary, $m = 1,\ldots,C$.
Step 2) Determine $q_j(\cdot)$ from (4) and (5). This is to determine the idle capacity distribution when link $j = 1 \ldots J$.
Step 3) Obtain new values of $\alpha_j(\cdot)$, $j = 1,\ldots,J$, using (6). (For two-hop routes, (7) is used instead of (6) and suitable generalizations are used for paths with more than two hops).

Step 4) Determine $L_R$, for all routes $R$ using (8). If $\max_R |L_R - \overline{L_R}| < \varepsilon$ (where $\varepsilon$ is suitably small positive value like 0.00001), then terminate else let $\overline{L_R} = L_R$, and go to Step 2.

Step 5) The average network blocking probability is then given by

$$\Pr_{network} = \frac{\sum_{i=1}^{R} a_i L_i}{a_{network}}$$ where $a_{network}$ is the network offered load.

## 6.5 Numerical and Simulation Results

The entire simulation is conducted on PCs with 1.8 GHz Intel Core Duo CPU Centrino processors on 32-bit MS Windows XP OS. Each PC has 2 Gigabits of RAM. The blocking performance is computed using OPNET for a network of seven nodes and nine links (Figure 6.4), the famous NSFNET (14 nodes, 21 links) topology (Figure 2.9), a three by eight mesh torus topology (Figure 6.9), and a five by five topology (Figure 6.11). At the first hop, a wavelength and a time-slot in the selected wavelength are randomly assigned. At subsequent hop(s), a time-slot in a wavelength is assigned based on the First-Fit heuristic since no wavelength converter is used. Simulations are run many times to obtain a 95% confidence interval. The reduced load algorithm is used in our method.

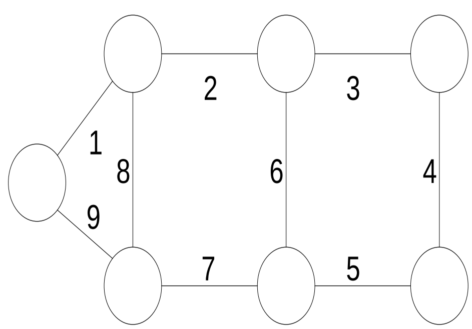


Figure 6.4: Seven nodes nine links network

The following assumptions are used in our proposed analytical model:

(i) Each connection is assumed to use an entire time-slot on a single wavelength on each link within its path. Each link is assumed to have the same number of wavelengths, and each wavelength contains the same number of time-slots. The capacity of each link denoted by *C* is the same for all the links in the network.

(ii) External calls arrive at each node according to the Poisson process with rate $\lambda$ .

(iii) Call holding time is exponentially distributed with unit mean.

(iv) Calls that cannot be routed in the network are blocked and never return.

(v) Random assignment of a wavelength and a time-slot in the selected wavelength.

(vi) Existing calls cannot be assigned another time-slot to accommodate new call requests.

For the seven nodes nine links network (Figure 6.4), we consider the possible 18 routes. Table 6.2 and Table 6.3 show the individual route blocking probabilities with different network offered loads. *R* denotes the selected set of routes labeled by the link IDs. $L_R^{sim}$ (%) denotes the blocking probability obtained by simulation. $L_R$ (%) denotes the blocking probability calculated analytically. Simulation results are given as 95% confidence intervals estimated by method of batch means. The number of batches is 30. Each link has eight wavelengths and each wavelength has eight time-slots. The total network offered load for Table 6.2 is 5 Erlangs. Since we assumed the load is uniformly distributed on all the routes, each route has a load of 0.277 Erlangs. The total network offered load for Table 6.3 is 10 Erlangs. The load is uniformly distributed on all the routes. Thus, each route has a load 0.555 Erlangs. We observe that there are good accuracies in the analytical results for a total network load of 5 Erlangs and a total network load of 10 Erlangs because for most cases the analytical results are within the range of simulated results.

For Figure 6.5 to Figure 6.8, routes are constructed using minimum fixed hop routing. The loads to all routes are assumed to be the same. Routes are considered from different parts of the network. If multiple routes are present between two node pairs, at most three routes are randomly selected. The inter-arrival time of a connection request is from 0.025 to 0.2 second. The simulated and analytical results of Figure 6.5 to Figure 6.8 are for NSFNET topology (Figure 2.9). For Figures 6.5 and 6.6, we consider 42 one-hop, 28 two-hop, and 28 three-hop routes. For Figure 6.5, similar results are obtained using the derived mathematical expressions and the proposed

Table 6.2: Total offered load of 5 Erlangs

| **No.** | **R** | $L_R^{sim}$ **(%)** | $L_R$ **(%)** |
|---|---|---|---|
| **1.** | {1} | (0.0062,0.0101) | 0.0087 |
| **2.** | {2} | (0.0171,0.0310) | 0.0191 |
| **3.** | {3} | (0.0172,0.0304) | 0.0190 |
| **4.** | {4} | (0.0049,0.0060) | 0.0055 |
| **5.** | {5} | (0.0030,0.0045) | 0.0043 |
| **6.** | {6} | (0.0000,0.0000) | 0.0000 |
| **7.** | {7} | (0.0041,0.0075) | 0.0070 |
| **8.** | {8} | (0.0000,0.0000) | 0.0000 |
| **9.** | {9} | (0.0000,0.0000) | 0.0000 |
| **10.** | {1,2} | (0.0347,0.0501) | 0.0325 |
| **11.** | {5,7} | (0.0196,0.0283) | 0.0245 |
| **12.** | {2,3} | (0.0225,0.0321) | 0.0245 |
| **13.** | {7,8} | (0.0228,0.0262) | 0.0254 |
| **14.** | {3,4} | (0.0221,0.0332) | 0.0323 |
| **15.** | {6,7} | (0.0101,0.0227) | 0.0136 |
| **16.** | {1,2,3} | (0.0521,0.0678) | 0.0516 |
| **17.** | {4,5,7} | (0.0495,0.0673) | 0.0545 |
| **18.** | {1,2,3,4} | (0.0637,0.0887) | 0.0801 |

algorithm. Figure 6.5 shows the simulation and analytical results of (i) two wavelengths per link, and each wavelength has eight time-slots ($W$=2,$T$=8), and (ii) two wavelengths per link, and each wavelength has 10 time-slots ($W$=2,$T$=10). We plot the average network blocking probability for these routes versus the total offered load to the network. The analytical results of the proposed model are in agreement with the

Table 6.3: Total offered load of 10 Erlangs

| **No.** | **R** | $L_R^{sim}$ **(%)** | $L_R$ **(%)** |
|---|---|---|---|
| **1.** | {1} | (0.0118,0.0204) | 0.0120 |
| **2.** | {2} | (0.0313,0.0607) | 0.0352 |
| **3.** | {3} | (0.0330,0.0612) | 0.0352 |
| **4.** | {4} | (0.0064,0.0092) | 0.0090 |
| **5.** | {5} | (0.0058,0.0075) | 0.0071 |
| **6.** | {6} | (0.0021,0.0042) | 0.0028 |
| **7.** | {7} | (0.0095,0.0145) | 0.0122 |
| **8.** | {8} | (0.0000,0.0000) | 0.0000 |
| **9.** | {9} | (0.0000,0.0000) | 0.0000 |
| **10.** | {1,2} | (0.0702,0.0881) | 0.0685 |
| **11.** | {5,7} | (0.0383,0.0534) | 0.0449 |
| **12.** | {2,3} | (0.0402,0.0597) | 0.0450 |
| **13.** | {7,8} | (0.0441,0.0512) | 0.0487 |
| **14.** | {3,4} | (0.0424,0.0653) | 0.0630 |
| **15.** | {6,7} | (0.0221,0.0432) | 0.0291 |
| **16.** | {1,2,3} | (0.1017,0.1388) | 0.1045 |
| **17.** | {4,5,7} | (0.1036,0.1337) | 0.1070 |
| **18.** | {1,2,3,4} | (0.1263,0.1753) | 0.1284 |

simulated results. For the purpose of analysis, we compare the simulated and analytical results of three wavelengths. This is shown in Figure 6.6. The figure shows the simulated and analytical results of three wavelengths per link, and each wavelength has eight time-slots ($W$=3,$T$=8). We plot the average network blocking probability for these routes versus the total offered load to the network. As the offered load (Erlangs) increases, the simulation results matches well with the analytical results.

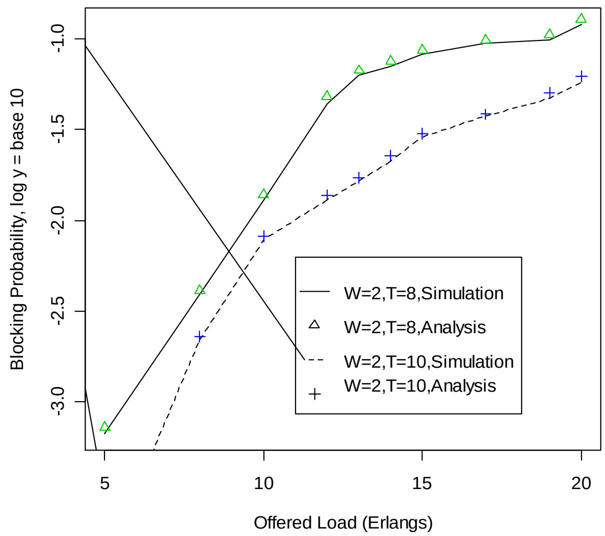


Figure 6.5: Results obtained through simulation and analysis for $W$=2, and $T$=8,10

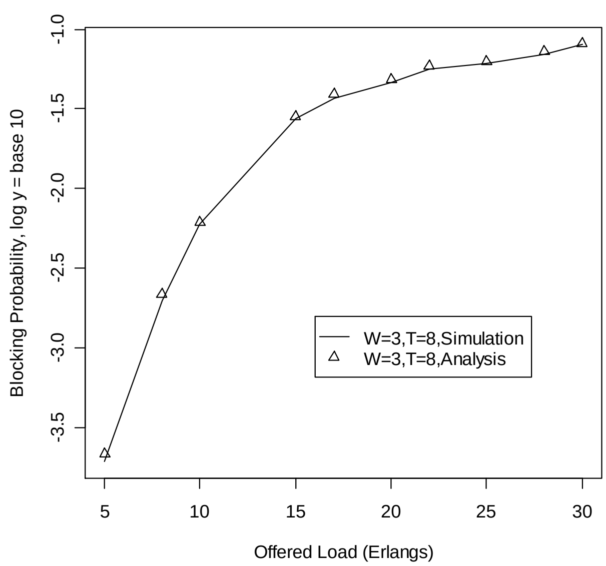


Figure 6.6: Results obtained through simulation and analysis for $W$=3 and $T$=8

For Figures 6.7 and 6.8, we consider 42 one-hop, 28 two-hop, 28 three-hop, and eight four-hop routes. Figure 6.7 shows the simulated and analytical results of eight wavelengths per link, and each wavelength has eight time-slots (*W*=8,*T*=8). Figure 6.8 shows the simulated and analytical results of 16 wavelengths per link, and each wavelength has four time-slots (*W*=16,*T*=4). For Figures 6.7 and 6.8, overall good accuracies are observed when the simulated and analytical results are compared.

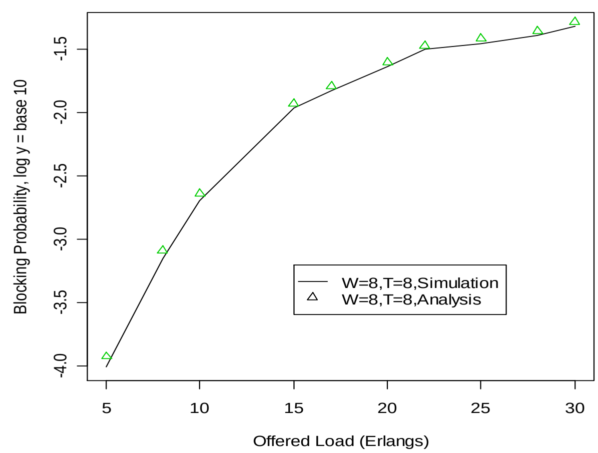


Figure 6.7: Results obtained through simulation and analysis for *W*=8 and *T*=8

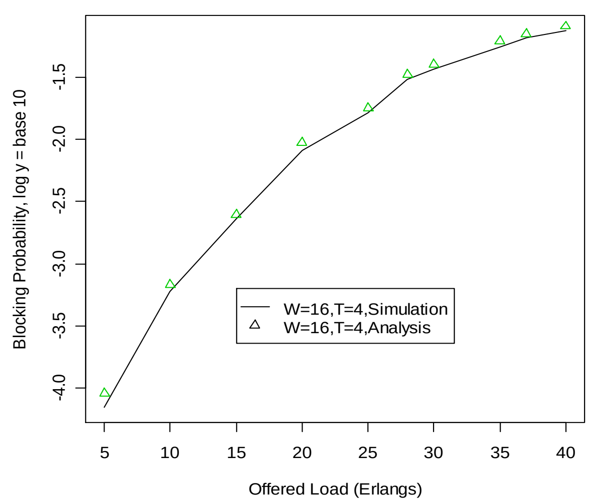


Figure 6.8: Results obtained through simulation and analysis for *W*=16 and *T*=4

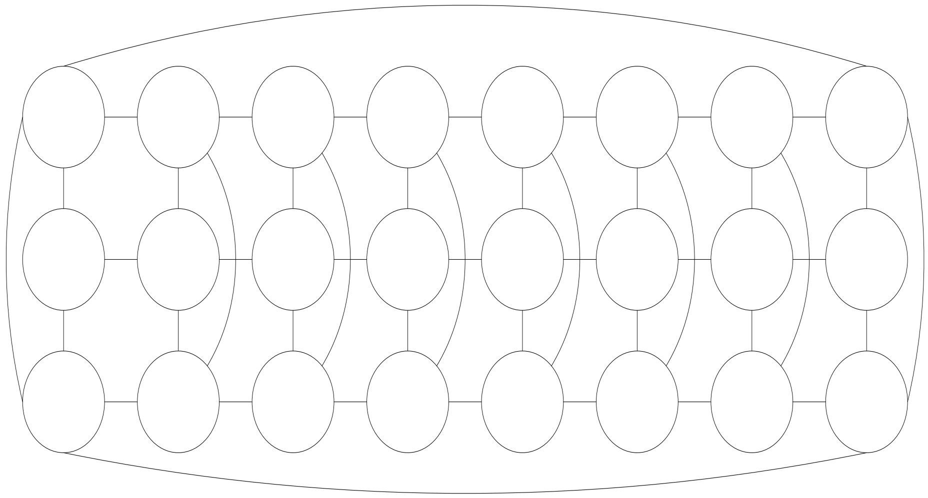

Figure 6.9: Three by eight mesh torus topology

The simulated and analytical results of Figure 6.10 are for the three by eight mesh torus topology (Figure 6.9). Figure 6.10 shows the simulated and analytical results of 16 wavelengths per link, and each wavelength has four time-slots ($W$=16,$T$=4). In this figure, we consider 44 one-hop, 28 two-hop, 28 three-hop, eight four-hop, and four five-hop routes. Similar conclusion is concluded as Figure 6.8.

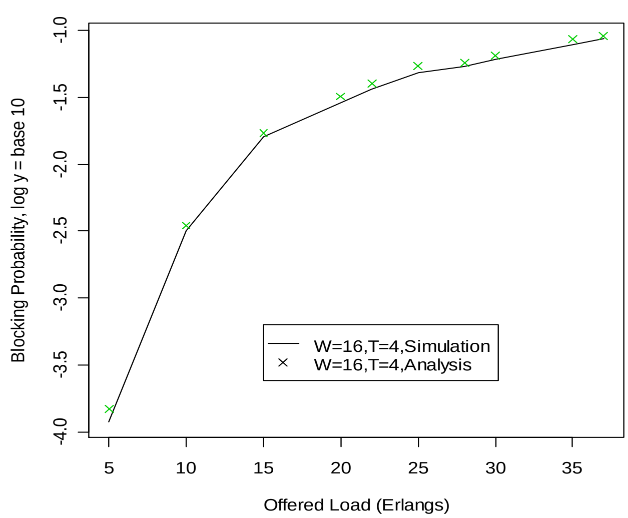


Figure 6.10: Results obtained through simulation and analysis for $W$=16 and $T$=4 (Three by eight mesh torus topology)

Our analytical model is suitable for small networks because it estimates the blocking probabilities of individual routes. Another disadvantage is that the reduced load algorithm requires intensive computation to calculate longer hops. Therefore, we suggest the use of mainframe to compute such routes.

## 6.6 Summary

In this research, the partition based approach is used to derive the mathematical expressions and calculate the blocking probabilities of TDM wavelength optical networks with OTSIs and without WC. As the number of wavelengths and links increases, the natural reasoning method has difficulty in deriving the mathematical expressions because of the large number of groupings. In order to make the analysis tractable, we proposed a schema that works for any number of partitions regardless of the numbers of links, wavelengths in each link, and time-slots in each wavelength. The fixed routing method is used to determine the route. This approach is accurate in estimating the blocking probabilities of individual routes and average network blocking probabilities.

# CHAPTER 7

# CONCLUSION and FUTURE RESEARCH

## 7.1 Summary

As the fiber bandwidth and the number of wavelengths in a fiber continue to increase, being able to better utilize the high bandwidth in each wavelength has become an important issue in optical networking research. The objectives of this thesis are to investigate various ways of effectively and efficiently using fiber bandwidth at the time-slot wavelength level and the mini-slot time-slot wavelength level, as well as to evaluate their feasibilities through performance studies and cost analysis.

Although research in traffic grooming at the time-slot wavelength level for optical networks is not new [76-82], they do not deal with the sharing of the time-slot among the successful connection requests. We have proposed a time-slot sharing scheme for TDM wavelength optical network with OTSIs and without WC. All the connections going to the same destination would share the same time-slot from the source to destination router, and the data is optically transmitted. We also proposed a shared time-slot TDM wavelength router architecture with OTSIs. The simulation results showed that our shared time-slot TDM wavelength optical WDM networks have a lower blocking probability than the conventional non-shared time-slot networks and typical wavelength optical network without WC. Our simulation results also reveal that the blocking probability of the networks is not strongly dependent on the routing methods as follow: fixed routing method, centralized least-cost routing method, and least-cost routing method with at least a free time-slot in a fiber link method.

Next, we believe it is feasible to realize the optical transmission system for transmitting data in a mini-slot of a time-slot in a wavelength, after taking the advancement of the enabling optical and electronic technologies into consideration (as presented in chapter 3). Although we have not design the OTSI and OMSI, we have discussed the research done in OTSI [88-91] in pages 13 and 14 and demonstrated theoretically that it is possible to switch mini-slots and synchronize mini-slots for our purpose in pages 52 and 53. We subsequently proposed a mini-slot router architecture and a mini-slot TDM wavelength optical networking scheme, in which each time-slot is further divided into mini-slots. Through extensive simulations study, we are able to show the effectiveness of fiber bandwidth utilization for different mini-slot requests. On the whole, our simulation results show that shared time-slot TDM wavelength optical WDM network has a lower blocking probability than the mini-slot TDM optical WDM network except for two cases at the offered load of 600 Erlangs.

Then, we performed a feasibility study of the shared time-slot TDM wavelength optical network and mini-slot TDM wavelength optical network from the perspectives of optical components availability and implementation costs. Both of our proposed networks are feasible to be implemented, in particular the shared time-slot TDM wavelength node where the major obstacle is the high development cost of an OTSI. At present, the cost of the mini-slot architecture is higher than the shared time-slot architecture. In future, as the cost of optical components decreases and fiber bandwidth increases, the mini-slot architecture may be a better alternative for low bandwidth requests.

Since the shared time-slot TDM wavelength optical WDM node and the mini-slot TDM wavelength optical node have their limitations in interchanging slots, it is importance to have a flexible optical architecture that can perform both time-slots and mini-slots operations. However, we felt that this architecture involves high complexities and hence the implementation cost would remain be very high in the foreseeable future due to the infancy stage of the required optical technology.

An analytical model for TDM wavelength optical network with OTSIs and without WC using the partition based approach was also proposed. To make the analysis tractable, a schema capable of working for any number of partition patterns regardless of the number of links, wavelengths in each fiber, and time-slots in each wavelength is proposed. Our analytical model yields good accuracies when compared with the simulation results. Instead of relying on simulation, network designers may instead use our analytical model to compute the blocking probabilities of desirable networks. However, our model requires intensive computation and the use of mainframe computers are recommended to generate analytical results, especially for long hops with many wavelength and time-slots in each link.

The next section suggests two possible enhancements of this thesis work.

## 7.2 Future Improvements

First, like many other researchers, we have focused our performance studies (both analytical and computer simulation) on common optical networks such as the NSFNET topology, 19-node EON[102], and 21-node ARPA-2 [161] and metropolitan area networks like the MSN [94]. The studies have become more tractable and manageable due to the smaller network sizes. However to ensure a better generalization of the findings, further studies should include networks of larger sizes with variety of topologies.

Second, we discovered that as the number of wavelengths and links continue to increase, the natural reasoning method of deriving the mathematical expressions for our analytical model becomes increasing difficult (see Section 6.2). Instead of using our proposed schema method, a generalized mathematical formula should be derived to calculate $p_o^{(l)}(x_1,...,x_r)$ so that the computation may be reduced.

The last section of this chapter outlines some future research directions of optical traffic grooming.

## 7.3 Directions for Future Research

The following are suggestions of further work for optical traffic grooming at the time-slot TDM WDM level and the mini-slot TDM WDM level:

(i) In chapter 2 of this thesis, some current wavelength switches architectures with WCs were first presented. Then different placements of SSWCs in the wavelength router were discussed. Taking a cue from the work report in [162], the optimal use of SSWCs in the wavelength router architecture and the behavior of this network warrant further investigation;

(ii) In chapter 6 of this thesis, the analytical model for the calculation of approximate blocking probabilities of TDM wavelength optical network with OTSIs and without WC using the partition based approach is proposed for the fixed routing method. It will be more challenging to derive the generalized formula for calculating the blocking probabilities for *m* links of *w* wavelengths in each link, each wavelength having $x$ empty time-slots, and each time-slot having $z$ mini-slots. Moreover, [105-106] reported that the analytical results for least cost routing method are good in moderate and heavy traffic loads. Future analysis using the least cost routing method should be done on our proposed model to see whether we can obtain similar results as what is being reported in [105-106], since these papers used the reduced load algorithm too. In addition, we can compare our analytical results with the output generated from other TDM wavelength performance models, for example the proposed model in [108];

(iii) [163] applies game theory to global traffic grooming at the time-slot wavelength level; [164-165] use game theory to analyze wireless Ad Hoc Networks. Interesting results may be obtained if game theory or its variations can be applied to global traffic grooming at the shared time-slot TDM wavelength optical WDM network. This network does not use WC;

(iv) [49] studies the effects of traffic changes and different buffer size on statistical multiplexing gain and bandwidth savings in OCS, OBS, and OPS. It is interesting to study traffic grooming in OBS and OPS on the shared time-slot TDM wavelength network. The OCS protocol cannot be used, and the size of each time-slot needs to be analyzed. A router architecture for each of the two traffic grooming methods – OBS and OPS – can be designed.

# BIBLIOGRAPHY

[1] J. M. H. Elmirghani and H. T. Mouftah, "Technologies and architectures for scalable dynamic dense WDM networks," IEEE Commun. Mag., vol. 38, no. 2, pp. 58-66, Feb. 2000.

[2] P. E. Green Jr., "Optical networking update," IEEE J. Select. Areas Commun., vol. 14, no. 5, pp. 764-779, June 1996.

[3] E. Karasan and S. Banerjee, "Performance of WDM transport networks," IEEE J. Select. Areas Commun., vol. 16, no. 7, pp. 1081-1096, Sept. 1998.

[4] L. D. Garrett, et al, "The MONET New Jersey network demonstration", IEEE J. Select. Areas Commun., vol. 16, no. 7, pp. 1199-1219, Sept. 1988.

[5] Alcatel-Lucent (http://www1.alcatellucent.com/products/productsbyfamily.jsp;jsessionid=0HJDH3VKG3OEPLAWFRSHJG3MCYWGQTNS?LUID=Product_Categories/Product_Category_39.xml&category=Optical).

[6] CISCO (http://www.cisco.com/en/US/products/hw/optical/index.html).

[7] Calient Networks (http://calient.net/products).

[8] ADVA (http://www.advaoptical.com).

[9] Tejas Networks (http://www.tejasnetworks.com/products.html).

[10] A. Gumaste and I. Chlamtac, "Mesh implementation of light-trails: A solution to IP centric communication," in ICCCN, Dallas, Texas, USA, 13$^{th}$-15$^{th}$ Oct. 2003, pp. 178-183.

[11] I. Chlamtac, A. Ganz, and G. Karmi, "Lightpath communications: An approach to high bandwidth optical WANs," IEEE Trans. Commun., vol. 40, no. 7, pp. 1171-1182, July 1992.

[12] S. Subramaniam and R. A. Barry, "Wavelength assignment in fixed-routing WDM networks," in ICC, Montreal, Canada, 8$^{th}$-12$^{th}$ June 1997, vol. 1, pp. 406-410.

[13] C. Chen and S. Banerjee, "A new model for optimal routing and wavelength assignment in wavelength division multiplexed optical networks," in INFOCOM, March 1996, vol. 1, pp. 164-171.

[14] X. Zhang and C. Qiao, "Wavelength assignment for dynamic traffic in multi-fiber WDM networks," in ICCCN, Lafayette, Louisiana, USA, 12th-15th Oct. 1998, pp. 479-485.

[15] J. Zheng and H. T. Mouftah, "Routing and wavelength assignment for advance reservation in wavelength-routed WDM optical networks," in ICC, New York, NY, USA, 28th Apr.-2nd May 2002, vol. 5, pp. 2722-2726.

[16] R. Ramaswami and K.N. Sivarajan, "Routing and wavelength assignment in all-optical networks," IEEE/ACM Trans. Networking, vol. 3, no. 5, pp. 489-500, Oct. 1995.

[17] A. Girard, Routing and Dimensioning in Circuit-Switched Networks, Addison-Wesley, Reading, MA, 1990.

[18] E. Lawler, Combinatorial Optimization: Networks and Matroids, Holt, Rinehart and Winston, 1976.

[19] J. Strand, A. L. Chiu, and R. Tkach, "Issues for routing in the optical layer," IEEE Commun. Mag., vol. 39, no. 2, pp. 81-96, Feb. 2001.

[20] M. Yoo, C. Qiao, and S. Dixit, "Optical burst switching for service differentiation in the next-generation optical Internet," IEEE Commun. Mag., vol. 39, no. 2, pp. 98-104, Feb. 2001.

[21] M. Renaud, et al, "Network and system concepts for optical packet switching," IEEE Commun. Magazine, vol. 35, no. 4, pp. 96-102, April 1997.

[22] L. Xu, H. G. Perros, and G. Rouskas, "Techniques for optical packet switching and optical burst switching," IEEE Commun. Mag., vol. 39, no. 1, pp. 136-142, Jan. 2001.

[23] S. Yao, B. Mukherjee, and S. Dixit, "Advances in photonic packet switching: an overview," IEEE Commun. Mag., vol. 38, no. 2, pp. 84-94, Feb. 2000.

[24] D. J. Blumenthal, P. R. Prucnal, and J. R. Sauer, "Photonic packet switches: architectures and experimental implementations," Proc. of the IEEE, vol. 82, no. 11, pp. 1650-1667, Nov. 1994.

[25] D. J. Blumenthal, et al, "All-optical label swapping networks and technologies," J. Lightwave Techno., vol. 18, no. 12, pp. 2058-2075, Dec. 2000.

[26] N. Yan, I. T. Monroy, and T. Koonen, "All-optical label swapping node architectures and contention resolution," in Conf. Optical Network Design and Modeling (ONDM), Milan, Italy, 7th-9th Feb. 2005, pp. 115-123.

[27] D. Chiaroni, "Packet switching matrix: a key element for the backbone and the metro," IEEE J. Select. Areas Commun., vol. 21, no. 7, pp. 1018-1025, Sept. 2003.

[28] H. Harai, M. Murata, and H. Miyahara, “Performance of alternate routing methods in all-optical switching networks,” in INFOCOM, Kobe, Japan, $7^{th}$-$11^{th}$ Apr. 1997, vol. 2, pp. 516-524.

[29] Y. Chen, C. Qiao, and X. Yu, “Optical Burst Switching (OBS): A new area in optical networking research,” IEEE Network, vol. 18, no. 3, pp. 16-23, May-June 2004.

[30] M. Klinkowski, D. Careglio, and J. Sole-Pareta, “Comparison of conventional and offset time-emulated optical burst architectures,” in Intl. Conf. Transparent Optical Networks, 2006, vol. 3, pp. 47-50.

[31] I. Widjaja, “Performance analysis of burst admission control protocols,” IEEE Proc. Commun., vol. 142, no. 1, pp. 7-14, Feb. 1995.

[32] E. Varvarigos and V. Sharma, “The ready-to-go virtual circuit protocol: a loss-free protocol for multigigabit networks using FIFO buffers,” IEEE/ACM Trans. Networking, vol. 5, no. 5, pp. 705-718, Oct. 1997.

[33] M. Yoo and C. Qiao, “Optical burst switching (OBS) – a new paradigm for an optical internet,” J. High Speed Networks, vol. 8, no. 1, pp. 69-84, 1999.

[34] J. Y. Wei and R. I. McFarland, “Just-in-time signaling for WDM optical burst switching networks,” J. Lightwave Techno., vol. 18, no. 12, pp. 2019-2037, Dec. 2000.

[35] A. Banerjee, et al, “Generalized Multiprotocol Label Switching: An overview of routing and management enhancements,” IEEE Commun. Mag., vol. 39, no. 1, pp. 144-150, Jan. 2001.

[36] A. Banerjee, et al, “Generalized Multiprotocol Label Switching: An overview of signaling enhancements and recovery techniques,” IEEE Commun. Mag., vol. 39, no. 7, pp. 144-151, July 2001.

[37] K. Kompella, et al, “OSPF extension in support of MPLS,” IETF Internet draft, work in progress, Feb. 2001.

[38] K. Kompella, et al, “IS-IS extensions in support of Generalized MPLS,” Internet draft, Dec. 2002.

[39] R. Braden, “Resource Reservation Protocol (RSVP) - version 1 functional specification,” RFC 2205, Sept. 1997.

[40] L. Berger, et al, “Generalized MPLS signaling - RSVP-TE extensions,” IETF RFC 3473, Jan. 2003.

[41] P. Ashwood-Smith, et al, "Generalized MPLS signaling - CR-LDP extensions," Internet draft, Nov. 2001.

[42] J. Lang, "Link management protocol," Internet draft, March 2001.

[43] D.O. Awduche, et al, "Multiprotocol lambda switching: Combining MPLS traffic engineering control with optical crossconnects," IEEE Commun. Mag., vol. 39, no. 4, pp. 111-116, March 2001.

[44] E. Mannie, et al, "Generalized Multi-Protocol Label Switching (GMPLS) architecture," Internet draft, May 2003.

[45] P. Ashwood-Smith, et al., "Generalized MPLS - Signaling Functional Description," IETF Internet Draft, work in progress, Nov. 2001.

[46] A. K. Somani, Survivability and Traffic Grooming in WDM Optical Networks, Cambridge University Press, 2006.

[47] F. Farahmand, Q. Zhang, and J. P. Jue, "Dynamic traffic grooming in optical burst-switched networks," J. Lightwave Techno., vol. 23, no. 10, pp. 3167-3177, Oct. 2005.

[48] Y-L Hsueh, et al, "Traffic grooming on WDM rings using optical burst transport," J. Lightwave Techno., vol. 24, no. 1, pp. 44-53, Jan. 2006.

[49] L. B. Sofman, A. Agrawal, and T. S. El-Bawab, "Traffic grooming and bandwidth efficiency in packet and burst switched networks," http://www.scs.org/getDoc.cfm?id=2086.

[50] X. Cao, V. Anand, Y. Xiong, and C. Qiao, "Performance evaluation of wavelength band switching in multi-fiber all-optical networks," in INFOCOM, San Francisco, California, USA, 30th March-3rd Apr. 2003, vol. 3, pp. 2251-2261.

[51] K. Harada, K. Shimizu, T. Kudou, and T. Ozeki, "Hierarchical optical path cross-connect systems for large scale WDM networks," in OFC, Feb. 1999, vol. 2, pp. 356-358.

[52] O. Gerstel, R. Ramaswami, and W. K. Wang, "Making use of a two-stage multiplexing scheme in a WDM network," in OFC, March 2000, vol. 3, pp. 44-46.

[53] R. Lingampalli and P. Vengalam, "Effect of wavelength and waveband grooming on all-optical networks with single layer photonic switching," in OFC, Anaheim, California, USA, 17th – 22nd March 2002, pp. 33-34.

[54] Y. Suemura, et al, "Hierarchical routing in layered ring and mesh optical networks," in ICC, New York, NY, USA, 28th Apr.-2nd May 2002, vol. 5, pp. 2727-2733.

[55] S. Yao, C. Ou, and B. Mukherjee, “Design of hybrid optical networks with waveband and electrical TDM switching,” in GLOBECOM, San Francisco, California, USA, 1st-5th Dec. 2003, vol. 5, pp. 2803-2808.

[56] E. Modiano and Philip J. Lin, “Traffic grooming in WDM networks,” IEEE Commun. Mag., vol. 39, no. 7, pp. 124-129, July 2001.

[57] O. Gerstel, P. Lin, and G. Sasaki, “Combined WDM and SONET network design,” in INFOCOM, San Francisco, California, USA, 29th March-3rd Apr. 1998, vol. 2, pp. 734-743.

[58] X. Zhang and C. Qiao, “On scheduling all-to-all personalized connections and cost-effective designs in WDM rings, “ IEEE/ACM Trans. Networking, vol. 7, no. 3, pp. 435-443, June 1999.

[59] J. Wang, W. Cho, V. R. Vemuri, and B. Mukherjee, “Improved approaches for cost-effective traffic grooming in WDM ring networks: ILP formulations and single-hop and multihop connections,” J. Lightwave Techno., vol. 19, no. 11, pp. 1645-1653, Nov. 2001.

[60] P. J. Wan, G. Calinescu, and O. Frieder, “Grooming of arbitrary traffic in SONET/WDM BLSR’s,” IEEE J. Select. Areas Commun., vol. 18, no. 10, pp. 1995-2003, Oct. 2000.

[61] J. Simmons, E. Goldstein, and A. Saleh, “Quantifying the benefit of wavelength add-drop in WDM rings with distance independent and dependent traffic,” J. Lightwave Techno., vol. 17, no. 1, pp. 48-57, Jan. 1999.

[62] R. Berrry and E. Modiano, “Reducing electronic multiplexing costs in SONET/WDM rings with dynamic changing traffic,” IEEE J. Select. Areas Commun., vol. 18, no. 10, pp. 1961-1971, Oct. 2000.

[63] O. Gerstel, R. Ramaswami, and G. H. Sasaki, “Cost-effective traffic grooming in WDM rings,” IEEE/ACM Trans. Networking, vol. 8, no. 5, pp. 618-630, Oct. 2000.

[64] V. R. Konda and T. Y. Chow, “Algorithm for traffic grooming in optical networks to minimize the number of transceivers,” in IEEE Workshop on HPSR, Dallas, Texas, USA, 29th-31st March 2001, pp. 218-221.

[65] J. Q. Hu and B. Leida, “Traffic grooming, routing, and wavelength assignment in optical WDM mesh networks,” in INFOCOM, Hong Kong, China, 7th-11th March 2004, vol. 1.

[66] R. Ranganathan, J. Berthold, L. Blair, and J. Berthold, “Architectural implications of core grooming in a 46-node USA optical network,” in OFC, Anaheim, California, USA, 17th – 22nd March. 2002, pp. 498-499.

[67] H. Zhu, H. Zang, K. Zhu, and B. Mukherjee, "A novel generic graph model for traffic grooming in heterogenous WDM mesh networks," IEEE/ACM Trans. Networking, vol. 11, no. 2, pp. 285-299, Apr. 2003.

[68] H. Zhu, H. Zang, K. Zhu, and B. Mukherjee, "Dynamic traffic grooming in WDM mesh networks using a novel graph model," in GLOBECOM, Taipei, Taiwan, 17th-21st Nov. 2002, vol. 3, pp. 2681-2685.

[69] S. Thiagarajan and A. K. Somani, "Capacity fairness of WDM networks with grooming capability," Optical Networks Mag., vol. 2, no. 3, pp. 203-210, May 2001.

[70] C. Xin, Y. Ye, S. Dixit, and C. Qiao, "An integrated lightpath provisioning approach in mesh optical networks," in OFC, Anaheim, California, USA, 17th – 22nd March 2002, pp. 547-549.

[71] K. Zhu and B. Mukherjee, "On-line provisioning connections of different bandwidth granularities in WDM mesh networks," in OFC, Anaheim, California, USA, 17th – 22nd March 2002, pp. 549-551.

[72] I. Cerutti and A. Fumagalli, "Traffic grooming in static wavelength-division multiplexing networks," IEEE Commun. Mag., vol. 43, no. 1, pp. 101-107, Jan. 2005.

[73] N. Ghani, et al, "Integrated traffic grooming in converged data-optical networks," in IEEE Intl. Symp. Computers and Commun. (ISCC), Alexandria, Egypt, 28th-1st July 2004, pp. 294-299.

[74] K. Zhu, H. Zang, and B. Mukherjee, "A comprehensive study on next-generation optical grooming switches," IEEE J. Select. Areas Commun., vol. 21, no. 7, pp. 1173-1186, Sept. 2003.

[75] K. Zhu, H. Zhu, and B. Mukherjee, "Traffic engineering in multigranularity, heterogenous optical WDM mesh networks through dynamic traffic grooming," IEEE Network, vol. 17, no. 2, pp. 8-15, March/April 2003.

[76] S. Subramaniam, E. J. Harder, and H. Choi, "Scheduling multi-rate sessions in TDM wavelength-routed networks," in GLOBECOM, Rio de Janeiro, Brazil, 5th-9th Dec. 1999, vol. 2, pp. 1466-1472.

[77] B. Wen, R. Shenai, and K. Sivalingam, "Routing, wavelength and time-slot assignment algorithms for wavelength-routed optical WDM/TDM networks," J. Lightwave Techno., vol. 23, no. 9, pp. 2598-2609, Sept. 2005.

[78] M. Sivakumar and S. Subramaniam, "A performance evaluation of time switching in TDM wavelength routing networks," in BROADNET, San Jose, California, USA, 25th-29th Oct. 2004, pp. 212-221.

[79] A. Chen, K-S Wong, and C-T Lea, “Routing and time-slot assignment in optical TDM networks,” IEEE J. Select. Areas Commun., vol. 22, no. 9, pp. 1648-1657, Nov. 2004.

[80] N-F. Huang, G-H Liaw, and C-P Wang, “A novel all-optical transport network with time-shared wavelength channels”, IEEE J. Select. Areas Commun., vol. 18, no. 10, pp. 1863-1875, Oct. 2000.

[81] I. Widjaja, I. Saniee, R. Giles, and D. Mitra, "Light core and intelligent edge for a flexible, thin-layered and cost-effective optical transport network," IEEE Optical Commun., vol. 1, no. 2, pp. S30-S36, May 2003.

[82] I. Widjaja and I. Saniee, “Simplified layering and flexible bandwidth with TWIN”, in SIGCOMM 2004 Workshop, Portland, Oregon, USA, 30th Aug.-3rd Sept. 2004, pp. 13-20.

[83] W. Stallings, Data and Computer Communications, 2nd edition, Upper Saddle River, NJ: Prentice-Hall, 1989.

[84] Peter’ De Dobbelaere, K. Falta, and S. Gloeckner, “Advances in integrated 2D MEMS-based solutions for optical network applications,” IEEE Commun. Mag., vol. 41, no. 5, pp. 516-523, May 2003.

[85] W. Goralski, Optical Networking & WDM, McGraw-Hill, 2001.

[86] P. J. Almeida, et al, “OTDM add-drop multiplexer based on time-frequency signal processing,” J. Lightwave Techno., vol. 24, no. 7, pp. 2720-2732, July 2006.

[87] H. J. R. Dutton, Understanding Optical Communications, Prentice-Hall, 1998.

[88] H. F. Jordan, D. Lee, K. Y. Lee, and S. V. Ramanan, “Serial array time slot interchangers and optical implementations,” IEEE Trans. on Computers, vol. 43, no. 11, pp. 1309-1318, Nov. 1994.

[89] D. K. Hunter and D. G. Smith, “New architectures for optical TDM switching,” J. Lightwave Techno., vol. 11, no. 3, pp. 495-511, Mar. 2003.

[90] J. Ramamirthan, and J. Turner, “Time sliced optical burst switching,” in INFOCOM, San Francisco, California, USA, 30th March-3rd Apr. 2003, vol. 3, pp. 2030-2038.

[91] M. C. Cardakli, et al, “Tunable all-optical time slot-interchange and wavelength conversion using difference-frequency-generation and optical buffers,” IEEE Photonics Technology Letters, vol. 14, no. 2, pp. 200-202, Feb. 2002.

[92] P. Gambini, et al, "Transparent optical packet switching: Network architecture and demonstrators in the KEOPS project", IEEE J. Select. Areas Commun., vol. 16, no. 7, pp. 1245-1257, Sept. 1988.

[93] T. Sakamoto, "Optical packet synchronizer using wavelength and space switching," IEEE Photonics Technology Letters, vol. 14, no. 9, pp. 1360-1362, Sept. 2002.

[94] B. Mukherjee, Optical Communication Networks, McGraw-Hill, 1997.

[95] V. Sharma and E. A. Varvarigos, "Limited wavelength translation in all-optical WDM mesh networks," in INFOCOM, San Francisco, California, 29th March-2nd Apr. 1998, vol. 2, pp. 893-901.

[96] S. Subramaniam, M. Azizoglu, and A. Somani, "All-optical networks with sparse wavelength conversion," IEEE/ACM Trans. Networking, vol. 4, no. 4, pp. 544-557, Aug. 1996.

[97] J. Yates, J. Lacey, D. Everitt, and M. Summerfield, "Limited range wavelength translation in all-optical networks," in INFOCOM, March 1996, pp. 954-961.

[98] L. Li and A. K. Somani, "A new analytical model for multifiber WDM networks," IEEE J. Select. Areas Commun., vol. 18, no. 10, pp. 2138-2145, Oct. 2000.

[99] A. Sridharan and K. N. Sivarajan, "Blocking in all-optical networks," IEEE/ACM Trans. Networking, vol. 12, no. 2, pp. 384-397, April 2004.

[100] Y. Zhu, G. N. Rouskas, and H. G. Perros, "A path decomposition approach for computing blocking probabilities in wavelength routing networks," IEEE/ACM Trans. Networking, vol. 8, no. 6, pp. 747-762, Dec. 2000.

[101] R. A. Barry and P. A. Humblet, "Models of blocking probability in all-optical networks with and without wavelength changers," IEEE J. Select. Areas Commun., vol. 14, no. 5, pp. 858-867, June 1996.

[102] M. Kovacevic and A. S. Acampora, "Benefits of wavelength translation in all-optical clear-channel networks," IEEE J. Select. Areas Commun., vol. 14, no. 5, pp. 868-880, June 1996.

[103] S. Gao, X. Jia, C. Huang, and D. Du, "An optimization model for placement of wavelength converters to minimize blocking probability in WDM networks," J. Lightwave Techno., vol. 21, no. 3, pp. 684-694, March 2003.

[104] F. P. Kelly, "Routing and capacity allocation in networks with trunk reservation," Math. Oper. Res., vol. 15, no. 14, pp. 771-792, 1990.

[105] S. Chung, A. Kashper, and K. W. Ross, “Computing approximate blocking probabilities for large loss networks with state-dependent routing,” IEEE/ACM Trans. Networking, vol. 1, no. 1, pp. 105-115, Feb. 1993.

[106] A. Birman, “Computing approximate blocking probabilities for a class of all-optical networks,” IEEE J. Select. Areas Commun., vol. 14, no. 5, pp. 852-857, June 1996.

[107] T. Tripathi and K. N. Sivarajan, “Computing approximate blocking probabilities in wavelength routed all-optical networks with limited-range wavelength conversion,” IEEE J. Select. Areas Commun., vol. 18, no. 10, pp. 2123-2129, Oct. 2000.

[108] J. Yates, J. Lacey, and D. Everitt, “Blocking in multiwavelength TDM networks,” in 4th Intl. Conf. Telecommunication Systems, Modeling, and Analysis, Nashville, Tennessee, 21st-24th March 1996, pp. 535-541.

[109] V. Tamilraj and S. Subramaniam, “An analytical blocking model for dual-rate sessions in multichannel optical networks,” in GLOBECOM, San Antonio, Texas, USA, 25th-29th Nov. 2001, pp. 515-519.

[110] R. Srinivasan and A. K. Somani, “A generalized framework for analyzing time-space switched optical networks,” IEEE J. Select. Areas Commun., vol. 20, no. 1, pp. 202-215, Jan. 2002.

[111] I. P. Kaminow, et al, “A wideband all-optical WDM network”, IEEE J Select. Areas Commun., vol. 14, no.5, pp. 780-799, June 1996.

[112] M. W. Chbat et al, “Toward wide-scale all-optical transparent networking: The ACTS optical PAN-European network (OPEN) project”, IEEE J. Select. Areas Commun., vol. 16, no. 7, pp. 1226-1244, Sept. 1988.

[113] R. Ramaswami and M.Mukherjee, “Routing and wavelength assignment in all-optical networks,” IEEE/ACM Trans. Networking, vol. 3, no. 5, pp. 489-500, Oct. 1995.

[114] I. Saniee, J. Morrison, and I. Widjaja, "Performance of a distributed scheduling protocol for TWIN," ACM SIGMetrics Performance Evaluation Review, vol. 32, no. 2, pp. 38-40, Sept. 2004.

[115] A. Myers, T.S. Eugene Ng, and Hui Zhang, “Rethinking the Service Model: Scaling Ethernet to a Million Nodes”, in Proc. ACM SIGCOMM Workshop on Hot Topics in Networking, Nov. 2004.

[116] W. Stallings, Data and Computer Communications, 6th edition, Upper Saddle River, NJ: Prentice-Hall, 2000.

[117] H. S. Hilton, An Introduction to Photonic Switching Fabrics, Plenum Press, 1993.

[118] M. J. Holmes, et al, “Low crosstalk devices for wavelength-routed networks,” in IEE Colloq. on Guided Wave Optical Signal Processing, 8th June 1995, pp. 2/1-2/10.

[119] M. M. Vaez and C. Lea, “Strictly and wide-sense nonblocking photonic switching systems under crosstalk constraint,” in INFOCOM, San Francisco, California, USA, 29th March-2nd Apr. 1998, vol. 1, pp. 118-125.

[120] F. N. Timofeev, “Free-space grating multi/demultiplexer and wavelength-router for densely spaced WDM networks,” in IEE Colloq. on WDM Technology and Applications, 6th Feb. 1997, pp. 11/1-11/5.

[121] K-W. Ke and C-T. Lea, “On Cost-Based Routing in Connection-Oriented Broadband Networks,” in GLOBECOM, Rio de Janeiro, Brazil, 5th-9th Dec. 1999, vol. 2, pp. 1522-1526.

[122] T. Field, U. Harder, and P. Harrison, “Network Traffic Behavior in Switched Ethernet Systems,” IEEE Intl. Symposium on Modeling, Analysis, & Simulation of Computer & Telecommunications Systems (MASCOTS’02), Fort Worth, Texas, USA, 12th-16th Oct. 2002, pp. 33-42.

[123] B. Ramamurthy and B. Mukherjee, “Wavelength conversion in WDM networking,” IEEE J. Select. Areas Commun., vol. 16, no. 7, pp. 1061-1073, Sept. 1998.

[124] E. Karasan and E. Ayanoglu, “Effects of wavelength routing and selection algorithms on wavelength conversion gain in WDM optical networks,” IEEE/ACM Trans. Networking, vol. 6, no. 2, pp. 186-196, Apr. 1998.

[125] S. Subramaniam, M. Azizoglu, and A. Somani, “On optimal converter placement in wavelength-routed networks,” IEEE/ACM Trans. Networking, vol. 7, no. 5, pp. 754-766, Oct. 1999.

[126] G. Jeong and E. Ayanoglu, “Comparison of wavelength-interchanging and wavelength-selective cross-connects in multi-wavelength all-optical networks,” in INFOCOM, March, 1996, vol. 1, pp. 156-163.

[127] R. Ramaswami and G. H. Sasaki, “Multiwavelength optical networks with limited wavelength conversion,” IEEE/ACM Trans. Networking, vol. 6, no. 6, pp. 744-754, Dec. 1998.

[118] K-C. Lee and Victor O. K. Li, “A wavelength-convertible optical network,” J. Lightwave Techno., vol. 11, no. 5, pp. 962-970, May/June 1993.

[129] J. Elmirghani and H. Mouftah, “All-optical wavelength conversion: Technologies and applications in DWDM networks,” IEEE Commun. Mag., vol. 38, no. 3, pp. 86-92, March 2000.

[130] C.Y. Li, G.M. Li, P. K. Wai, V. O. K. Li, "A wavelength-switched time-slot routing scheme for wavelength-routed networks," in ICC, Paris, France, 27th June-1st July 2004, vol. 3, pp. 1689-1693.

[131] S. Kodama, et al, "2.3 picoseconds optical gate monolithically integrating photodiode and electroabsorption modulator," Electronic Letters, vol. 37, no. 19, pp. 1185-1186, Sept. 2001.

[132] I. Ogura, et al, "Picosecond all-optical gate using a saturable absorber in mode-locked laser diodes," IEEE Photonics Technology Letters, vol. 10, no. 4, pp. 603-605, Apr. 1998.

[133] L. Zucchelli, et al, "An experimental optical packet synchronizer with 100ns range and 200ps resolution," in ECOC, 20th-24th Sept. 2004, vol. 1, pp. 587-588.

[134] R. Ramaswami and K. N. Sivarajan, Optical Networks – A Practical Perspective, Morgan Kauffman, 2002, 2nd Edition.

[135] B. M. Waxman, "Routing of multipoint connections," IEEE J. Select. Areas Commun., vol. 6, no. 9, pp. 1617-1622, Dec. 1988.

[136] http://www-iepm.slac.stanford.edu/monitoring/bulk/window-vs-streams.html]

[137] M. Roughan, et al "Class-of-Service Mapping for QoS: A Statistical Signature-based Approach to IP Traffic Classification," in 4th. Proceeding of ACM SIGCOMM Conference on Internet Measurement, ACM Press, 2004, pp. 135-148.

[138] Photonik Technologies, German Center, #04-102, 25 International Business Park, Singapore 609916.

[139] ADC at http://www.adc.com/search/search.jsp?q=tunable+laser

[140] Zugo Photonics Pte. Ltd., 55 Kaki Bukit View, Kaki Bukit Techpark II, Singapore 415976.

[141] Hardwarezone.com at
http://www.hardwarezone.com/core/search.php?q=gigabit+ethernet+card

[142] Vitesse.com at http://www.vitesse.com/technologies/index.php?id=10

[143] L. G. Roberts, "Beyond Moore's law: Internet growth trends," Computer, vol. 33, no. 1, pp. 117-119, Jan. 2000.

[144] R. J. Bates, Optical Switching and Networking Handbook, McGraw-Hill, 2001.

[145] J. Zheng and H. T. Mouftah, Optical WDM Networks – Concepts and Design Principles. John Wiley & Sons, 2004.

[146] http://www.mrv.com/products/line/optiswitch.php

[147] http://www.ghipsystems.com/en/Products/TDM41xx-en/TDM41xx-en.html

[148] P. Bedell, Gigabit Ethernet for Metro Area Networks, McGraw-Hill, 2003.

[149] G. Kramer and G. Pesavento, "Ethernet passive optical network (EPON): Building a next-generation optical access network," ", J. Lightwave Techno., vol. 40, no. 2, pp. 66-73, Feb. 2002.

[150] T-P. Lin and K-P Fan, "EPON testbed and field trial environment in Taiwan," in 2nd Intl. Conf. on Testbeds and Research Infrastructure for Dev. Of Networks and Communities (TRIDENTCOM), Barcelona, Spain, 1st-3rd March, 2006, pp. -.

[151] N. Ghani, A. Shami, C. Assi, and M. Y. A. Raja, "Quality of service in Ethernet passive optical networks," in IEEE Sarnoff Sym. Advances in Wired and Wireless Commun., Princeton, New Jersey, USA, 26th-27th Apr. 2004, pp. 161-165.

[152] H. S. Nam, et al, "TDM over EPON in access network," ," in 6th. Intl. Advanced Commun. Technology (ICACT), Phoenix Park, Korea, 9th-11th Feb. 2004, vol. 1, pp. 279-282.

[153] M. Nakamura, H. Ueda, T. Yokotani, and K. Oshima, "Proposal of networking by PON technologies for full and Ethernet services in FTTx", J. Lightwave Techno., vol. 22, no. 11, pp. 2631-2640, Nov. 2004.

[154] P. Kloppenburg, "Optical Ethernet is evolving as a delivery vehicle for retail metro services," in Optical Fiber Commun. Conf. and 2006 National Fiber Optic Eng. Conf. (OFC/NFOEC), 5th-10th March 2006.

[155] S. Keshav, An Engineering Approach to Computer Networking, Addison-Wesley, 2000.

[156] S. Pau, et al, "160 Gb/s all optical MEMS time-slot switch for OTDM and WDM application", IEEE Photonics Technology Letters, vol. 14, no. 10, pp. 1460-1462, Oct. 2002.

[157] C. K. Yow, et al, "A novel ultra-fast optical router using time-slot switching," Lasers and Electro-Optics (CLEO), 16th-21st May 2004, vol. 1.

[158] K. Y. Eng and M. Santoro, "Multi-Gb/s Optical Cross-connect Switch Architecture: TDM versus FDM Techniques," in GLOBECOM, Nov. 1989, vol. 2, pp. 999-1003.

[159] M. Hall, Combinatorial Theory, John Wiley & Sons, 1986.

[160] K. P. Bogart, Introductory Combinatorics, 2nd edition, Harcourt Brace Jovanovich (HBJ) Publishers, 1990.

[161] A. Mokhtar and M. Azizoglu, "Adaptive wavelength routing in all-optical networks," IEEE/ACM Trans. Networking, vol. 6, no. 2, pp. 197-206, Apr. 1998.

[162] Z. Zhang and Y. Yang, "On-line optimal wavelength assignment in WDM networks with shared wavelength converter pool," IEEE/ACM Trans. Networking, vol. 15, no. 1, pp. 234-245, Feb. 2007.

[163] V. V. Minh Nhat, A. Obaid, and P. Poirier, "Application of game theory in traffic grooming," in IEEE and IFIP Intl. Conf. on Wireless and Optical Commun. Networks (WOCN), Dubai, UAE, 6th-8th March 2005, pp. 383-387.

[164] V. Srivastava, et al, "Using game theory to analyze wireless ad hoc networks," IEEE Commun. Surveys & Tutorials, vol. 7, no. 4, pp. 46-56, Fourth Quarter, 2005.

[165] V. Srivastava and L. A. DaSilva, "Equilibria for node participation in ad hoc networks – an imperfect monitoring approach," in ICC, Istanbul, Turkey, 10th-16th June 2006, vol. 8, pp. 3850-3855.